

Aus der Abteilung Genvektoren des Helmholtz Zentrums München

Leitung: Prof. Dr. Wolfgang Hammerschmidt

Patients' acute lymphoblastic leukemia cells show
heterogeneous growth behavior and drug sensitivity in vivo

Dissertation
zum Erwerb des Doktorgrades
der Naturwissenschaften
(Dr. rer. nat.)



an der Medizinischen Fakultät der
Ludwig-Maximilians-Universität München

vorgelegt von
Cornelia Finkenzeller
aus Ingolstadt

2015

Für meine Eltern

**Gedruckt mit Genehmigung der Medizinischen Fakultät der
Ludwig-Maximilians-Universität München**

| | |
|-----------------------------|--------------------------------------|
| Betreuer: | PD Dr. Ursula Zimmer-Strobl |
| Zweitgutachter: | Prof. Dr. Roland Kappler |
| Dekan: | Prof. Dr. med. dent. Reinhard Hickel |
| Tag der mündlichen Prüfung: | 15.12.2016 |

Eidesstattliche Versicherung

Finkenzeller, Cornelia

Name, Vorname

Ich erkläre hiermit an Eides statt, dass ich die vorliegende Dissertation mit dem Thema

Patients' acute lymphoblastic leukemia cells show heterogeneous growth behavior and drug sensitivity in vivo

selbständig verfasst, mich außer der angegebenen keiner weiteren Hilfsmittel bedient und alle Erkenntnisse, die aus dem Schrifttum ganz oder annähernd übernommen sind, als solche kenntlich gemacht und nach ihrer Herkunft unter Bezeichnung der Fundstelle einzeln nachgewiesen habe.

Ich erkläre des Weiteren, dass die hier vorgelegte Dissertation nicht in gleicher oder in ähnlicher Form bei einer anderen Stelle zur Erlangung eines akademischen Grades eingereicht wurde.

Ort, Datum

Unterschrift Doktorandin

Table of contents

| | |
|---|----|
| 1. Zusammenfassung..... | 9 |
| 2. Abstract | 11 |
| 3. Introduction..... | 12 |
| 3.1. Acute leukemias | 12 |
| 3.1.1. Treatment and prognosis of patients | 12 |
| 3.1.2. Minimal residual disease as hallmark of intra-tumor heterogeneity..... | 13 |
| 3.1.3. Acute leukemia as suitable model disease to study clonal heterogeneity | 14 |
| 3.2. Adverse characteristics of tumor cells | 15 |
| 3.2.1. Quiescence | 15 |
| 3.2.2. Drug resistance..... | 16 |
| 3.2.3. Stemness | 16 |
| 3.3. Intra-tumor heterogeneity..... | 18 |
| 3.3.1. Genetic heterogeneity..... | 19 |
| 3.3.2. Epigenetic heterogeneity | 22 |
| 3.3.3. Functional heterogeneity | 23 |
| 3.4. Aim of this work | 25 |
| 4. Material | 26 |
| 4.1. Equipment..... | 26 |
| 4.2. Substances..... | 26 |
| 4.3. Primers, enzymes, plasmids | 27 |
| 4.4. Cell lines | 29 |
| 4.5. Antibodies for flow cytometry | 29 |
| 4.6. Kits..... | 29 |
| 4.7. Software | 30 |
| 4.8. Statistics | 30 |

| | |
|--|----|
| 5. Methods | 31 |
| 5.1. Ethical issues | 31 |
| 5.1.1. Work with human material | 31 |
| 5.1.2. Work with animals..... | 31 |
| 5.2. The individualized xenograft mouse model of acute leukemia | 31 |
| 5.2.1. Expansion and purification of primary patient cells..... | 32 |
| 5.2.2. Limiting dilution transplantation assay | 32 |
| 5.2.3. Competitive transplantation assay..... | 32 |
| 5.2.4. Bioluminescence in vivo imaging..... | 33 |
| 5.2.5. In vivo therapy with dexamethasone | 33 |
| 5.2.6. Analysis of bone marrow of mice treated with dexamethasone | 34 |
| 5.3. In vitro cell culture of cell lines and PDX cells..... | 34 |
| 5.3.1. Determination of cell numbers | 34 |
| 5.3.2. Freezing and thawing of cell line cells and PDX cells..... | 34 |
| 5.3.3. In vitro cultivation of cell line cells and PDX cells..... | 35 |
| 5.3.4. Co-culture of transduced PDX cells | 35 |
| 5.3.5. Limiting dilution of RGB marked NALM-6 cell line cells | 35 |
| 5.3.6. Antibody staining of PDX cells and staining of apoptotic cells..... | 36 |
| 5.3.7. Drug stimulation in vitro..... | 36 |
| 5.4. Molecular biology..... | 37 |
| 5.4.1. Agarose gel electrophoresis of DNA..... | 37 |
| 5.4.2. DNA gel extraction..... | 37 |
| 5.4.3. Polymerase chain reaction | 37 |
| 5.4.4. Colony-PCR | 38 |
| 5.4.5. Purification of PCR products..... | 39 |
| 5.4.6. Restriction digestion of DNA | 40 |
| 5.4.7. Ligation of DNA fragments | 40 |
| 5.4.8. Plasmid miniprep and midiprep..... | 40 |

| | |
|---|----|
| 5.4.9. Isolation of genomic DNA..... | 41 |
| 5.4.10. Determination of DNA quantity and quality | 41 |
| 5.5. Genetic engineering of cell lines and PDX cells..... | 42 |
| 5.5.1. Cultivation of E. coli DH5 α cells..... | 42 |
| 5.5.2. Generation of competent cells for heat shock transformation | 42 |
| 5.5.3. Heat shock transformation of plasmid DNA into competent E. coli cells | 42 |
| 5.5.4. Lentivirus production using HEK-293T packaging cells | 42 |
| 5.5.5. Determination of virus titers | 43 |
| 5.5.6. Lentiviral transduction of cell line cells and PDX cells..... | 43 |
| 5.5.7. Flow cytometry analysis of cell line cells and PDX cells | 44 |
| 5.5.8. Sorting of RGB PDX single cell clones | 45 |
| 6. Results | 46 |
| 6.1. AL patients, the individualized xenograft mouse model of AL; genetic engineering in AL PDX cells and in vivo imaging of mice | 46 |
| 6.2. Multicolor staining using lentiviral molecular marking..... | 48 |
| 6.2.1. Cloning of RGB transfer vectors for lentivirus production | 49 |
| 6.2.2. RGB marking enabled color marking of individual cell clones | 50 |
| 6.2.3. RGB marking of PDX AL cells..... | 54 |
| 6.2.4. RGB marking uncovered clonal outgrowth upon in vivo transplantation of AML | 56 |
| 6.2.5. Clonal outgrowth aggravated upon serial transplantation in ALL-265 | 59 |
| 6.3. Limiting dilution transplantation of RGB PDX cells to generate single cell clones | 60 |
| 6.3.1. Stem cell frequencies of PDX ALL-265 and PDX AML-393..... | 60 |
| 6.3.2. Transplantation of low cell numbers delayed disease progression in recipient mice ... | 62 |
| 6.3.3. Transplantation of low cell numbers allowed isolation of specifically colored single cell clones | 62 |
| 6.3.4. Generating single cell clones of ALL-265..... | 66 |
| 6.4. Single cell clones differed in growth behavior in vivo..... | 69 |

| | |
|---|-----|
| 6.4.1. Competitive transplantation of five single cell clones uncovered divergent growth properties among clones..... | 70 |
| 6.4.2. Competitive transplantation of two single cell clones confirmed differences in growth behavior | 71 |
| 6.5. Single cell clones differed in chemosensitivity in vitro and in vivo..... | 76 |
| 6.5.1. Single cell clones differed in drug sensitivity in vitro | 77 |
| 6.5.2. Single cell clones differed in drug sensitivity in vivo | 82 |
| 7. Discussion | 86 |
| 7.1. Molecular marking of PDX cells using RGB | 86 |
| 7.2. Limiting dilution transplantation allowed visualization of selective engraftment of leukemic stem cells..... | 88 |
| 7.3. Competitive transplantation experiments revealed divergent growth behavior of clonal subpopulations..... | 90 |
| 7.4. Drug treatment of single cell clones revealed heterogeneity in drug response..... | 92 |
| 7.5. Conclusion and outlook..... | 94 |
| 8. List of tables and list of figures..... | 96 |
| 9. List of abbreviations | 98 |
| 10.References..... | 100 |
| 11.Acknowledgment..... | 110 |

1. Zusammenfassung

Akute Leukämien bestehen aus heterogenen Zellpopulationen, die sich sowohl in genetischen als auch in funktionellen Eigenschaften unterscheiden können. Letztendlich ist die jeweils aggressivste Subpopulation eines Tumors entscheidend für die Prognose und den Krankheitsverlauf des Patienten. Ein besseres Verständnis von aggressiven Subklonen sowohl bezüglich Genotyp als auch funktionellem Phänotyp ist erforderlich, um neue Angriffspunkte für Chemotherapeutika zu finden und so die Prognose und Heilungsrate von Krebspatienten zu verbessern.

Ziel der vorliegenden Arbeit war es, Einzelzellklone zu charakterisieren, um neue therapeutische Targets zu identifizieren. Dafür wurden primäre Tumorzellen von einem Mädchen mit akuter lymphatischer Leukämie (ALL) im ersten Rezidiv in immunsupprimierte Mäuse transplantiert und mit Lentiviren genetisch so modifiziert, dass sie ein rotes, ein grünes und ein blaues Fluoreszenzprotein in verschiedenen Mengen und Kombinationen exprimierten (RGB marking, (Weber et al., 2011)). Im Anschluss wurden Einzelzellklone der Leukämieprobe hergestellt, indem wenige RGB-gefärbte Xenograftzellen in Mäuse transplantiert wurden und dadurch individuell gefärbt Einzelzellen amplifiziert wurden. Die Identität der Zellen der Einzelzellklone wurde mittels LM-PCR bestätigt.

Um aggressive Subklone aufzuspüren, wurden verschiedene Klone gemischt, zusammen in Mäuse transplantiert und in vivo Proliferationsassays und Chemoresistenzassays durchgeführt. Dabei konnten die Klone mittels Durchflusszytometrie anhand ihrer unterschiedlichen molekularen Farbmarkierungen klar voneinander unterschieden werden.

Bei gemeinsamer Transplantation von Mischungen von verschiedenen Klonen zusammen in eine Maus wurden einige Klone von anderen überwachsen, was auf ein aggressives, langsames Wachstumsverhalten der überwachsenen Klone schließen lässt. Außerdem wurden zwei Klone gemeinsam in Mäuse transplantiert und diese Mäuse mit Glucocorticoiden behandelt. Dabei wies ein Klon eine erheblich geringere Sensitivität gegenüber in vivo Glucocorticoid-Behandlung in Kombination mit einem langsamen Wachstumsverhalten auf, was diesen Klon als besonders aggressiv und schwer zu behandeln identifizierte.

Zusammenfassend wurde in der vorliegenden Arbeit eine neue Methode etabliert, um aggressive Subklone sowohl hinsichtlich funktioneller Besonderheiten als auch bezüglich genetischer Merkmale zu charakterisieren, was helfen wird, neue effiziente

Behandlungsmethoden zu entwickeln, um aggressive Subklone in Zukunft besser eliminieren zu können.

2. Abstract

Acute leukemias consist of heterogeneous cell populations and the most aggressive subpopulation determines prognosis and outcome in each patient. A better understanding of challenging subclones is intensively desired, regarding both genotype and functional phenotype. New therapies are required which eradicate aggressive subpopulations in order to improve the prognosis and cure rate of patients with cancer.

Here, we aimed at characterizing single cell clones in order to find putative therapeutic targets. Primary tumor cells from a girl with acute lymphoblastic leukemia (ALL) at first relapse were transplanted into severely immunocompromised mice and lentivirally modified to express the fluorochromes red, green and blue at different amounts and combinations (RGB marking, (Weber et al., 2011)). Single cell clones were generated by limiting dilution transplantation and their uniqueness was verified by LM-PCR.

In order to identify challenging subclones, molecularly marked clone mixtures were transplanted into the same recipient mouse to perform competitive *in vivo* proliferation and drug sensitivity assays and analyzed separately by flow cytometry using their unique expression of molecular markers. In clone mixtures, certain clones were overgrown by others indicating unfavorable slow proliferation. When two clones were mixed and transplanted in groups of mice and animals were treated with glucocorticoids, one clone showed significantly reduced sensitivity against *in vivo* glucocorticoid treatment which was accompanied by slow growth, identifying this clone as especially aggressive and challenging for treatment.

Taken together, the present work established a novel approach to characterize challenging subclones regarding functional features and genetic characteristics which will help to develop efficient novel treatment approaches to eliminate aggressive cell clones in the future.

3. Introduction

Tumors consist of heterogeneous cells and the subpopulation with the most adverse characteristics determines the prognosis of cancer patients. Here, we used acute leukemia (AL) as a model disease in order to characterize unfavorable subclones in a patient's sample with the final aim to develop future therapies which eliminate unfavorable subclones for the save of cancer patients.

3.1. Acute leukemias

Acute leukemias are hematologic malignancies that are characterized by the accumulation of immature, non-functional white blood cells in the bone marrow. They can be classified according to the cell-type affected by the disease: In acute lymphoblastic leukemia (ALL) the amount of abnormal lymphocytes is increased whereas in acute myeloid leukemia (AML) myeloblasts are affected. The symptoms of these diseases, such as fever, fatigue, pallor, weight loss, bleeding and an enhanced risk of infections, are rather unspecific. They are mainly based on the accumulation of not fully developed, non-functional leukemic blasts in the bone marrow that interfere with normal hematopoiesis leading to bone marrow failure (Esparza & Sakamoto, 2005; E. H. Estey, 2014).

3.1.1. Treatment and prognosis of patients

In children, ALL occurs primarily between two and five years of age. Improved therapeutic strategies have markedly increased cure rates of pediatric ALL: in 1961, only 20% of all children diagnosed with ALL survived the disease, whereas 5-year survival rates today are above 90% (Pui & Evans, 2013). However, prognosis is still dismal in infant and adult patients. Especially relapsed disease is generally much less susceptible to treatment and associated with a poor overall survival rate. Current treatment strategies include a glucocorticoid in combination with vincristine and L-asparaginase or drugs such as anthracyclines and cytarabine (Inaba, Greaves, & Mullighan, 2013; Pui, Mullighan, Evans, & Relling, 2012).

Patients suffering from AML are mainly adults and have a 5-year survival rate of only 30 to 40%. Particularly, for elderly patients over 65 years of age, prognosis is eminently poor with survival rates of just a few months. Chemotherapy of AML patients usually includes aggressive drugs such as anthracyclines and cytarabine which are often associated with severe side-effects. This is

a problem especially for elderly patients and contributes to an increased treatment-related mortality in this group (Dohner, Paschka, & Dohner, 2015; E. Estey & Dohner, 2006).

In summary, despite improved survival rates especially for childhood ALL and for younger adults suffering from AML, prognosis for some groups of patients is still dismal, for instance for infant and adult ALL patients and for elderly AML patients. Thus, new treatment options are intensively desired in order to overcome treatment resistance and prevent relapse.

3.1.2. Minimal residual disease as hallmark of intra-tumor heterogeneity

While most tumor cells are in general sensitive to initial treatment and can be eradicated by chemotherapy, others escape and persist in the patient being a potential source of relapse.

The development of the tumor load in leukemia patients during treatment is illustrated in Figure 1. Chemotherapy reduces the amount of leukemic blasts within the patient by eradicating sensitive cells (green circle) so that complete remission is achieved in most patients. However, within some patients, few leukemic blasts that are resistant to treatment may persist after chemotherapy inducing minimal residual disease (MRD, red circles). In particular, MRD levels indicate the initial response to therapy. The existence of MRD reflects the diverse nature of cancer cells comprising tumor cells with enhanced survival properties compared to others. Therefore, the occurrence of MRD represents a hallmark of intra-tumor heterogeneity indicating that cells of the same tumor exhibit major differences regarding essential characteristics so that some cells are able to survive treatment.

MRD has further proven to be of highly prognostic value (Inaba et al., 2013; Pui & Evans, 2013). Even minute proportions of MRD cells that cannot be detected using conventional methods (“complete MRD response”) may act as source of relapsed disease. Thus, MRD detection and monitoring is important to assess treatment efficacy and to start treatment upon regrowth of resistant cells as early as possible (Bruggemann, Raff, & Kneba, 2012; Pui et al., 2012; Stow et al., 2010).

Development of cell numbers during treatment

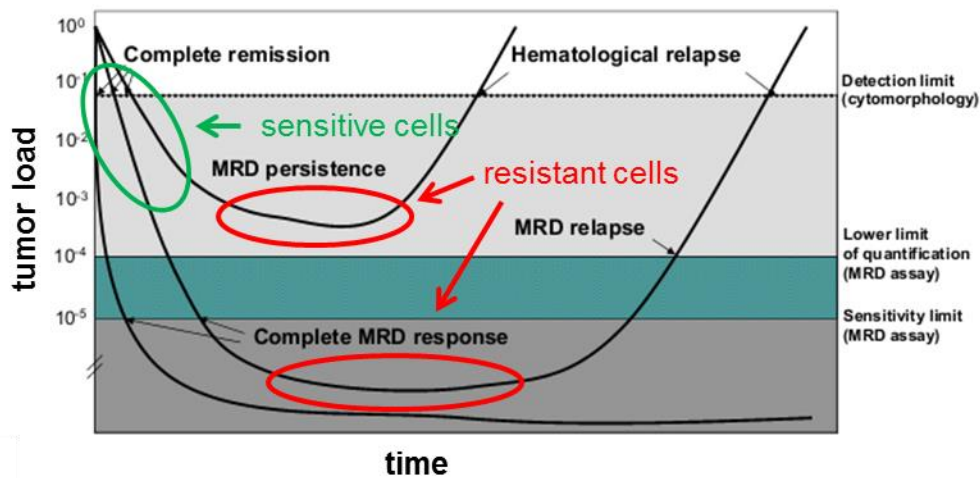


Figure 1: Functional heterogeneity of acute leukemia cells.

Tumor load (proportion of leukemic cells among healthy cells) in leukemia patients can be reduced by chemotherapy. Persistence of therapy resistant MRD cells may cause treatment-refractory relapsed disease (hematological relapse). Leukemias are composed of functionally diverse subpopulations which differ in regard to drug sensitivity so that sensitive cells (green circle) are eliminated by therapy while resistant cells (red circles) may persist and induce relapse. Adapted from (Bruggemann et al., 2012)

Permanent success of every cancer therapy is based on the elimination of as many tumor cells as possible in order to prevent relapse and consider the patient as cured. However, relapse occurs quite frequently and, in many cases, is caused by few cells that survived chemotherapy. Considering that most patients suffering from relapsed cancer finally succumb to the disease, a better understanding of the adverse clones of persistent, treatment-refractory disease during MRD is urgently needed.

3.1.3. Acute leukemia as suitable model disease to study clonal heterogeneity

Intra-tumor heterogeneity including subclones which differ in important features demonstrates the need of studying clonal heterogeneity by investigating the differences between single clones of the tumor. However, subclonal heterogeneity cannot be assessed in in vitro systems using cell line cells because cell lines do not represent the clonal composition existing in the original patient sample. In particular, cell lines may have changed clonal composition during the process of immortalization and extensive in vitro passaging. Therefore, suitable model systems are required which mimic the situation in the patient in the best possible manner.

In this context, leukemia represents a suitable model disease to study clonal heterogeneity since the individualized xenograft mouse model of acute leukemia allows amplification of primary patient cells derived from acute leukemia patients (Kamel-Reid et al., 1989; Lee, Bachmann, & Lock, 2007; Liem et al., 2004; Terziyska et al., 2012; Vick et al., 2015). Engrafting primary cells from leukemia patients in severely immunocompromised NSG mice lacking T-cells, B-cells and functional natural killer cells, allows stable engraftment and propagation of patient-derived xenograft (PDX) cells (Jacoby, Chien, & Fry, 2014; Schmitz et al., 2011; Shultz, Ishikawa, & Greiner, 2007; Shultz, Pearson, et al., 2007). Orthotopic disease distribution involving the leukemia-typical organs bone marrow, spleen, liver and blood enables a clinic-close modeling of acute leukemia in contrast to many xenograft models of solid tumors so that adverse clones relying on different niches throughout the body find their required environment. Xenograft samples are more closely related to the original patient's leukemia and reproduce the heterogeneity of ALL and AML. For this reason, patients' acute leukemia cells studied in the xenograft mouse model represent an especially suitable model for studying questions on clonal distribution of tumors in general.

3.2. Adverse characteristics of tumor cells

As described in 3.1.2, the existence of MRD represents a hallmark of intra-tumor heterogeneity suggesting that some cells exhibit features that are associated with a survival benefit. In detail, important unfavorable characteristics of tumor cells are quiescence, drug resistance and stemness rendering tumor cells difficult to eliminate. Since elimination of all tumor cells is the ultimate goal of therapy in order to cure the patient and prevent relapse, studies to further explore these features are of utmost importance.

3.2.1. Quiescence

Therapeutic failure may be related to persistence of tumor cells existing in an inactive, quiescent state. Eradication of inactive, non-cycling tumor cells is particularly challenging because many conventionally used therapeutic agents are developed to kill cycling cells and therefore do not eradicate resting, non-proliferating cells, for instance antimetabolites like cytarabine. Antimetabolites are incorporated into DNA instead of normal purine and pyrimidine bases and inhibit DNA polymerase causing chain termination (Galmarini, Mackey, & Dumontet, 2001). As a consequence, non-cycling tumor cells may be protected from eradication by cytotoxic drugs. Therapy-refractory, dormant cells may be able to survive for many years after treatment and be

responsible for relapse even after a long time (Clevers, 2011; Dick, 2008; Greaves, 2013). Therefore, new therapy concepts aim at targeting quiescent tumor cells by interrupting their dormancy and bringing them back to cycle (Saito et al., 2010).

Notably, quiescence is a feature of cancer stem cells (CSCs, described in 3.2.3) which represents a challenge for cancer therapy since only CSCs maintain the tumor and, in theory, one single, surviving CSC should be enough to give rise to a whole tumor again.

3.2.2. Drug resistance

Another reason for treatment failure is caused by the emergence of resistant cells which are not eradicated by therapeutic drugs and may cause relapse in patients upon regrowth.

The mechanisms leading to drug resistant variants are still poorly understood. Acquired genetic alterations may impair sensitivity of tumor cells towards drugs. In addition, chemotherapy may select for resistant cells leading to a more aggressive, drug resistant tumor or induce alterations conferring drug resistance. For instance, resistance towards glucocorticoids (GCs) is a major problem in the treatment of childhood ALL and the mechanisms leading to GC resistance are still unclear. In this context, GC resistance represents an important prognostic marker so that patients with a poor response to initial GC treatment have, in general, a worse prognosis compared to good responders (Bhadri, Trahair, & Lock, 2012; Inaba & Pui, 2010).

As described in 3.2.1, drug resistance may be associated with dormancy of tumor cells since it is challenging to target and eliminate cells that do not actively cycle because many conventional drugs interfere with the cell cycle. Besides, cells might be protected against chemotherapeutic agents by the surrounding environment where therapeutic agents cannot reach them or have impaired activity due to micro-environmental conditions (Ishikawa et al., 2007; Shlush et al., 2012).

Considering that relapsed disease is associated with a poor prognosis, eradication of drug resistant cells is a major issue for therapy of cancer patients.

3.2.3. Stemness

Ultimately, stemness has to be considered as an adverse characteristic of cancer cells. Stem cells may exist in an inactive, dormant state and consequently be drug resistant as described in 3.2.1 and 3.2.2.

According to the cancer stem cell model, tumors are heterogeneous regarding growth capacities and a small rare subpopulation exists of cancer stem cells. CSCs maintain the tumor while non-CSCs do not contribute to disease propagation, because only CSCs have the capacity to self-renew. CSCs can in turn divide into CSCs and non-CSCs (Clevers, 2011; Dick, 2008; Magee, Piskounova, & Morrison, 2012). CSCs might be diverse regarding their genotype and their phenotype. Accordingly, subclones originating from different CSCs within one tumor might be heterogeneous in terms of genetic and phenotypic features as well. Survival benefit is only profitable for the tumor if it takes place in a tumor stem cell. Only then the survival advantages are passed on to daughter CSCs and will be stably present in the tumor. In contrast, as non-CSCs do not propagate the tumor, survival benefit in those cells is only temporary (Clevers, 2011; Greaves, 2013; Kreso & Dick, 2014; Magee et al., 2012). If only a subfraction of the tumor is able to propagate the disease, elimination of these cells is sufficient for the eradication of the whole tumor. It is thus not necessary to eliminate extensive numbers of non-CSCs as they cannot permanently maintain the tumor. Therapies that target only non-tumorigenic non-CSCs lead to relapse when CSCs regrow. Consequently, eradication of CSCs should be the goal of every cancer therapy (Dick, 2008; Eppert et al., 2011; Shackleton, Quintana, Fearon, & Morrison, 2009; Wang, 2007).

Leukemia cells that have the capacity to give rise to leukemia upon xenotransplantation are termed leukemia initiating cells or leukemic stem cells (LSCs) (Bonnet & Dick, 1997; Lapidot et al., 1994). Accordingly, LSCs are leukemic blasts which are capable of generating a xenograft in immunocompromised mice upon serial transplantation (Hope, Jin, & Dick, 2004). Like all CSCs, LSCs do also create non-LSCs that are incapable of tumor propagation upon serial transplantation (Clarke et al., 2006; Kreso & Dick, 2014). As leukemia growth is driven by LSCs, each therapy should aim at eradicating LSCs, respectively (Guzman & Allan, 2014). Each subclone within one patient's leukemia originates from a different LSC and subclonal heterogeneity in leukemia is consequently based on the diversity of LSCs.

At present, the gold standard assay to experimentally quantify cancer stem cells and their ability to self-renew is the xenograft assay (Hope et al., 2004; Lapidot et al., 1994). Stem cell frequencies in cancer samples can be estimated by transplanting limiting amounts of tumor cells into groups of immunocompromised mice. CSC frequencies can subsequently be calculated according to the number of engrafted mice upon injection of specific cell numbers. However, it has to be considered that tumor initiating potential of CSCs may be hampered by stress due to experimental settings and therefore CSC frequencies may be underestimated (Clarke et al., 2006; Clevers, 2011).

Cancers were believed to be composed of a large mass of non-tumorigenic cells that are sustained by only a small subgroup of cancer stem cells with the ability to self-renew. However, it has been shown that CSCs do not necessarily need to be a minor part of the tumor mass. In some ALLs for example, LSCs are quite frequent (Kelly, Dakic, Adams, Nutt, & Strasser, 2007). Additionally, recent studies demonstrated that stem cell frequencies vary with respect to different cancer types: LSC frequencies in AML are generally rather low, whereas leukemia propagating activity in ALL is typically pretty high (Eppert et al., 2011; Rehe et al., 2013; Sarry et al., 2011; Shackleton et al., 2009).

Taken together, quiescence, drug resistance and stemness represent adverse characteristics of tumor cells which may induce therapy failure.

3.3. Intra-tumor heterogeneity

Tumors are composed of heterogeneous cellular subpopulations which may differ in respect to genetic and epigenetic characteristics and in essential functional features such as growth behavior, drug resistance, self-renewal and other hallmarks of cancer (Hanahan & Weinberg, 2011; Marusyk, Almendro, & Polyak, 2012). The presence of multiple subpopulations within one tumor and their diversity regarding genotype and functional phenotype makes the tumor less susceptible to cancer treatment. The intra-tumor heterogeneity provides a survival advantage for the tumor as evolution can continue from diverse subclones. Therefore, an efficient chemotherapy is challenging as it has to be directed against diverse subclones at the same time and relapse may still be initiated by a small amount of surviving cells. Hence, the most aggressive subpopulation will ultimately define the patient's prognosis. Cancer therapy should therefore specifically aim at eradicating all subpopulations in order to prevent relapse.

In 1976, Nowell developed the "clonal evolution concept" which was the cornerstone for considering cancer as a Darwinian evolutionary process (Nowell, 1976). According to his model, tumor progression is a dynamic process, meaning that subclonal architecture of tumors changes over time. Selective pressure induces the emergence of divergent subclones with different characteristics. In addition, chemotherapy may select for resistant subpopulations and thus contribute to a more aggressive disease (Choi et al., 2007). Moreover, mutagenic chemotherapy might even induce occurrence of drug resistance by inducing genetic alterations that lead to drug resistance (Landau, Carter, Getz, & Wu, 2014). Likewise, single cells that have acquired resistance to therapeutic drugs induce a treatment-refractory disease so that drugs that were effective at the beginning will be inefficient after some time (Almendro, Marusyk, & Polyak,

2013; Gerlinger et al., 2014; Swanton, 2012). The cause for phenotypic evolution towards more aggressive cancer cells might be associated with changes in their genotype that yield a survival benefit (Barber, Davies, & Gerlinger, 2014; Meacham & Morrison, 2013; Yates & Campbell, 2012). As a consequence, clones that exhibit superior characteristics will outcompete less fit clones over time (Burrell, McGranahan, Bartek, & Swanton, 2013; Greaves & Maley, 2012).

Future cancer therapies should therefore aim at targeting all subclones within the tumor of each patient as its efficiency relies on the capacity to eliminate the last, most aggressive subclone.

3.3.1. Genetic heterogeneity

Genomic profiling based on recent advances in sequencing technologies has uncovered substantial genetic complexity within one tumor (Burrell et al., 2013; Greaves & Maley, 2012). Tumors consist of various genetically distinct subpopulations which can be related to each other in a complex architecture (Ding et al., 2012; Greaves, 2010). Different approaches of single cell sequencing technologies have revealed further insights into the genomic architecture of leukemia on the single cell level. Genetic analysis of many single cells of one patient's leukemia allows detection of cell-specific genetic aberrations. The occurrence of specific alterations may be used to track individual subpopulations and to estimate the number of genetic subclones within one tumor (Jan & Majeti, 2013; Klco et al., 2014). Moreover, clonal relationships can be reconstructed due to shared alterations of genetic subclones (Anderson et al., 2011; Gawad, Koh, & Quake, 2014; Saadatpour, Guo, Orkin, & Yuan, 2014; Shlush et al., 2012). Anderson and colleagues analyzed single cells of individual patients suffering from ETV6-RUNX1 positive ALL by fluorescence in situ hybridization. They have discovered a pronounced subclonal genetic heterogeneity of leukemic blasts following a complex architecture (Anderson et al., 2011). The type and amount of genetic lesions enabled the visualization of complex relationships between single clones. They observed that mutations occurred randomly and independently from each other. Hence, some ALLs consisted of only few subclones but, more often, they could detect up to ten subclones related to each other (Figure 2).

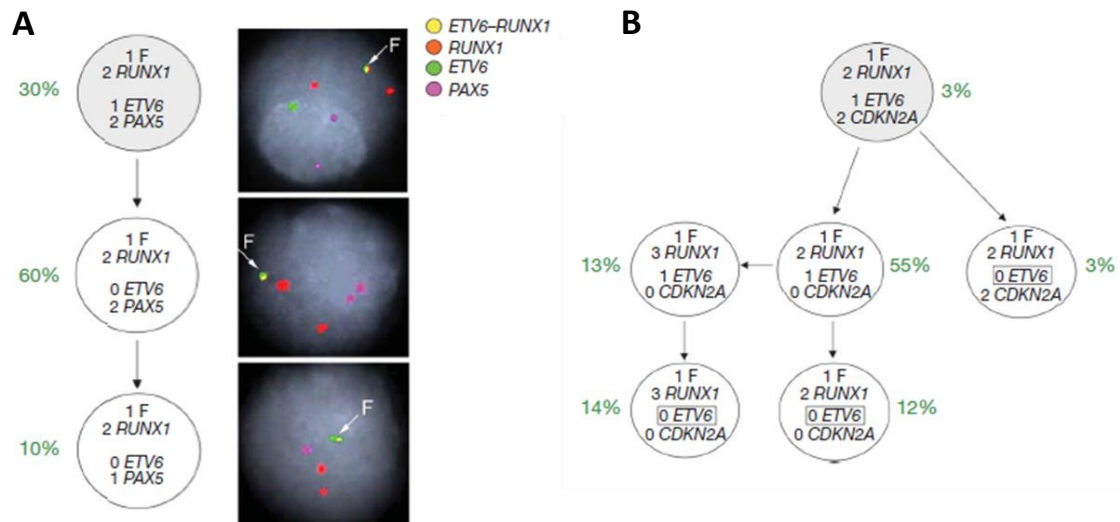


Figure 2: Subclonal architecture in ALL is complex.

Multiplex fluorescence in situ hybridization (FISH) analysis of ETV6-RUNX1 positive ALL revealed diverse subclonal architecture. According to individual genetic alterations, the relationship of subclones can be assessed. (A) ALL consisting of three clones which can be aligned in a linear architecture based on different genetic alterations (loss of the untranslocated ETV6 allele and PAX5 allele) detected by FISH as shown on the right. (B) More complex architecture with six clones. Three subclones lost the untranslocated ETV6 allele (boxes) independently from each other. yellow signal (F): ETV6-RUNX1 fusion gene; red signals: RUNX1 (one large and one small signal resulting from one normal RUNX1 allele and the residue from the translocation); green signal: untranslocated ETV6 allele; pink signal: PAX5. Adapted from (Anderson et al., 2011).

In addition, genomic profiling showed that some pathways are commonly altered in ALL (Kuiper et al., 2007; Mullighan, 2012; Mullighan et al., 2011; Zhang et al., 2011). Changes in genotype might be associated with changes in functional phenotype. Therefore, a better understanding of how genotype and phenotype relate to each other would offer the possibility to develop novel agents that specifically target mutated pathways (Pui et al., 2012; Roberts & Mullighan, 2015).

Subclones may be defined by their individual mutations. Hence, genetic aberrations could be used as markers to trace single clones in order to investigate clonal evolution from diagnosis to relapse (Jan & Majeti, 2013). Recent studies in AML (Ding et al., 2012; Kronke et al., 2013; Parkin et al., 2013) and ALL (Anderson et al., 2011; Ma et al., 2015; Mullighan et al., 2008; van Delft et al., 2011) have explored the evolutionary trajectory from diagnosis to relapse by comparing the subclonal architecture of diagnosis and corresponding relapse samples. These studies have shown that subclonal diversity changed from diagnosis to relapse suggesting that some clones had a functional survival advantage which might be based on the acquisition of additional

mutations that contributed to drug resistance. Some pathways were observed to be frequently mutated in the relapse clone, for instance cell cycle regulation and B-cell development (Ma et al., 2015; Mullighan et al., 2008; Mullighan et al., 2011; van Delft et al., 2011). These studies have revealed that diagnosis and relapse samples were genetically related to each other in the majority of all cases suggesting clonal evolution from diagnosis to relapse or a common ancestral clone. Besides, the relapse clone was frequently present already at diagnosis as a minor subclone, strengthening the idea that additional mutations may confer resistance to therapy. Only in a minority of the cases (6%), the relapse clone was genetically not related to diagnosis (Figure 3).

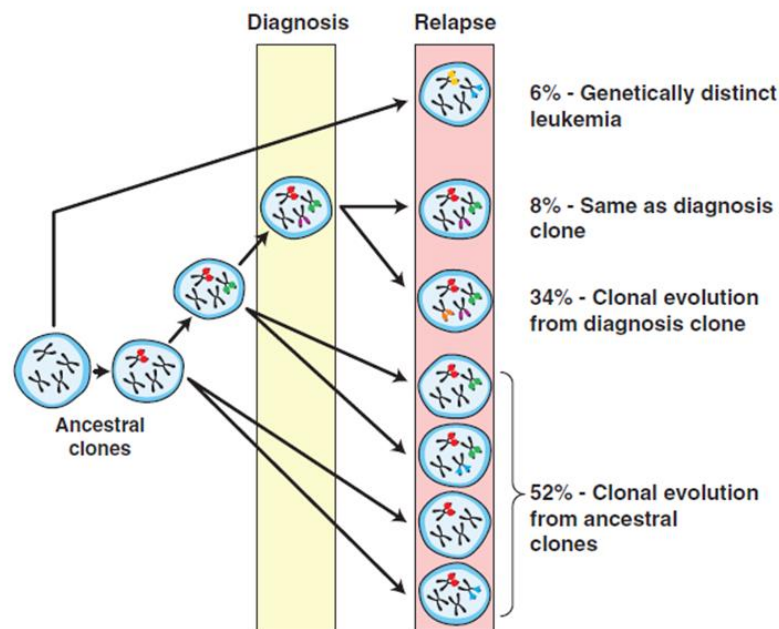


Figure 3: Relationship of diagnosis and relapse samples in ALL.

In most cases, relapse ALL is genetically related to the diagnosis sample either originating from an ancestral pre-leukemic clone or from the diagnosis clone. Only in a minority of all cases, relapse is a genetically unrelated leukemia (6%). In general, the relapse clone has acquired additional mutations compared to the diagnosis clone. However, in many cases, the relapse clone is already present as a minority in the diagnosis sample. Adapted from (Mullighan et al., 2008).

Remarkably, some studies have demonstrated that in general, more alterations could be detected at relapse compared to diagnosis proposing that mutagenic chemotherapy triggered DNA damage or additional spontaneously acquired mutations caused a survival benefit for the

respective cell population (Ding et al., 2012; Kronke et al., 2013; Mullighan et al., 2008; Shlush et al., 2012).

In this regard, cytogenetic analyses are part of clinical routine diagnostic in AML and ALL and the prognostic value of chromosomal abnormalities is known since many years (Harrison, 2009; Secker-Walker, Lawler, & Hardisty, 1978; Williams et al., 1984).

Individual genetic lesions may serve as potential targets for individualized therapies and allow a risk-adapted treatment of each patient according to specific genetic abnormalities (Downing et al., 2012; Hogan et al., 2011; Mullighan, 2012; Patel et al., 2012; Schlenk & Dohner, 2013). The use of tyrosine kinase inhibitors for the treatment of BCR-ABL positive leukemia for instance, has eminently improved survival rates in this group of patients (Pui, Carroll, Meshinchi, & Arceci, 2011). Since the use of chemotherapeutic drugs is often limited by their toxicity and side-effects, targeted therapies are desperately needed in order to reduce chemotherapy related mortality and increase life quality of the patients. Novel treatment strategies should be based on the individual genetic alterations of each patient's leukemia in order to eradicate all subpopulations present at diagnosis and to prevent relapse (Bhatla et al., 2014; Evans, Crews, & Pui, 2013). Besides, targeting of single resistance mechanisms might not be sufficient to reliably eliminate resistant subclones since cells might acquire resistance via various pathways simultaneously. Therefore, combination therapies consisting of several drugs targeting different lesions may be required in order to circumvent these resistance mechanisms (Aparicio & Caldas, 2013; Burrell & Swanton, 2014; Garraway & Janne, 2012; Roberts & Mullighan, 2015).

3.3.2. Epigenetic heterogeneity

Very recent studies have shown that epigenetic heterogeneity based on epigenetic instability of CSCs has to be taken into account as well. Subclones with the same genotype may still differ on the epigenetic level (Landau et al., 2014; Swanton & Beck, 2014). Specific leukemia subtypes may be defined by an individual epigenetic signature, for instance an increased global promoter hypermethylation (Figueroa et al., 2013; Figueroa et al., 2010; Schafer et al., 2010). Epigenetic modifications, such as differences in DNA methylation are accompanied by changes in gene expression: hypermethylation of cytosine rich regions in promoters mediates gene silencing in cancer cells whereas hypomethylation induces gene transcription (Berdasco & Esteller, 2010). Epigenetic changes may also be the reason for differences regarding functional features like proliferation rates or drug sensitivity (Figueroa et al., 2013; Figueroa et al., 2010). Thus, methylation of gene promoters directly influences gene expression levels and some genes are

recurrently found to be abnormally methylated in ALL and AML (Dawson & Kouzarides, 2012; Roberts & Mullighan, 2015). Accordingly, epigenetic mutations provide novel targets for personalized epigenetic therapies: 5-Azacitidine for example, an inhibitor of DNA methyltransferases was the first epigenetic drug in clinical use for treatment of leukemia patients (Bullinger & Armstrong, 2010; Geng et al., 2012; Mehdipour, Santoro, & Minucci, 2014; Yang, Lay, Han, & Jones, 2010).

3.3.3. Functional heterogeneity

In order to clearly define LSCs and to distinguish them from non-LSCs, extensive effort was put into characterizing LSCs phenotypically since expression of particular cell surface markers on LSCs would facilitate targeted therapies against LSCs. Earlier studies in AML demonstrated that LSCs, according to normal hematopoietic stem cells, were defined by expression of CD34 and CD38: the LSC phenotype was primarily found in CD34⁺CD38⁻ cells (Bonnet & Dick, 1997; Lapidot et al., 1994). However, subsequent studies have revealed that LSCs in AML have a more heterogeneous phenotype. They are not restricted to the CD34⁺CD38⁻ compartment, but can also be found in other compartments (Eppert et al., 2011; Sarry et al., 2011; Taussig et al., 2008; Taussig et al., 2010). Concordantly, no phenotypic marker exists to exactly define LSCs in ALL either. Definition of LSCs via cell surface markers is thus misleading because none of their markers are uniquely expressed by stem cells. Further studies have proven that leukemogenic activity can be enriched in subsets with particular phenotypic markers but is nevertheless not strictly defined by a definite immunophenotype (Anderson et al., 2011; Chiu, Jiang, & Dick, 2010; Klco et al., 2014; le Viseur et al., 2008; Notta et al., 2011; Rehe et al., 2013). In summary, this indicates that despite the increased expression of some markers on LSCs, targeted therapies against particular cell surface markers might not be sufficient as no marker is exclusively expressed by LSCs.

Diversity of leukemic stem cells regarding functional features such as self-renewal ability, growth behavior, apoptosis, response to therapy, and other hallmarks of cancer is a major problem for treatment (Hope et al., 2004; Kreso & Dick, 2014). Since every subclone originates from a different LSC, each patient's leukemia is composed of functionally heterogeneous subclones. Accordingly, clones with favorable growth properties will outcompete clones with dismal growth behavior over time. In contrast, clones that are less susceptible to treatment will overgrow sensitive clones during therapy. Importantly, clonal evolution during disease progression can emerge from diverse subpopulations, which makes leukemia difficult to treat.

Until now, the knowledge about the differences between resistant and sensitive cells is still fragmentary. In order to prevent relapse, a better understanding of the underlying mechanisms which cause functional phenotypes that, for instance, enable resistance towards chemotherapy is urgently needed. Thus, eradication of all relevant subpopulations present at diagnosis should be the goal for every cancer therapy in order to prevent relapse sustained by the regrowth of resistant cells showing advantageous survival properties leading to a treatment-refractory disease.

Taken together, acute leukemias are heterogeneous diseases which involve diverse subpopulations with distinct survival properties. Intra-tumor heterogeneity acts as a reservoir for relapse clones providing genetically and functionally diverse subpopulations which help the tumor to adapt. Genetic and epigenetic variations may be linked with changes in phenotype and function providing a survival benefit. However it is still unclear which genetic changes are associated with which functional features (Klco et al., 2014; Kreso & Dick, 2014; Meacham & Morrison, 2013). Hence, possible connections between genotype and functional phenotype have to be further investigated in order to develop novel drugs that specifically target challenging subpopulations.

3.4. Aim of this work

Despite improved treatment regimens for acute leukemia patients, survival rates still need to be improved. Particularly, patients suffering from relapsed disease have an extremely poor prognosis. Acute leukemias consist of heterogeneous cell populations and the most aggressive subpopulation determines prognosis and outcome in each patient. Thus, new therapies that eliminate all relevant subpopulations are urgently needed in order to cure the patient and prevent relapse. A better characterization of challenging subclones would help to find new targets for the eradication of treatment refractory subpopulations. Clonal evolution within one tumor can originate from divergent subclones which might differ regarding genotype and functional phenotype. In this regard, therapy is challenging as it should be directed against diverse subpopulations at the same time in order to eliminate all tumor cells. A better understanding of the biology of subclones with an aggressive phenotype is required to develop novel treatments that specifically target these challenging clones.

Many studies have proven clonal heterogeneity of leukemias regarding their genotype, while clinic courses of patients, especially residual disease after treatment, suggest functional heterogeneity within a single tumor. Due to technical limitations, it remains unclear which genetic characteristics cause which functional phenotypes in tumor subclones.

The present study aimed at establishing a method for studying single cell clones regarding functional phenotype *in vivo* in order to identify clones with unfavorable functional characteristics in an exemplary sample of a child with relapsed acute lymphoblastic leukemia.

A better understanding of the genetic background of these clones may help to identify new targets for future therapy in order to develop efficient novel treatment approaches to eliminate aggressive cell clones in ALL. The present work envisions eliminating aggressive subclones to increase prognosis and cure rate of patients with cancer.

4. Material

4.1. Equipment

| | |
|--------------------------|--|
| Incubator (bacteria) | B 6060 microbiological incubator, Heraeus, Hanau, Germany |
| Flow cytometry | BD LSRFortessa, BD Bioscience, Heidelberg, Germany |
| Cell sorting | BD FACSAriaIII, BD Bioscience, Heidelberg, Germany |
| Incubator (cell culture) | Hera Cell, Heraeus, Hanau, Germany |
| Light microscopy | Carl Zeiss 550 1317, Zeiss, Jena, Germany |
| Fluorescence microscopy | Carl Zeiss Axioplan, Zeiss, Jena, Germany |
| PCR machine | Primus 25 advanced Thermocycler, PeqLab, Erlangen, Germany |
| Gel documentation | E-BOX VX5, Vilbert Lourmat, Eberhardzelle, Germany |
| Nanophotometer | Nanodrop 2000, Thermo Fischer Scientific, Waltham, MA, USA |
| In vivo Imaging | IVIS Lumina II Imaging System, Caliper Life Sciences, Mainz, Germany |

4.2. Substances

| | |
|------------------------|---|
| Agarose | Biozym Scientific GmbH, Hessisch Oldendorf, Germany |
| Ampicillin solution | 25 mg / ml, sterile filtered, Sigma-Aldrich, St. Louis, MO, USA |
| α -Thioglycerol | Sigma-Aldrich, St. Louis, MO, USA |
| Coelenterazine | Synchem OHG, Felsberg, Germany |
| DAPI (1 mg / ml) | Sigma-Aldrich, St. Louis, MO, USA |
| DMEM | cell culture medium, Gibco, San Diego, CA, USA |
| DMSO | Sigma-Aldrich, St. Louis, MO USA |
| DNA Ladder Mix | Thermo Fischer Scientific, Waltham, MA, USA |
| DNA-loading dye6x | Thermo Fischer Scientific, Waltham, MA, USA |
| dNTP mix | Thermo Fischer Scientific, Waltham, MA, USA |
| Ethidium Bromide | Carl Roth, Karlsruhe, Germany |
| FCS | fetal calf serum, Biochrome, Berlin, Germany |
| Ficoll | GE Healthcare, Freiburg, Germany |

| | |
|----------------|--|
| HBG buffer | HEPES-buffered glucose containing 20 mM HEPES at pH 7.1, 5% glucose w / v |
| ITS | Insulin-Transferrin-Selenium, Gibco, San Diego, CA, USA |
| LB medium | 10 g tryptone, 5 g yeast extract, 5 g NaCl ad 1 l H ₂ O, (1 ml Ampicillin, 25 mg / ml), autoclaved |
| LB agar | 15 g / l agar in 1 l LB medium, autoclaved, 800 µl ampicillin solution were added before pouring into petridishes |
| Patient medium | RPMI-1640 supplemented with 20% FCS, 1% pen/strep, 1% gentamycin and 2 mM glutamine |
| PBS (1x) | 8 g NaCl, 0.2 g KaCl, 1.42 g Na ₂ HPO ₄ , ad 1 l H ₂ O |
| Pen/Strep | Penicillin-Streptomycin 5000 U / ml, Gibco, San Diego, CA, USA |
| Polybrene | 2 mg / ml, Sigma-Aldrich, St. Louis, MO, USA |
| RPMI-1640 | cell culture medium, Gibco, San Diego, CA, USA |
| Sodim pyruvat | 100 mM, Sigma-Aldrich, St. Louis, MO, USA |
| TAE-Buffer | 1.8 g Tris / HCl, 1.14 ml acetic acid, 0.7 g EDTA, ad 1 l H ₂ O (pH 8.5) |
| Trypsin (1x) | 0.5% Trypsin-EDTA, Invitrogen, Karlsruhe, Germany |
| TFB I | 1.491 g 100 mM KCl, 0.294 g 10 mM CaCl ₂ , 0.588 g 30 mM K-acetate, 1.979 g 50 mM MnCl ₂ , 30.6 g 15% glycerol; pH 5.8, sterile filtered |
| TFB II | 0.074 g 10 mM KCl, 1.102 g 75 mM CaCl ₂ , 0.209 g 10 mM MOPS, 15.3 g 15% glycerol; pH 7.0, sterile filtered |
| TurboFect | Tansfection Reagent, Thermo Fischer Scientific, Waltham, MA, USA |

4.3. Primers, enzymes, plasmids

Table 1: Primers.

| Number | Sequence | Application | T _m (°C) |
|--------|-----------------------------------|--|---------------------|
| 305 | CCAATGCATATGGTGAGCAAGGGCGAG | Amplification of mCherry, Venus, mtagBFP FWR | 65.5 |
| 306 | ACGCGTCGACTTACTTGTACAGCTCGTCCATGC | Amplification of mCherry, Venus, mtagBFP REV | 66.5 |

Table 2: Enzymes.

| Enzyme | Application | Manufacturer |
|------------------|--------------------|---|
| GoTaq Polymerase | Colony PCR | Promega, Madison, WI, USA |
| Pfu Polymerase | PCR | Thermo Fischer Scientific, Waltham, MA, USA |
| T4 DNA Ligase | Ligation | Thermo Fischer Scientific, Waltham, MA, USA |
| Sall | Restriction digest | New England Biolabs, Frankfurt am Main, Germany |
| Nsil | Restriction digest | New England Biolabs, Frankfurt am Main, Germany |
| BamHI | Restriction digest | New England Biolabs, Frankfurt am Main, Germany |

Table 3: Plasmids.

| Plasmid | Manufacturer | Size (bp) |
|--|---|-----------|
| pRSV-Rev (392) | Addgene, Cambridge, MA, USA | 4174 |
| pMDLg/pRRE (393) | Addgene, Cambridge, MA, USA | 8895 |
| pMD2.G | Addgene, Cambridge, MA, USA | 5824 |
| pCDH-EF1 α -extGLuc-T2A-copGFP | Research Group Apoptosis (Terziyska et al., 2012) | 8053 |
| pSicoR-U6-EF1 α -mCherry | Addgene, Cambridge, MA, USA | 7484 |
| pRRL-PPT-SFFV-Venus | Provided by Tim Schroeder | 7304 |
| pmTagBFP-C1 | Provided by Michael Schindler | 4750 |
| pCDH-EF1 α -MCS-T2A-copGFP | System Bioscience, CA, USA | 7253 |
| pCDH-EF1 α -extGLuc-T2A-mCherry | Cloned by Michela Carlet | 7993 |
| pCDH-EF1 α -extGLuc-T2A-Venus | Cloned by Michela Carlet | 8002 |
| pCDH-EF1 α -extGLuc-T2A-mTagBFP | Cloned by Michela Carlet | 7984 |
| pCDH-EF1 α -mCherry | Cloned for this study | 7193 |
| pCDH-EF1 α -Venus | Cloned for this study | 7002 |
| pCDH-EF1 α -mTagBFP | Cloned for this study | 7184 |

4.4. Cell lines

All cell lines indicated below were tested negative for mycoplasma infection.

Table 4: Cell lines.

| Cell line | Source | Use |
|-----------|-----------------------------|---|
| HEK-293T | DSMZ, Braunschweig, Germany | Packaging cell line for lentiviral particles |
| NALM-6 | DSMZ, Braunschweig, Germany | Used to establish RGB marking |
| EL08 | DSMZ, Braunschweig, Germany | Feeder cell line for in vitro culture of transduced PDX cells |

4.5. Antibodies for flow cytometry

Table 5: Antibodies.

| Name | Manufacturer |
|--|------------------------------------|
| APC-Cy7 anti-mouse CD45 (30-F11) (rat) | Biolegend, San Diego, CA, USA |
| APC anti-Annexin V | BD Bioscience, Heidelberg, Germany |

4.6. Kits

Table 6: Commercial kits.

| Name | Application | Manufacturer |
|---------------------------------------|---|------------------------------------|
| Annexin V APC Apoptosis Detection Kit | Staining of apoptotic cells | BD Bioscience, Heidelberg, Germany |
| NucleoSpin Gel and PCR Clean-up | Purification of PCR products, extraction of DNA from agarose gels | Macherey Nagel, Duren, Germany |
| NucleoSpin Plasmid EasyPure | Isolation of plasmid DNA (mini) | Macherey Nagel, Duren, Germany |
| NucleoBond Xtra Midi | Isolation of plasmid DNA (midi) | Macherey Nagel, Duren, Germany |
| QIAamp DNA Mini Kit | Isolation of genomic DNA | Qiagen, Venlo, NL |

4.7. Software

Microsoft Office

Adobe Photoshop CS3

Axio Vision Zeiss

Clone Manager 7

FlowJo V10

GraphPad Prism 6

Living Image software 4.4

4.8. Statistics

Two-tailed unpaired t-test was applied to determine the significance of differences in specific apoptosis rates upon drug testing between single cell clones. F-test was applied to compare variances and in cases in which variances differed significantly, Welch's correction was employed. All statistical analyses were calculated using GraphPad Prism 6 software.

5. Methods

5.1. Ethical issues

5.1.1. Work with human material

Fresh bone marrow or peripheral blood samples from adult AML patients were obtained from the Department of Internal Medicine III, Ludwig-Maximilians-Universität, Munich. Specimens were collected for diagnostic purposes before start of treatment. Written informed consent was obtained from the patients. The study was performed in accordance with the ethical standards of the responsible committee on human experimentation (written approval by Ethikkommission des Klinikums der Ludwig-Maximilians-Universität, Munich, number 068-08) and with the Helsinki Declaration of 1975, as revised in 2000.

5.1.2. Work with animals

NSG (NOD/scid, IL2 receptor gamma chain knockout) mice from The Jackson Laboratory (Lund, Sweden) were maintained under specific pathogen-free conditions in the research animal facility of the Helmholtz Zentrum München. Animals had free access to food and water, and were housed with a 12-hour light-dark cycle and constant temperature. All animal trials were performed in accordance with the current ethical standards of the official committee on animal experimentation (written approval by Regierung von Oberbayern, number 55.2-1-54-2532-95-10). When clinical signs of illness became apparent (more than 60% leukemic cells within peripheral blood, rough fur, hunchback, or reduced motility), mice were sacrificed equally in all passages. If leukemia became not apparent, mice were killed and analyzed 25 weeks after cell injection by latest.

5.2. The individualized xenograft mouse model of acute leukemia

We amplified cells from acute leukemia patients in immunocompromised NSG (NOD/scid, IL2 receptor gamma chain knockout) mice from The Jackson Laboratory (Lund, Sweden) using the individualized xenograft mouse model as established in the lab (Kamel-Reid et al., 1989; Lee et al., 2007; Liem et al., 2004; Terziyska et al., 2012; Vick et al., 2015).

5.2.1. Expansion and purification of primary patient cells

To amplify leukemic blasts from acute leukemia patients, peripheral blood or bone marrow aspirates were injected into 6 to 8 weeks old NSG mice via the tail vein (in 250 µl autoclaved and sterile filtered PBS). After injection, mice were treated with ciprofloxacin which was added to the drinking water in order to prevent infections. For expansion of PDX cells, freshly thawed PDX cells were injected into the tail vein of NSG mice (in 250 µl autoclaved and sterile filtered PBS). All animals were maintained under specific pathogen-free conditions in the research animal facility of the Helmholtz Zentrum München. Mice were sacrificed when blood measurement indicated leukemia disease or as soon as they showed any clinical signs of illness and human cells were isolated out of spleen or bone marrow subsequently. The spleen was homogenized through a 70 µm cell strainer and cells were purified using Ficoll gradient centrifugation (400 g, 30 min, rt, without rotor brake). After centrifugation, mononuclear cells could be harvested as a layer at the interphase. Cells were washed twice with PBS and once with patient medium (RPMI supplemented with 20% FCS, 1% pen/strep, 1% gentamycin and 2 mM glutamine) (400 g, 10 min, rt). After washing, cells were re-suspended in patient medium and stored at 37 °C for further use. Isolated bones were crushed in a porcelain mortar and suspended in PBS. The suspension was filtered through a 70 µm cell strainer and washed twice with PBS. Cells were re-suspended in patient medium and stored at 37 °C, respectively. Accuracy of sample identity was verified by repetitive finger printing using PCR of mitochondrial DNA (Hutter et al., 2004).

5.2.2. Limiting dilution transplantation assay

For limiting dilution transplantation assays (LDA), fresh cells of the RGB ALL-265 sample or freshly thawed cells of the RGB AML-393 sample were counted with trypan blue (5.3.6) and suspended in PBS. Cells of RGB ALL-265 and RGB AML-393 were diluted and intravenously injected into groups of NSG mice at cell numbers indicated in Table 12 and Table 11. The amount of human cells in blood of mice was determined every second week to monitor disease progression. Mice were sacrificed and PDX cells were purified out of spleen and bone marrow. Stem cell frequencies were determined according to Poisson statistics, using the ELDA software application (<http://bioinf.wehi.edu.au/software/elda/>) (Hu & Smyth, 2009).

5.2.3. Competitive transplantation assay

For competitive engraftment experiments, cells of each cell clone were thawed and counted using trypan blue (5.3.6). Cells were mixed in equal parts and 5×10^5 cells of the mixture were

stained with mouse CD45-APC-Cy7 antibody (Biolegend, San Diego, CA, USA) as described in 5.3.6. Correct mixing was confirmed by flow cytometry before injection.

For competitive xenograft experiments with five clones (6.4.1), cells of clone #1, clone #5, clone #6, clone #7 and clone #8 were mixed in equal parts and 2.5×10^5 cells of the mixture were subsequently injected into each mouse.

For competitive transplantation of two clones (6.4.2), cells of clone #5 and clone #6, clone #5 and clone #8 or clone #6 and clone #8 were mixed in equal parts and 1×10^5 cells of the mixtures were injected into mice.

For in vivo therapy with dexamethasone (6.5.2), cells of clone #5 and clone #6 were mixed in equal parts and 1×10^5 cells of the mixture were injected into mice, respectively.

For re-transplantation of samples of competitive transplantation experiments of combinations of two clones, 1×10^4 cells of two representative samples consisting either of clone #5 and clone #6 or of clone #5 and clone #8 after one mouse passage (6.4.2), were injected into secondary recipient mice.

5.2.4. Bioluminescence in vivo imaging

For in vivo imaging of NSG mice engrafted with PDX cells expressing Gaussia luciferase, we used the IVIS Lumina II Imaging System (Caliper Life Sciences, Mainz, Germany) (Barrett et al., 2011; Bomken et al., 2013; Terziyska et al., 2012). Mice were anesthetized with isoflurane and fastened in the imaging chamber. Coelenterazine (Synchem OHG, Felsberg, Germany) was dissolved in acidified methanol to a final concentration of 10 mg / ml and diluted shortly before injection in sterile HBG buffer (HEPES-buffered glucose containing 20 mM HEPES at pH 7.1, 5% glucose w / v). 100 µg of Coelenterazin were injected into the tail vein of the mice and pictures were taken immediately after injection (field of view: 12.5 cm, binning: 8, f / stop: 1 and open filter setting). Pictures were analyzed using Living Image software 4.4 (Caliper Life Sciences, Mainz, Germany)

5.2.5. In vivo therapy with dexamethasone

For dexamethasone (Dexa) treatment of mice engrafted with clone #5 and clone #6, stock solutions of Dexa were diluted in sterile PBS in a manner that all mice received 8 µl of the dilution per g body weight. Control mice received the same amounts of PBS. Mice were treated

with either PBS control or different concentrations of Dexa (2 mg or 8 mg per kg body weight) by intraperitoneal injection from Monday to Friday for five consecutive weeks. Body weights of treated animals were determined every second day. The loss of body weight never exceeded 13% during treatment time. Bioluminescence in vivo imaging (5.2.4) was performed once a week to monitor disease progression. Control mice were sacrificed at advanced disease and treated mice were sacrificed subsequently.

5.2.6. Analysis of bone marrow of mice treated with dexamethasone

Dexa treated mice were sacrificed and bones (pelvis, long bones of the legs, backbone and sternum) were isolated. Cells were purified as described in 5.2.1 and 1 / 10 of the total bone marrow was stained with anti muCD45 antibody (Biolegend, San Diego, CA, USA) and in whole measured by flow cytometry.

5.3. In vitro cell culture of cell lines and PDX cells

5.3.1. Determination of cell numbers

The density of PDX cells and cell line cells was determined using a “Neubauer” counting chamber. Adherent cells were detached from the flask and re-suspended prior to counting. 10 μ l adequately diluted cell suspension were pipetted into the counting chamber and cells within the chamber were counted using light microscopy (Carl Zeiss 550 1317 with phase contrast filter). Cell suspension densities (cells per ml) were calculated as follows:

Mean of counted cells x dilution factor x 10^4 cells / ml.

5.3.2. Freezing and thawing of cell line cells and PDX cells

All cells were viably frozen at -80 °C in 1 ml FCS with 10% DMSO. To thaw cells, the cryotube containing the frozen cells was incubated at 37 °C for 1 min and then transferred into 9 ml fresh medium. After centrifugation (400 g, 5 min, rt) the pellet was dissolved in fresh medium and transferred into a new culture flask. Frozen PDX cells for re-passaging in NSG mice were thawed as described and re-suspended in a final volume of 250 μ l of sterile PBS. Cells were injected into mice shortly after thawing.

5.3.3. In vitro cultivation of cell line cells and PDX cells

Adherent cell lines HEK-293T (DSMZ, Braunschweig, Germany) for virus production and the mouse stromal cell line EL08 (DSMZ, Braunschweig, Germany) for co-culture of PDX cells, were grown in 75 cm² culture flasks at 37 °C. HEK-293T cells were cultured in DMEM supplemented with 10% FCS and 1% glutamine and EL08 feeder cells were grown in RPMI supplemented with 20% FCS and 1% glutamine. Every 2 to 3 days, confluent cells were split in a 1:10 ratio by taking away the old medium and adding 1 mL of trypsin solution to the cells and incubating for 5 min at 37 °C. Subsequently, cells were re-suspended in fresh medium.

NALM-6 cell line cells (DSMZ, Braunschweig, Germany) were kept in RPMI supplemented with 10% FCS at a concentration of 0.5 to 2 x 10⁶ cells / ml in 25 cm² or 75 cm² culture flasks. Cells were split every 2 to 3 days so that the concentration never exceeded 2 x 10⁶ cells / ml.

For in vitro culture of PDX cells, we used patient medium (RPMI supplemented with 20% FCS, 1% pen/strep, 1% gentamycin and 2 mM glutamine) further supplemented with 6 mg / l insulin, 3 mg / l transferrin, 4 µg / l selenium (ITS-G, Gibco, San Diego, CA, USA), 1 mM sodium pyruvate, 50 µM α-thioglycerol (Sigma-Aldrich, St. Louis, MO, USA).

5.3.4. Co-culture of transduced PDX cells

For co-culture experiments, we used the mouse stromal cell line EL08 (DSMZ, Braunschweig, Germany). To detach adherent cells from the flask, 1 ml of trypsin was added to one 75 cm² culture flask of confluent cells and incubated for 5 min. Cells were re-suspended in fresh RPMI medium supplemented with 20% FCS and 1% glutamine and counted. In 24-well plates, 40,000 cells were seeded per well in 1 ml medium. The next day, the cells were irradiated (16 Gy). Old medium was taken away and 0.5 x 10⁶ transduced PDX cells were added per well in 500 µl patient medium supplemented with 6 mg / l insulin, 3 mg / l transferrin, 4 µg / l selenium, 1 mM sodium pyruvate, 50 µM α-thioglycerol.

5.3.5. Limiting dilution of RGB marked NALM-6 cell line cells

RGB marked NALM-6 cells were counted and stepwise diluted to a final concentration of 5 cells / ml. 100 µl of the cell suspension were added to each well of a 96-well plate to a final concentration of 0.5 cells / well. Plates were incubated at 37 °C for 4 weeks. In those wells, where cells had regrown, color expression was determined by flow cytometry to verify clonal expansion of single cells.

5.3.6. Antibody staining of PDX cells and staining of apoptotic cells

To exclude mouse cells, PDX cells were stained with mouse CD45-APC-Cy7 (Biolegend, San Diego, CA, USA). Fresh PDX cells were washed with PBS and re-suspended in PBS. Antibody was added according to the manufacturer's instructions (1:100). To assess cell viability, Annexin V-APC detection kit (BD Biosciences, Heidelberg, Germany) and DAPI (at a final concentration of 1 µg / ml) were used. To exclude dead cells, trypan blue was added (1:2) and cells were counted. All antibodies and reagents were diluted according to the manufacturer's instructions.

5.3.7. Drug stimulation in vitro

For in vitro apoptosis assays of single cell clones, cells were diluted to a final concentration of 1×10^6 cells / ml and seeded in 96-well plates (1×10^5 cells / well). Stock solutions of all drugs were diluted as indicated in Table 7 and 1 µl drug dilution was added to 100 µl cell suspension. Cells were treated with the indicated drug concentrations in duplicate wells.

Table 7: Drugs and dilutions for in vitro stimulation of single cell clones.

| Drug | stock | Final concentration | Manufacturer |
|----------------|------------|---------------------|--|
| Dexamethasone | 10.19 mM | 500 nM | mibe GmbH Arzneimittel, Brehna, Germany |
| | | 50 nM | |
| Prednisolone | 27.22 mM | 1.6 µM | mibe GmbH Arzneimittel, Brehna, Germany |
| | | 160 nM | |
| Daunorubicine | 3.55 mM | 250 nM | PFIZER PHARMA GmbH, Berlin, Germany |
| | | 25 nM | |
| Doxorubicine | 3.68 mM | 500 nM | TEVA GmbH, Ulm, Germany |
| | | 50 nM | |
| Epirubicine | 3.7 mM | 370 nM | TEVA GmbH, Ulm, Germany |
| | | 37 nM | |
| L-Asparaginase | 2,500 U/ml | 1 U/ml | medac, Gesellschaft für klinische Spezialpräparate mbH, Wedel, Germany |
| | | 0.1 U/ml | |
| Cytarabine | 206 mM | 4 µM | Mundipharma GmbH, Limburg an der Lahn, Germany |
| | | 400 nM | |

72 hours after stimulation, 96-well plates were measured using the high throughput sampler of the BD LSRfortessa (5.5.7). Percentage of specific apoptosis was assessed by gating on dead cells in forward-side scatter and calculated as follows:

$$\% \text{ specific apoptosis} = \left(\frac{\text{apoptosis (stimulated)} - \text{apoptosis (control)}}{100 - \text{apoptosis (control)}} \right) \cdot 100$$

5.4. Molecular biology

5.4.1. Agarose gel electrophoresis of DNA

Agarose gel electrophoresis to separate DNA fragments by size was performed on 1% agarose gels. Gels contained 1 g agarose (Biozym Scientific GmbH, Hessian Oldendorf, Germany), 100 ml 1xTAE buffer and 5 µl ethidium bromide (Carl Roth, Karlsruhe, Germany). Agarose and buffer were microwaved and ethidium bromide was added. Electrophoresis was performed in a gel electrophoresis chamber with 1xTAE buffer at 60 to 80 V. 10 µl DNA suspension were mixed with 5 µl 6xDNA-loading dye and run on the gel for one to two hours. The gel was checked under UV light and the respective bands were cut out from the gel.

5.4.2. DNA gel extraction

To extract and purify DNA from gels, NucleoSpin Gel and PCR Clean-up Kit (Macherey Nagel, Duren, Germany) was used. The gel slices were completely dissolved in membrane binding buffer by incubating at 50 °C for 10 min and vortexing. The mixture was loaded onto NucleoSpin Gel and PCR Clean-up Columns and centrifuged for 30 sec at 11,000 g to bind the DNA to the silica membrane of the column. The flow through was discarded and the column washed twice with ethanolic wash buffer to remove contaminations. The membrane was dried and DNA was eluted by adding elution buffer and centrifuging.

5.4.3. Polymerase chain reaction

Polymerase chain reaction (PCR) was applied to amplify the coding sequences for mCherry (from pSicoR-U6-EF1α-mCherry; Addgene, Cambridge, MA, USA), Venus (from plasmid

pRRL-PPT-SFFV-Venus, provided by Tim Schroeder) and mTagBFP (from plasmid pmTagBFP-C1, provided by Michael Schindler) using Pfu DNA Polymerase (Thermo Fischer Scientific, Waltham, MA, USA).

The following components were used for 50 μ l of PCR reaction:

- 5 μ l 10xPfu-Buffer with MgSO₄
- 2 μ l dNTP mix
- 1 μ l forward primer
- 1 μ l reverse primer
- 50 ng template DNA
- 1 μ l Pfu DNA Polymerase
- Ad 50 μ l H₂O (nuclease free)

PCR was run in a PCR machine with the following program:

| | | |
|-------|--------------|-------|
| 95 °C | 2 min | |
| 95 °C | 30 sec | } 35x |
| 60 °C | 30 sec | |
| 72 °C | 1 min 30 sec | |
| 72 °C | 5 min | |
| 40 °C | 10 min | |

Subsequently, PCR products were checked on an agarose gel and purified.

5.4.4. Colony-PCR

One colony was picked and shaken over one day at room temperature in a 24-well plate containing 2 ml LB-medium with ampicillin. As template for the PCR, 2 μ l of culture medium were used.

For colony PCR we used the following components (sufficient for 25 PCR products):

104 μ l GoTaq-Buffer
10.4 μ l dNTP mix
20.8 μ l forward primer
20.8 μ l reverse primer
2 μ l template
3.25 μ l GoTaq Polymerase
361 μ l H₂O

PCR was run in a PCR machine with the following program:

| | | | |
|-------|--------|--|-----|
| 95 °C | 2 min | | |
| 95 °C | 30 sec | ┌──────────┐ │ │ │ │ └──────────┘ | 35x |
| 53 °C | 30 sec | | |
| 72 °C | 2 min | | |
| 72 °C | 5 min | | |

PCR products were subsequently checked on an agarose gel to detect the right colonies.

5.4.5. Purification of PCR products

PCR products were purified using the NucleoSpin Gel and PCR Clean-up Kit (Macherey Nagel, Duren, Germany). In short, two volumes of binding buffer were added to one volume of PCR product, loaded onto a NucleoSpin Gel and PCR Clean-up Column and centrifuged (30 s, 11,000 g). The flow through was discarded and the silica membrane of the column was washed twice with ethanolic wash buffer. The membrane was dried by centrifuging for 1 min at 11,000 g. Finally, DNA was eluted by incubating with 15 to 30 μ l elution buffer and centrifuging (1 min, 11,000 g).

5.4.6. Restriction digestion of DNA

PCR products and the vector backbone were digested with the respective restriction enzymes (Table 2).

Digestion took place at 37 °C for 45 min.

10 U restriction enzyme
1-2 µg DNA
3 µl restriction enzyme buffer (10x)
0.5 µl BSA
ad 30 µl H₂O

After digestion of the plasmids, the efficiency was checked on an agarose gel. The bands were cut out and DNA was purified using NucleoSpin Gel and PCR Clean-up Kit (Macherey Nagel, Duren, Germany).

5.4.7. Ligation of DNA fragments

T4 DNA Ligase was used to ligate the DNA of the vector backbone with the corresponding fragment. The fragments were added at a 1:1 ratio. Usually, we used 100 ng DNA of the vector backbone and calculated the right amount of fragment which had to be ligated into the vector using the ligation calculator:

<http://www.promega.com/a/apps/biomath/index.html?calc=ratio>

Example:

calculated amounts of vector and fragment
1 µl Ligase Buffer 10x
1 µl T4 DNA Ligase
ad 10 µl H₂O

Ligations were incubated on a PCR thermoblock for 2 h at 22 °C.

5.4.8. Plasmid minipreparation and midipreparation

For plasmid minipreparations and midipreparations, cultures of *E. coli* in LB-medium with ampicillin were inoculated with starter cultures. Overnight cultures (5 ml for minipreparations,

50 ml for midipreparations) were pelleted (6,000 g, 4 °C, 10 - 30 min) and DNA was purified using NucleoSpin Plasmid EasyPure Kit for a minipreparation or NucleoBond Xtra Midi Kit for a maxipreparation (both from Macherey Nagel, Duren, Germany) according to the manufacturer's instructions. In brief, pellets were re-suspended in buffer. DNA was released from the cells by adding lysis buffer and incubating for 2 to 5 min at room temperature. Subsequently, the mixture was neutralized by adding neutralization buffer, mixed and clarified by centrifugation.

For a miniprep, the lysate was loaded onto a NucleoSpin Plasmid EasyPure Column and centrifuged (30 sec, 2,000 g). The column was washed and dried and DNA was eluted by adding 50 µl elution buffer and centrifuging for 1 min at 12,000 g.

For a midiprep, the lysate was filled into an equilibrated NucleoBond Xtra Column Filter which was put into a column. The filter was washed by adding equilibration buffer. Then, the filter was removed, the column was washed and DNA was eluted. The plasmid DNA was precipitated by adding isopropanol and centrifuging (30 min, 15,000 g, 4 °C). The supernatant was discarded and the pellet was washed with 70% ethanol (5 min, 15,000 g) and dried at room temperature. Finally, the pelleted plasmid DNA was dissolved in sterile water.

5.4.9. Isolation of genomic DNA

Genomic DNA was isolated out of 5×10^6 freshly thawed PDX cells using the QIAamp DNA Mini Kit (Qiagen, Venlo, NL). Briefly, cells were pelleted and re-suspended in PBS to a final volume of 200 µl and 20 µl of protease were added. Subsequently, lysis buffer was added to the cell suspension and incubated at 56 °C for 10 min. Pure ethanol was added and the mixture was loaded onto a column and centrifuged (1 min, 6,000 g). After two washing steps, DNA was eluted from the column by adding elution buffer, incubating for 1 min and centrifuging.

5.4.10. Determination of DNA quantity and quality

DNA concentration and purity was determined by measuring 1 µl of DNA solution in a nanophotometer (Nanodrop 2000, Thermo Fisher Scientific, Waltham, MA, USA).

5.5. Genetic engineering of cell lines and PDX cells

5.5.1. Cultivation of E. coli DH5 α cells

E. coli DH5 α cells were cultured at 37 °C. For long-term storage, cells were maintained in glycerol stocks. 1.5 ml of a bacterial culture were mixed with 100 μ l of sterile glycerol solution, incubated for 30 min on ice and stored at -20 °C.

5.5.2. Generation of competent cells for heat shock transformation

100 ml LB medium was inoculated with 1 ml of an overnight culture of E. coli DH5 α cells and cultured to an OD₆₀₀ of 0.4 to 0.5. The OD₆₀₀ of the culture was regularly checked on a photometer and as soon as the optimal density was reached, the culture was incubated on ice for 2 min. The cells were pelleted by centrifugation (5 min, 4,000 rpm, 4 °C) and the pellet was re-suspended in 15 ml TFB I on ice. After 5 min incubation on ice, the cells were centrifuged for a second time (5 min, 4,000 rpm, 4 °C) and the pellet was re-suspended in 4 ml TFB II on ice. Cells were stored in aliquots of 100 μ l at -80 °C.

5.5.3. Heat shock transformation of plasmid DNA into competent E. coli cells

100 ng DNA were added to 50 μ l of freshly thawed E. coli DH5 α cells and gently mixed. The mixture was incubated on ice for 30 min, put at 42 °C for 90 sec and put back on ice for 2 min. The whole amount was transferred into 400 μ l LB-medium and incubated at 37 °C for 45 min. Aliquots of 200 to 250 μ l were plated onto agar-plates containing ampicillin and incubated at 37 °C overnight. Plates were checked for colonies the next day.

5.5.4. Lentivirus production using HEK-293T packaging cells

Human cells were genetically engineered using third generation lentiviruses (Dull et al., 1998; Zufferey, Donello, Trono, & Hope, 1999). Lentiviruses were produced using the adherent cell line HEK-293T (human embryonic kidney cell line, DSMZ, Braunschweig, Germany) as packaging cell line. HEK-293T cells were grown in 75 cm² culture flasks in DMEM supplemented with 10% FCS and 1% glutamine. At a confluency of 50 to 80%, cells of one 75 cm² culture flask were transfected with the packaging plasmids 392 (2.5 μ g), 393 (5 μ g) und pMD2.G (1.25 μ g) and the desired transfer vector (2.5 μ g). Therefore, DNA suspension and 24 μ l Turbofect (Thermo Fischer

Scientific, Waltham, MA, USA) were mixed with 1 ml DMEM (without FCS) and incubated for 20 min at room temperature. Exhausted medium of HEK-293T cells was exchanged with fresh medium prior to transfection. DNA was added dropwise to the packaging cells. Transfected HEK-293T cells were incubated at 37 °C and 5% CO₂ for 70 h. Subsequently, the supernatant was transferred into 15 ml falcons and centrifuged (400 g, 5 min, rt) to get rid of remaining cells. The supernatant was filtered and concentrated by centrifugation using Amicon-Ultra 15 centrifugal filter units (Merck Millipore, Darmstadt, Germany). The supernatant was centrifuged (2,000 g, 30 min, rt) to a remaining volume of 200 to 250 µl and the virus concentrate was stored at -80 °C in aliquots of 10 µl.

5.5.5. Determination of virus titers

Titers of produced lentiviruses were determined on NALM-6 B-ALL cell line cells. 0.7×10^6 cells were seeded in 1 ml RPMI medium with supplements in a 24-well plate and virus was added at increasing concentrations (0.25 µl; 0.5 µl; 1 µl; 2 µl; 4 µl per well) together with 8 µg/ml polybrene. After 7 days, the amount of transduced cells for each virus concentration was assessed by flow cytometry and the virus titer was calculated as follows:

$$titer = \left(\frac{F \cdot Z}{V} \right) TU/ml$$

F = % of transduced cells

Z = number of cells at infection

V = volume of virus

5.5.6. Lentiviral transduction of cell line cells and PDX cells

For genetic engineering of cell line cells and PDX cells, we used the third generation lentiviral vector system described in 5.5.4. Prior to transduction, exhausted medium was exchanged with fresh medium. To increase transduction efficiencies, polybrene was added to a final concentration of 8 µg/ml. Polybrene reduces the charge repulsion between the viral particles and the cell surface (Davis, Rosinski, Morgan, & Yarmush, 2004). Subsequently, cell line cells or PDX cells were incubated with the lentivirus(es) encoding the desired transgene(s) at a multiplicity of infection of 300 to 1300. After 24 h, PDX cells were washed twice with PBS and either injected into a mouse or seeded on EL08 feeder cells. Transduced cell line cells were cultured in vitro. Transgene expression was assessed by flow cytometry.

5.5.7. Flow cytometry analysis of cell line cells and PDX cells

All flow cytometry analyses were performed using a BD LSRFortessa (BD Biosciences, Heidelberg, Germany). Fluorescent proteins (mCherry, Venus, mTagBFP) and other fluorochromes (APC, APC-Cy7, DAPI) were measured using the laser and filter settings indicated in Table 8.

Table 8: Filter settings of the BD LSRfortessa.

| Laser (nm) | Longpass Filter | Bandpass Filter | Parameter |
|------------|-----------------|-----------------|-----------------|
| 355 | 505 | 450/50 | DAPI |
| 405 | 595 | 605/12 | Qdot 605 |
| | 475 | 525/50 | Qdot 525 |
| | | 450/50 | mTagBFP |
| 488 | 600 | 695/40 | PerCP-Cy5.5 |
| | 505 | 530/30 | Venus |
| | | 488/10 | SSC |
| 561 | 750 | 780/60 | PE-Cy7 |
| | 685 | 710/50 | PE-Cy5.5 |
| | 635 | 670/30 | PE-Cy5 |
| | 600 | 610/20 | mCherry |
| | 570 | 585/15 | PE |
| 640 | 750 | 780/60 | APC-Cy7 |
| | 710 | 730/45 | Alexa Fluor 700 |
| | | 670/14 | APC-Cy7 |

96-well plates were measured using the High Throughput Sampler (HTS) option of the BD LSRFortessa.

PDX samples were gated for living cells and for muCD45 negative cells to exclude mouse cells as shown in Figure 4.

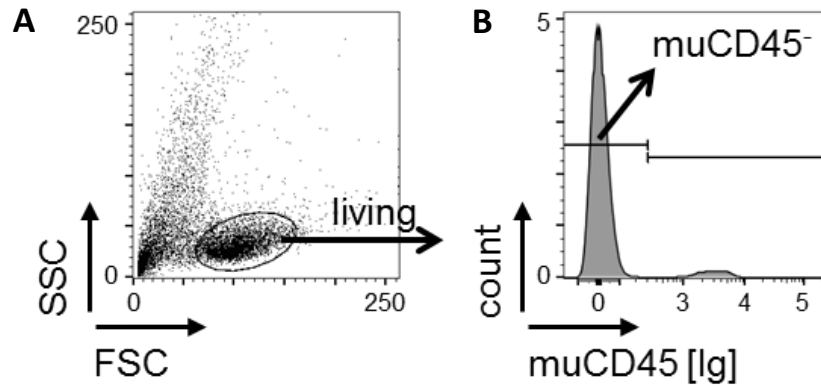


Figure 4: Gating strategy for analysis of PDX cells by flow cytometry.

Cells were gated on living cells in FSC/SSC (A) and on muCD45 negative cells to exclude mouse hematopoietic cells (B).

5.5.8. Sorting of RGB PDX single cell clones

ALL-265 single cell clones were sorted using the BD FACSAriaIII (BD Biosciences, Heidelberg, Germany). Cells were thawed and re-suspended in patient medium at a final concentration of 10×10^6 cells / ml. Cells were sorted into a flow cytometry tube containing 500 μ l RPMI medium. Finally, 1×10^5 cells of each cell clone were transplanted into two recipient mice in order to amplify each clone in two biological replicates.

6. Results

Malignant tumors consist of heterogeneous tumor cells, and the most adverse clones within a tumor require effective treatment to cure the patient. Here, we aimed at a better understanding of clones with unfavorable characteristics with the final vision to eradicate aggressive subclones in the future. In this regard, we characterized single cell clones from a child with acute lymphoblastic leukemia regarding functional properties focusing on growth behavior and drug resistance. Our findings serve as basis to develop therapeutic strategies that eradicate aggressive subclones in the future.

6.1. AL patients, the individualized xenograft mouse model of AL; genetic engineering in AL PDX cells and in vivo imaging of mice

We aimed at characterizing functional characteristics of different subclones within a population of leukemia cells. Subclonal diversity cannot be investigated in leukemia cell lines because cell lines putatively changed clonal composition during the process of immortalization and in vitro passaging. However, primary leukemia cells from patients do not grow in vitro.

To nevertheless be able to study patients' cells, we amplified primary tumor cells derived from acute leukemia (AL) patients in severely immunocompromised mice, NSG mice, within the individualized xenograft mouse model (5.2). NSG mice lack T-cells, B-cells and functional natural killer cells and allow stable engraftment and propagation of acute leukemia patient samples (Jacoby et al., 2014; Schmitz et al., 2011; Shultz, Ishikawa, et al., 2007; Shultz, Pearson, et al., 2007). Patient-derived xenograft (PDX) cells represent an attractive alternative to cell lines because they are more closely related to the original patient's leukemia and reproduce the heterogeneity of ALL and AML. For this reason, PDX samples represent a suitable model for functional studies.

For the experiments performed within this study, the PDX samples listed in Table 9 derived from three different acute leukemia patients were used: AML-393, AML-346 and ALL-265.

Table 9: PDX samples.

| PDX sample | Patient | Disease stage | Passaging time (1 – 2 x 10⁶ cells / mouse) |
|-------------------|----------------|---|--|
| AML-393 | Adult | Relapse after stem cell transplantation | 35 days |
| AML-346 | Pediatric | Relapse | 42 days |
| ALL-265 | Pediatric | Relapse | 40 days |

All patients suffered from relapsed disease and thus aggressive and poor prognostic disease and are rather not to be considered representative. PDX samples of these patients were established by engrafting primary patient cells in mice to propagate patients' leukemia cells. Primary blasts of AML-393 were obtained from an adult patient treated at the Department of Internal Medicine III, Ludwig-Maximilians-Universität, Munich, and the xenograft sample was established in our lab. PDX AML-346 is derived from a child treated at the Kinderonkologie in Tübingen and the xenograft was established in Tübingen. PDX ALL-265 was established at the Kinderonkologie in Zürich by xenografting primary tumor cells from a child treated in Zürich.

The time to cause a full leukemia in a mouse was similar for all three xenograft samples and varied between five and six weeks upon transplantation of 1 to 2 x 10⁶ cells per mouse which is quite fast indicating that all three xenografts were derived from rather aggressive leukemia cells. When mice showed clinical signs of the disease, expanded PDX cells were recovered as described in 5.2.1 from mice spleens and bone marrows. Thus, PDX samples could be stably propagated in mice by serial re-passaging over multiple passages. Besides, PDX cells could be preserved by viably freezing at -80 °C and after thawing these cells could be re-injected into secondary recipient mice representing an enormous reservoir of PDX leukemia cells for experiments (5.3.2).

Using a third generation lentiviral vector system, genetic engineering of PDX cells was successfully established in our lab in order to express diverse transgenes such as fluorescent proteins or luciferases in PDX cells (Terziyska et al., 2012) (5.5). In particular, expression of fluorescent proteins enables sorting and tracking of PDX cells while expression of luciferases allows monitoring of disease progression in a living mouse engrafted with leukemic cells. Expression of recombinant luciferase enables highly reliable and sensitive in vivo imaging for monitoring disease progression and treatment effects (Terziyska et al., 2012)(5.2.4).

Furthermore, as lentiviral transduction leads to an integration of the viral genome into the recipient genome, transgenes are stably expressed and hereditary.

Unfortunately, in contrast to leukemic cell line cells, PDX cells are rather reluctant to lentiviral transduction and to receive high transduction efficiencies is challenging. Therefore, we aimed at working with PDX samples which could be efficiently lentivirally transduced in order to mark a representative amount of PDX cells which ensured to study a representative part of the whole patient sample. Besides, for the experiments performed in this study, preferably PDX samples with a short passaging time were chosen which could concomitantly be efficiently lentivirally transduced which was the case for all three PDX samples described here.

Taken together, three PDX samples, AML-393, AML-346 and ALL-265, had been established in my lab or by others; samples exhibited reasonable passaging times in mice and enhanced susceptibility to lentiviral transduction and served as tools for my studies.

6.2. Multicolor staining using lentiviral molecular marking

In order to discriminate single cells from each other as prerequisite to generate single cell clones, I first molecularly marked cells of the chosen PDX AL samples with different colors.

I used an innovative lentiviral multicolor staining termed red-green-blue (RGB) marking based on the RGB color model (Weber et al., 2011). The principle is that by mixing the three basic colors red, green and blue at different intensities, all colors of the rainbow can be generated. The RGB system is commonly used in electronic devices such as TV screens or video cameras.

Weber and colleagues adapted the RGB technology to molecular marking of cells by simultaneously transducing cells with three different lentiviral vectors each coding for another fluorescent protein. If cells are transduced with three lentiviral vectors encoding a red, a green and a blue fluorescent protein at the same time, colors mix due to different numbers of each vector integrated per cell. Each cell can potentially be transduced with none, one, two, or three colors at a time and after transduction can contain different numbers of genomic integrations of each color. Consequently, each cell will express a specific, individual mixed color depending on the color transduced and the number of genomic integrations per color (Figure 5).

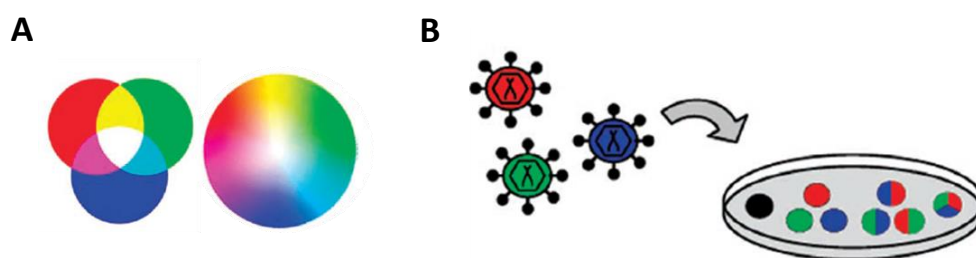


Figure 5: The principle of RGB marking.

(A) Mixing of the basic colors red, green and blue at different intensities enables generation of various mixed colors. (B) Transduction of cells with three lentiviral vectors coding for a red, a green, and a blue fluorescent protein results in cells expressing numerous colors. Adapted from (Weber et al., 2011).

To achieve mixed colors, more than one, at best multiple lentiviruses must enter the cell and transduction efficiencies must be high, at best above 50% for each color. Thus, high transduction efficiencies are crucial to obtain a sufficient color overlap in order to discriminate as many cells as possible based on their specific color. If efficiencies are too low, only single transgenic cells expressing either red or green or blue will be generated but no double transgenic and triple transgenic cells expressing more than one color.

As a consequence, RGB marking allows tracking of individually marked cell clones over time. Moreover and in contrast to other methods, the great advantage of molecular color marking is that it allows separating living cells according to their specific colors and using these viable cells for further functional assays.

6.2.1. Cloning of RGB transfer vectors for lentivirus production

To perform molecular RGB marking in acute leukemia cell lines and PDX cells, we adapted the published RGB system to our vector system successfully used in our group before.

Therefore, my colleague Michela Carlet cloned new lentiviral transfer vectors encoding a red, a green and a blue fluorescent protein together with Gaussia luciferase by replacing the copGFP gene in pCDH-EF1 α -GLuc-copGFP by mCherry, Venus or mTagBFP. The copGFP gene was removed from the vector and the coding sequences for mCherry (from plasmid pSicoR-U6-EF1 α -mCherry; Addgene, Cambridge, MA, USA), Venus (from plasmid pRRL-PPT-SFFV-Venus, provided by Tim Schroeder) and mTagBFP (from plasmid pmTagBFP-C1, provided by Michael Schindler), were PCR amplified (5.4.3) and cloned into the pCDH-EF1 α -GLuc-copGFP vector using NsiI and Sall.

In addition, I cloned novel smaller lentiviral transfer vectors encoding mCherry, Venus or mTagBFP without Gaussia luciferase allowing to produce lentiviruses with enhanced titers due to decreased vector size. Therefore, the coding sequences for the three fluorescent proteins mCherry, Venus and mTagBFP were cloned downstream of the EF1 α promoter using BamHI and Sall.

These lentiviral vectors depicted in Figure 6 encoding three different fluorescent proteins with or without Gaussia luciferase were ultimately used to produce lentiviruses for transduction of cell line cells and PDX cells with the RGB system.

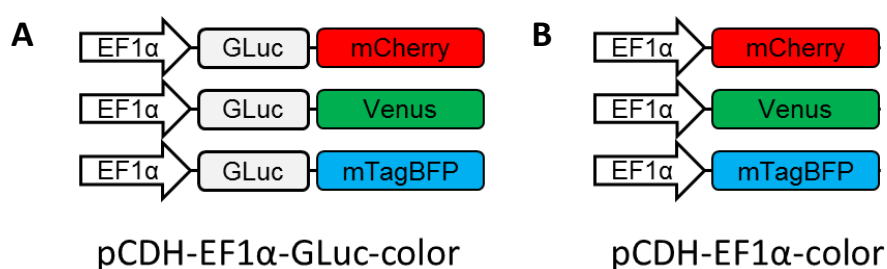


Figure 6: Transfer vectors for production of third generation lentiviruses.

(A) Transfer vectors encoding Gaussia luciferase and the three fluorescent proteins mCherry, Venus and mTagBFP. (B) Transfer vectors encoding the three fluorescent proteins without luciferase. EF1 α = elongation factor 1 alpha promoter; GLuc = Gaussia luciferase; mCherry = red fluorescent protein; Venus = green fluorescent protein; mTagBFP = blue fluorescent protein; color indicates mCherry, Venus or mTagBFP.

6.2.2. RGB marking enabled color marking of individual cell clones

For RGB marking of cell line cells and PDX cells, we used lentiviruses that were produced with the plasmids depicted in Figure 6 coding for the fluorescent proteins mCherry, Venus and mTagBFP with or without Gaussia luciferase (5.5.4). Additional expression of Gaussia luciferase in the cells enabled bioluminescence in vivo imaging to follow leukemia development in living mice (Santos et al., 2009; Terziyska et al., 2012)(5.2.4).

I established RGB marking in cell line cells first. Hence, NALM-6 pre-B-ALL cell line cells were transduced as described in 5.5.6 with lentivirus produced with the three different transfer vectors depicted in Figure 6A using a third generation lentiviral vector system (Dull et al., 1998; Zufferey et al., 1999). In comparison to PDX cells, lentiviral transduction of ALL cell lines is highly

efficient so that transduction efficiencies of 50% for each RGB virus were achieved in NALM-6 cells in one single transduction. Fluorescence microscopy of RGB marked NALM-6 cells confirmed expression of different colors as shown in Figure 7 indicating color mixing of red, green and blue.

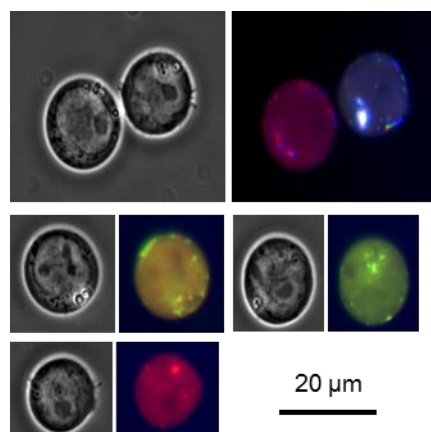


Figure 7: Color expression of RGB marked cell line cells assessed by fluorescence microscopy.

NALM-6 cell line cells were transduced with lentiviruses produced with the three constructs shown in Figure 6A and transgene expression was determined by fluorescence microscopy.

Since flow cytometry allows analysis of a higher number of cells in parallel compared to fluorescence microscopy, I developed the published RGB method further and established flow cytometry analysis of RGB marked cells. Using a BD LSRfortessa with the filter settings indicated in Table 8 enabled to measure mCherry, Venus and mTagBFP in parallel (5.5.7). Flow cytometry analysis of RGB marked NALM-6 cells, 50% positive for each color, revealed expression of each mCherry, Venus and mTagBFP at different intensities suggesting different numbers of genomic integrations per color. Importantly, expression of only one color does not allow clear separation of subclones. Cells must express at least two or even better three colors at different intensities in order to be distinguishable from each other. A major number of cells were successfully transduced with several colors at the same time indicated by expression of several colors per cell (Figure 8A). As expected, expression of multiple colors appeared as homogeneous clouds in 2-dimensional or 3-dimensional plots indicating multiple Gaussian distributions in each color in parallel.

Because it was unknown how single cell clones would look like in flow cytometry, we generated single cells of the RGB marked NALM-6 cell line depicted in Figure 8A by limiting dilution and

seeding 0.5 cells per well in 96-well plates (5.3.5). Flow cytometric analysis of regrown cells confirmed clonal expansion of single cells: individual cell clones expressed unique colors and could be distinguished from each other using flow cytometry. Remarkably, RGB marking also enabled to detect that in some wells not only one cell but two cells had been seeded and amplified. Accordingly, cells in these wells did not consist of one but of two cell clones which could clearly be separated from each other due to individual color expression using flow cytometry (Figure 8B). Expansion of not one single cell but two cells occurred even in two out of five wells where RGB marked NALM-6 cells had regrown after limiting dilution. Using RGB marking, we could easily identify the wells containing more than one single cell clone.

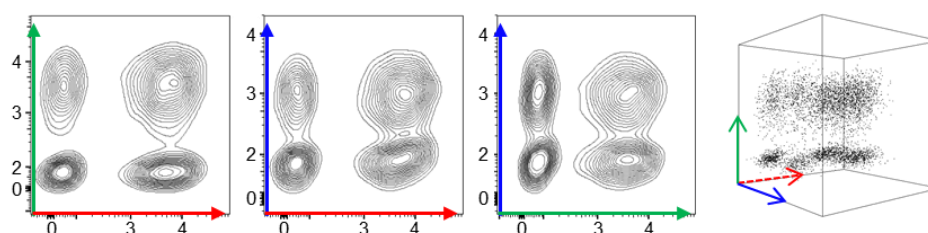
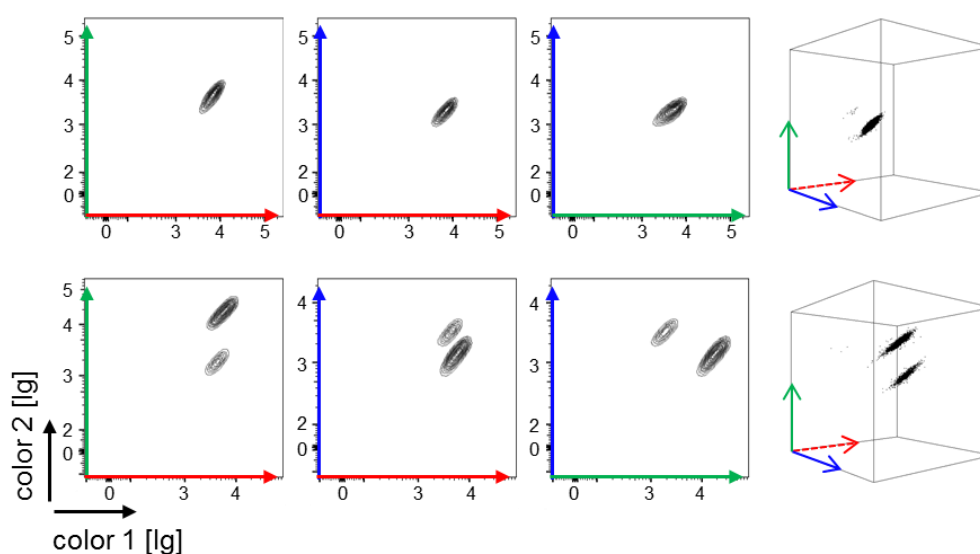
A RGB NALM-6 cell line cells**B** RGB NALM-6 single cell clones

Figure 8: Color expression of RGB marked cell line cells assessed by flow cytometry.

(A) NALM-6 cell line cells were transduced (50% for each color) with lentiviruses produced with the three constructs shown in Figure 6A and transgene expression was determined by flow cytometry. Shown are three dot plots displaying expression of mCherry, Venus and mTagBFP and one cube illustrating color distribution in 3D; red arrow = mCherry, green arrow = Venus, blue arrow = mTagBFP; depicted dot plots are pregated on living cells in FSC/SSC. (B) RGB NALM-6 cells of (A) were seeded at a concentration of 0.5 cells / well and expanded. Color expression was determined by flow cytometry upon regrowth of the cells in each well. Upper panel: amplification of one cell in one well, lower panel: amplification of two cells in one well.

Single clones appeared ellipsoid in 2-dimensional and egg-shaped in 3-dimensional flow cytometry plots according to Gaussian distribution of each color. Unfortunately, single cell clones absorbed a large area or volume in 2-dimensional or 3-dimensional flow cytometry plots. This unexpected heterogeneity in color expression in genetically identical cells of one clone unpleasantly limited the number of single cell clones which could be monitored simultaneously using flow cytometry.

In summary, these data indicate that RGB marking could be used to individually stain and track single cell clones as it enabled clear separation of single cell clones by their unique color using flow cytometry.

6.2.3. RGB marking of PDX AL cells

We aimed at studying subclonal heterogeneity in patients' cells and not in leukemia cell lines. As ideal tool, we aimed at generating PDX samples with numerous cells expressing two or at best three colors and each color in Gaussian distribution. This proved a technically highly demanding task due to two major challenges - lentiviral transduction efficiency in PDX AL cells (described here) and homing efficiency of PDX AL cells in NSG mice (described in 6.2.4).

Since PDX AL cells are rather reluctant towards lentiviral transduction, our studies were restricted to these patient samples which could be transduced to a high extent to perform a sufficient RGB marking and to discriminate as many cells as possible. Furthermore, we preferred AL PDX samples with a rather short passaging time in order to perform the experiments within a reasonable time frame.

In the beginning, various attempts to generate an efficiently RGB marked PDX sample by simultaneous transduction with lentiviruses produced from the three lentiviral vectors encoding Gaussia luciferase and the different fluorescent proteins depicted in Figure 6A were unsuccessful due to too low transduction efficiencies. This one step transduction with all three viruses did not result in transduction efficiencies that were high enough to generate RGB marked PDX cells containing double colored and triple colored cells expressing multiple individual mixed colors besides single colored cells.

We assumed that transduction with only one single vector per transduction round might yield a higher transduction rate for each single vector alone compared to transduction with three vectors at the same time. Therefore, I performed sequential rounds of lentiviral transduction with only one single vector per transduction round over three mouse passages to increase the efficiency for each single color. Indeed, sufficiently RGB marked PDX cells of PDX sample ALL-265 cells could be generated by successive transduction with the three vectors depicted in Figure 6A encoding Gaussia luciferase and mCherry, Venus or mTagBFP (Figure 9). In detail, transduction of PDX ALL-265 cells in three steps yielded cells 40% transgenic for mCherry, 81% for Venus and 18% for mTagBFP (see Table 10 and Figure 15A, upper panel).

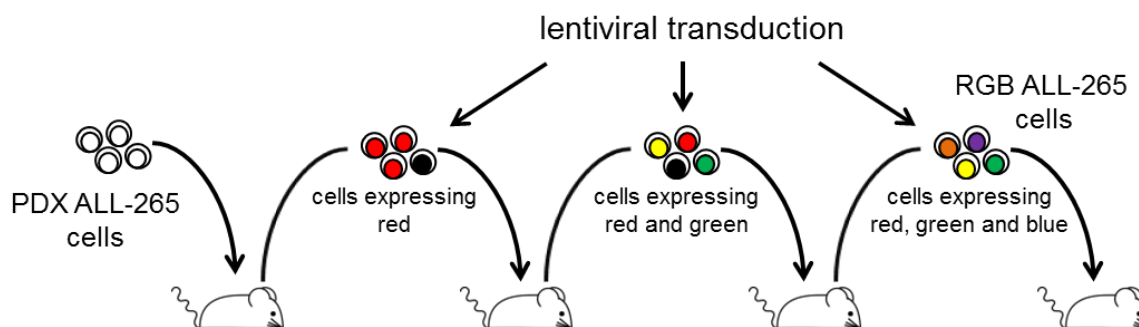


Figure 9: Experimental procedure for generation of RGB ALL-265.

PDX ALL-265 cells were successively RGB marked by consecutive transduction with the 3 lentiviruses depicted in Figure 6A encoding *Gaussia luciferase* and red, green or blue over 3 mouse passages resulting in RGB marked ALL-265 cells 40% transgenic for *mCherry*, 81% for *Venus* and 18% for *mTagBFP* (see Table 10 and Figure 15A, upper panel).

In addition, since it was known in the lab that smaller transfer vectors in general resulted in viruses with higher virus titers, we intended to increase virus titers by cloning of smaller constructs without expressing *Gaussia luciferase* depicted in Figure 6B. Indeed, compared to lentiviruses produced from transfer vectors encoding *Gaussia luciferase* and additionally one color, the smaller transfer vectors encoding one color but no *Gaussia luciferase* exhibited in general enhanced virus titers ranging from 1×10^{10} TU / ml to 1×10^{11} TU / ml compared to titers of big constructs (Figure 6A) which mainly varied between 1×10^9 TU / ml to 1×10^{10} TU / ml as determined on NALM-6 cell line cells (5.5.5).

Finally, RGB marked cells of two AML samples, AML-393 and AML-346, could be generated by simultaneous transduction with the three viruses produced with these smaller constructs illustrated in Figure 10 indicating that decreased vector size resulted in increased transduction efficiencies. In detail, RGB marked AML-393 cells were 40% transgenic for *mCherry*, 66% for *Venus* and 82% for *mTagBFP*, while RGB marked AML-346 cells were 20% positive for *mCherry*, 36% for *Venus* and 58% for *mTagBFP* (see Table 10 and Figure 12).

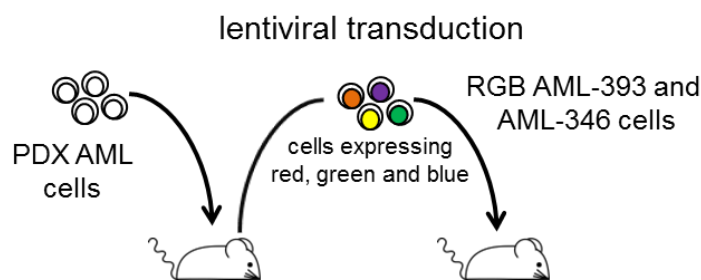


Figure 10: Experimental procedure for generation of RGB AML-393 and RGB AML-346.

PDX AML-393 and AML-346 cells were RGB marked by simultaneous transduction with the 3 lentiviruses (encoding red, green and blue) depicted in Figure 6B resulting in RGB marked AML-393 cells expressing 40% mCherry, 66% Venus and 82% mTagBFP and in RGB marked AML-346 cells 20% transgenic for mCherry, 36% for Venus and 58% for mTagBFP (see Table 10 and Figure 12A and B, upper panels).

Taken together, three RGB marked PDX samples, ALL-265, AML-393 and AML-346, described in the following table, were successfully generated by one or three step transduction with lentiviruses encoding three different fluorescent proteins with or without Gaussia luciferase.

Table 10: Transduction efficiencies of lentivirally transduced RGB PDX samples
color = mCherry, Venus or mTagBFP; GLuc = Gaussia luciferase

| Sample | Lentiviral vectors | Transduction performed | Transduction efficiencies (%) | | |
|---------|-------------------------------|-----------------------------|-------------------------------|-------|------|
| | | | red | green | blue |
| ALL-265 | pCDH-EF1 α -GLuc-color | successively in three steps | 40 | 81 | 18 |
| AML-393 | pCDH-EF1 α -color | in one step | 40 | 66 | 82 |
| AML-346 | pCDH-EF1 α -color | in one step | 20 | 36 | 58 |

6.2.4. RGB marking uncovered clonal outgrowth upon in vivo transplantation of AML

We aimed at generating RGB marked PDX AL cells as stable tools for future series of experiments. As PDX AL cells are reluctant towards growth in vitro, we relied on amplifying cells in NSG mice.

Hence, as described, we transduced freshly isolated PDX cells with the RGB lentiviruses and transplanted RGB marked cells into one mouse for amplification. In parallel and in order to control for any influence that mouse passaging might have, transduced PDX cells were seeded on irradiated EL08 feeder cells and co-cultured in vitro (5.3.3, Figure 11). Generally, PDX cells do

not grow in vitro, however co-culture with EL08 feeder cells enabled to keep them alive in culture for several days allowing to monitor transgene expression. Accordingly, PDX cells of AML-393 and AML-346 were simultaneously transduced with the three RGB lentiviruses each encoding a different fluorescent protein (Figure 6B) as described in 6.2.3. RGB marked cells of both PDX samples were transplanted into mice and, in addition, co-cultured on feeder layer for several days until they expressed the transgenes.

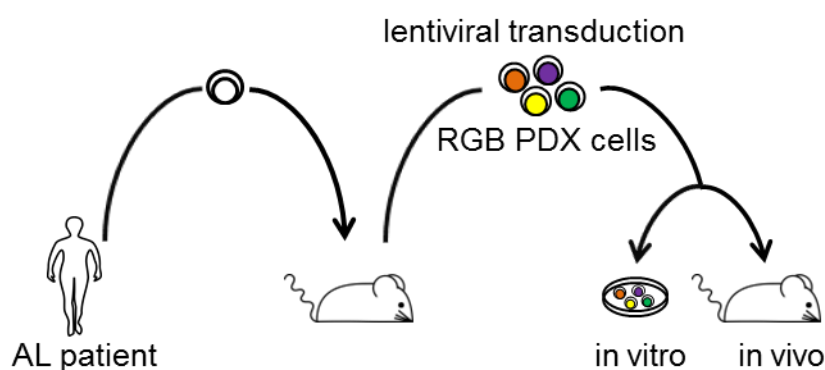


Figure 11: Amplification, lentiviral transduction and in vitro co-culture of RGB PDX cells.

2.5×10^6 PDX cells of AML-393 and AML-346 were RGB marked as described using three lentiviruses encoding red, green and blue depicted in Figure 6B. Transduced cells were either transplanted into recipient mice (1×10^6 cells per mouse) or co-cultured with irradiated EL08 feeder cells. Transgene expression was measured by flow cytometry after 6 days of in vitro culture and after mouse passage.

Flow cytometry analysis of in vitro co-cultured PDX AML-393 and AML-346 cells revealed sufficient transduction efficiencies, although unfortunately still well below cell lines; color expression revealed a Gaussian distribution for each color indicating that PDX cells were homogeneously transduced with red, green and blue (Figure 12A and B, upper panels). In contrast, when the same RGB marked PDX AML cells were amplified in mice, color expression in double and triple colored cells became patchy, while ellipsoid, egg-shaped clones started to appear (Figure 12A and B, lower panels). Patchiness is best analyzed in double and triple colored cells (upper right in the dot plots and upper right in the 3D cubes) because cells expressing two or three colors at different intensities can more easily be distinguished from each other than cells expressing only one color.

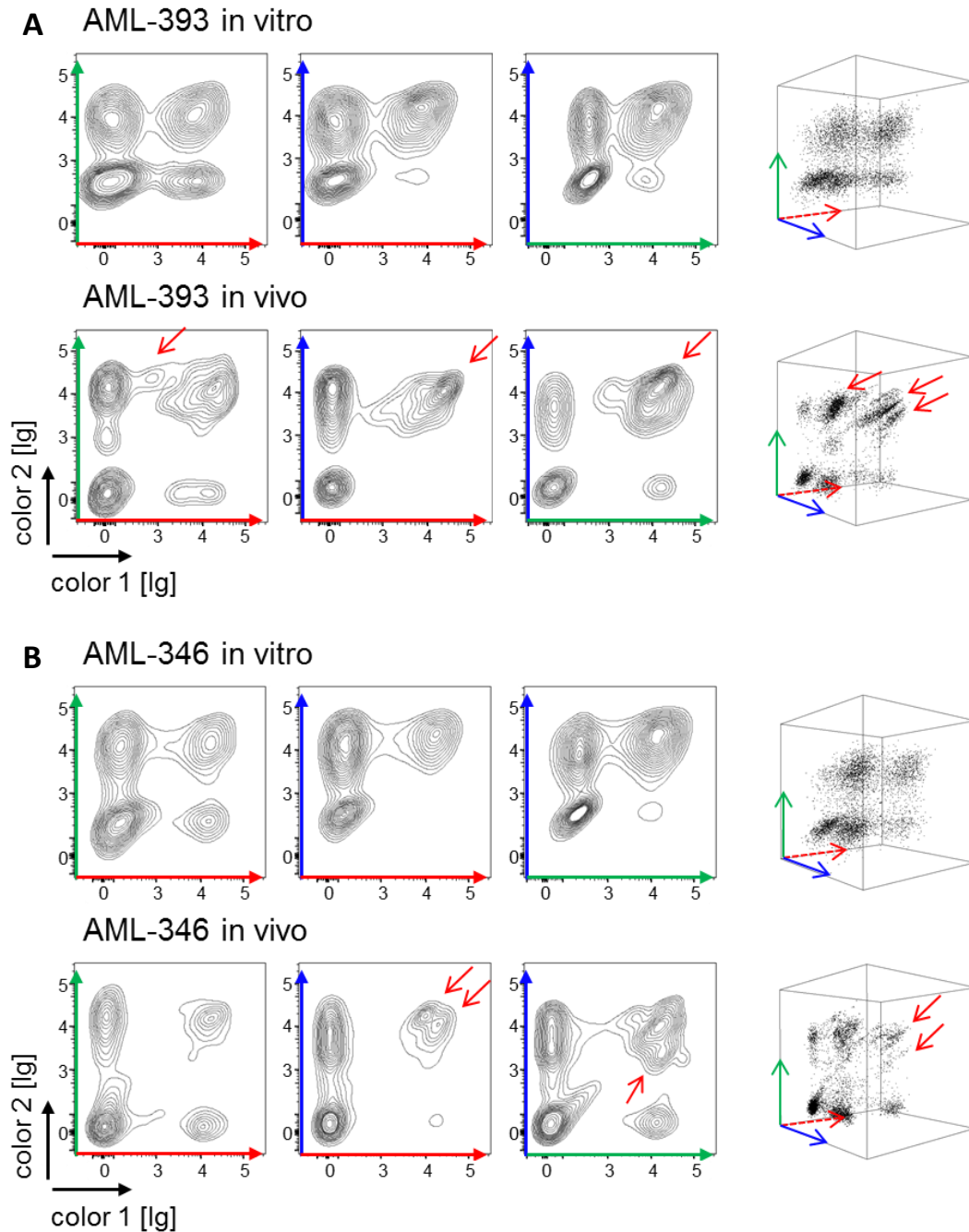


Figure 12: RGB marking of AML PDX cells revealed clonal outgrowth upon in vivo transplantation.

Transgene expression of RGB AML-393 (A) and AML-346 (B) was determined by flow cytometry after 6 days of in vitro co-culture (upper panel) and after xenotransplantation (1×10^6 cells/mouse, lower panel). Red arrows highlight dominant clones. Cells are pregated on living cells in FSC/SSC.

These data indicated that homing and growth of PDX AML cells in mice was not homogeneous, but rather some cells had homing and growth advantage, while other cells were completely lost resulting in areas in flow cytometry not covered by cells upon passaging. Thus, RGB marking of PDX AML cells detected that PDX AML samples changed during one mouse passage equaling

approximately six weeks and that the clonal composition of the sample was severely disturbed by passaging through mice. These data are in line with published data indicating that the individualized PDX mouse model of AML is associated with certain clonal selection (Klco et al., 2014).

6.2.5. Clonal outgrowth aggravated upon serial transplantation in ALL-265

As mouse model-based clonal selection could potentially interfere with the scientific questions, we next changed the AL subtype and studied ALL cells which are known from the literature to suffer only limited clonal alterations upon passaging through mice (Schmitz et al., 2011). Fortunately, ALL-265 showed an only slightly altered color distribution upon amplification in mice. Nevertheless, clonal selection aggravated over serial transplantation as illustrated in Figure 13. 1×10^6 PDX ALL-265 cells expressing mCherry and Venus at different intensities (passage 1) were serially passaged through mice and transgene expression was checked after each additional mouse passage. Flow cytometric analysis uncovered slight clonal outgrowth already after passage 2 while after passage 3, we could clearly detect outgrowth of three double colored clones located in the upper right section of the dot plots.

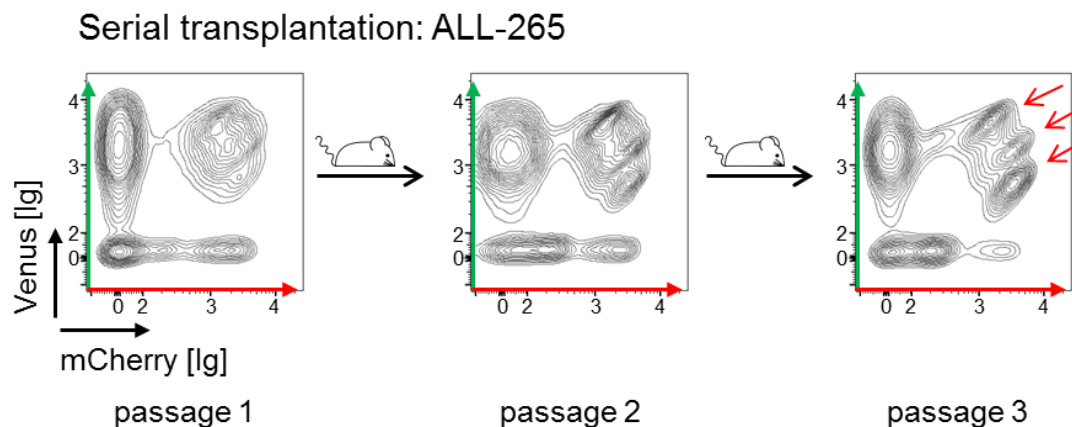


Figure 13: Clonal outgrowth aggravated upon passaging in ALL-265.

Cells of a red and green colored PDX ALL-265 sample were serially passaged through mice (1×10^6 cells/mouse, $n = 5$ for passage 2 and passage 3). Color distribution was checked by flow cytometry after each mouse passage. Shown is one dot plot out of five identical for passage 2 and passage 3. Red arrows highlight dominant cell clones. Cells are gated on living cells in FSC/SSC and on *muCD45* negative cells as shown in Figure 4.

In summary, clonal selection aggravated upon passaging in PDX ALL-265 suggesting that some clones were more dominant compared to others and that during each mouse passage certain

cells got lost; nevertheless, we considered the color distribution of the three colored sample PDX ALL-265 (see Figure 15A, upper panel) generated as described in Figure 9 as sufficient for the planned studies.

6.3. Limiting dilution transplantation of RGB PDX cells to generate single cell clones

We next aimed at generating single PDX cell clones from our RGB stained samples. As described in 3.2.3, leukemias are maintained by their LSCs since only LSCs have the potential to initiate leukemia in xenografts and to propagate the disease upon serial transplantation. In contrast, non-LSCs without cancer initiating potential are lost upon serial transplantation. Such, each single cell clone originates from a single RGB marked PDX stem cell and all cells developing thereof are putatively genetically identical.

Towards this aim, we performed a limiting dilution transplantation assay (LDA, 5.2.2) in which we transplanted different numbers of RGB marked PDX cells into groups of mice. Subsequently, cells were recovered from spleen of diseased mice and analyzed by flow cytometry for color expression which was compared between the groups. In this context, we performed two LDAs with generated RBG marked PDX samples AML-393 and ALL-265.

6.3.1. Stem cell frequencies of PDX ALL-265 and PDX AML-393

AML-393 cells that were RBG marked by simultaneous transduction with the three lentiviruses as illustrated in Figure 10 were transplanted at limiting dilution into groups of mice as described in Table 11.

Table 11: Numbers of cells and mice used for LDA of RGB AML-393.

Calculated LSC frequency: 1/2,000 cells or higher.

| cells / mouse | engraftment | days to full leukemia (mean) |
|-----------------|-------------|------------------------------|
| 2×10^6 | 3/3 | 35 |
| 2×10^5 | 3/3 | 39 |
| 2×10^4 | 3/3 | 49 |
| 2×10^3 | 3/3 | 56 |

Accordingly, RGB ALL-265 cells generated as described in Figure 9 were subsequently transplanted at limiting dilution into groups of mice as shown in Table 12.

Table 12: Numbers of cells and mice used for LDA of RGB ALL-265.

Calculated LSC frequency: 1/27 cells (CI = 95%) (lower = 57.8; upper = 12.5).

| cells / mouse | engraftment | days to full leukemia (mean) |
|-----------------|-------------|------------------------------|
| 1×10^5 | 3/3 | 41 |
| 1×10^4 | 3/3 | 54 |
| 1×10^3 | 3/3 | 65 |
| 333 | 5/5 | 83 |
| 1×10^2 | 10/10 | 81 |
| 33 | 3/5 | 92 |

Table 11 and Table 12 illustrate the amount of cells transplanted per mouse, the number of engrafted mice per group and the mean value of days until the mice had to be sacrificed due to leukemia for each group for both LDAs.

Stem cell frequencies of RGB AML-393 and RGB ALL-265 were calculated based on the amount of transplanted cells and the total number of engrafted mice per group according to Poisson statistics, using the ELDA software application (<http://bioinf.wehi.edu.au/software/elda/>) (Hu & Smyth, 2009).

For RGB AML-393, we could not clearly determine the LSC frequency because we observed engraftment in all mice that had received 2×10^3 cells but we did not check if a lower amount of cells would have initiated leukemia as well. Therefore, the stem cell frequency for RGB AML-393 is at least 1 LSC in 2,000 cells or even higher and thus rather high compared to published data, although published data determined LSC frequency mostly upon transplanting primary AML cells and not PDX AML cells (Eppert et al., 2011; Sarry et al., 2011).

For RGB ALL-265, we calculated a stem cell frequency of 1 LSC in 27 cells which is in line with published data showing that in ALL stem cell frequencies tend to be rather high (Kelly et al., 2007; Rehe et al., 2013). Precisely, all ten mice that were injected with 100 cells engrafted and even 3 of 5 mice injected with only 33 cells engrafted suggesting that in line with published results nearly every cell of this ALL sample has stem cell properties and is able to propagate the disease.

6.3.2. Transplantation of low cell numbers delayed disease progression in recipient mice

Both LDAs revealed a close correlation of the amount of transplanted cells and the survival time of the recipient mice. Mice transplanted with as many as 1×10^5 cells of RGB ALL-265, succumbed to the disease within 41 days, whereas mice that had been injected with only 33 cells survived for up to 92 days (Table 12; Figure 14A). In the LDA of RGB AML-393, survival time of recipient mice ranged from 35 days for 2×10^6 transplanted cells up to 56 days for mice injected with solely 2×10^3 cells (Table 11; Figure 14B). In general, mice that had received more cells died quicker, while disease progression was delayed upon transplantation of low cell numbers. These results are illustrated in the Kaplan Meier survival curves depicted in the following.

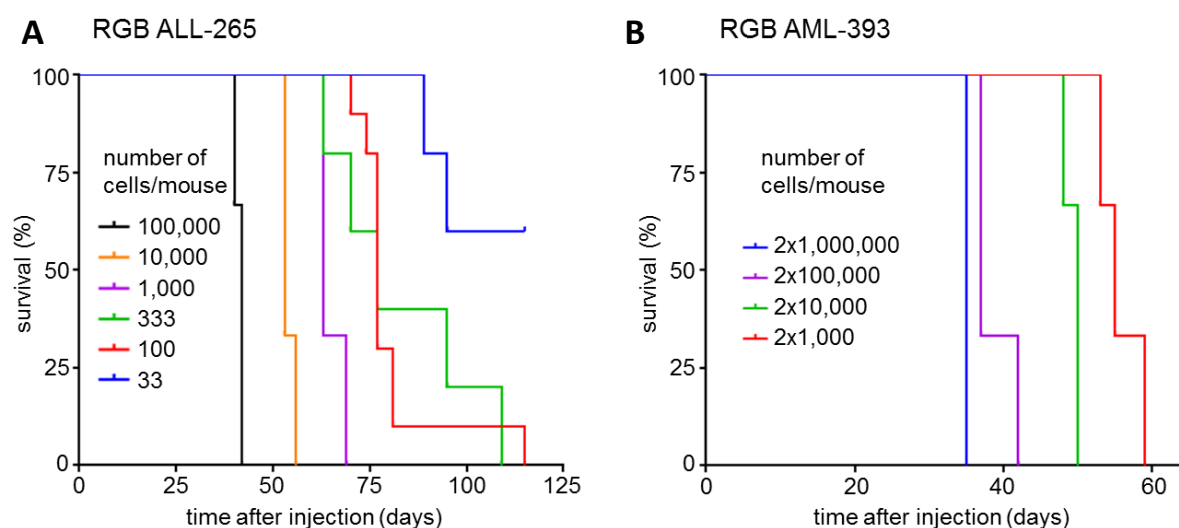


Figure 14: Kaplan Meier survival curves for LDAs with cells of RGB ALL-265 and AML-393.

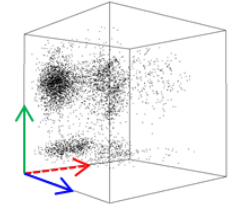
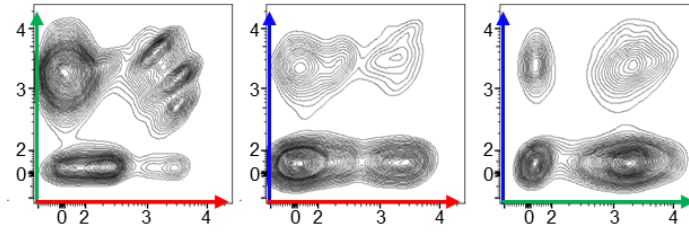
Kaplan Meier survival curves for mice engrafted with different amounts of cells of RGB ALL-265 (A) and RGB AML-393 (B) as described in Table 11 and Table 12. Mice were sacrificed as soon as they showed clinical signs of the disease.

6.3.3. Transplantation of low cell numbers allowed isolation of specifically colored single cell clones

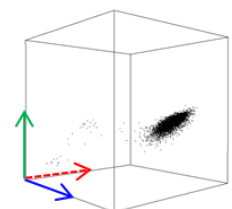
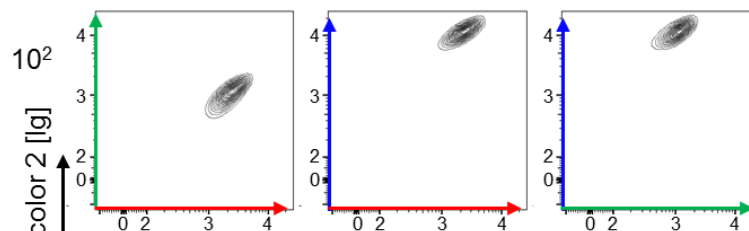
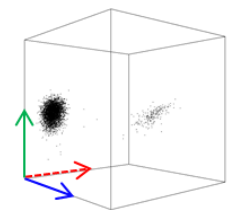
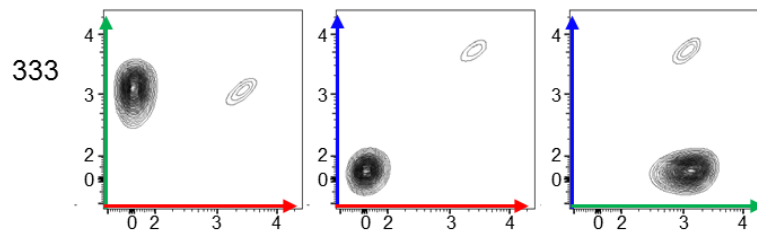
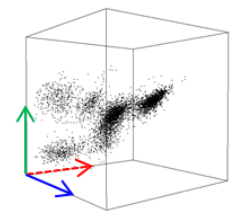
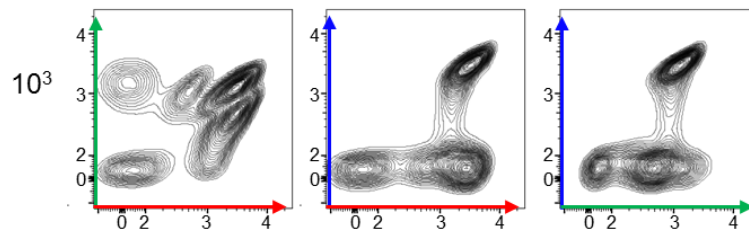
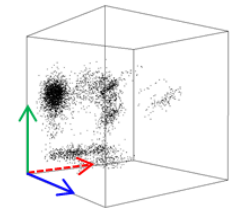
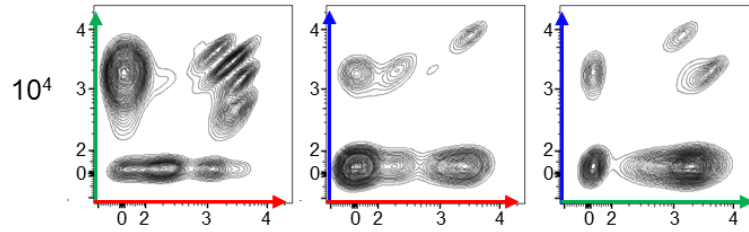
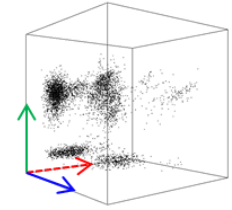
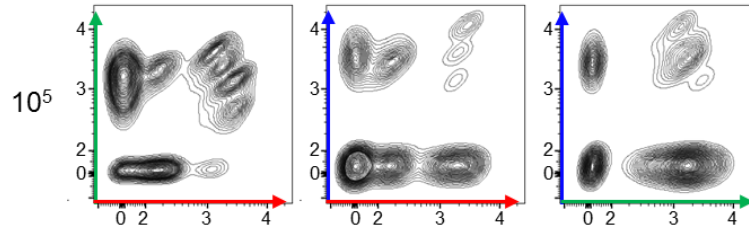
To investigate whether the amount of colors correlated with the amount of transplanted cells, color expression in spleen derived cells of each LDA mouse was determined when the mouse was sacrificed. Human cells in mouse spleens were purified and analyzed by flow cytometry for expression of mCherry, Venus and mTagBFP. For both PDX samples, ALL-265 and AML-393, we

found the amount of expressed colors to be dependent on the amount of transplanted cells. In general, the more cells were transplanted, the more colors were obtained (Figure 15). Accordingly, transplantation of many cells yielded only a slight decrease in colors whereas transplantation of marginal amounts of cells resulted in a profound reduction of colors. Upon transplantation of few cells, clonal outgrowth was more prominent in both samples and single cell clones could be distinguished from each other based on their individual colors. Ultimately, when only minute amounts of cells were injected into mice, flow cytometric analysis revealed clonal expansion of only one single clone.

A

RGB ALL-265
(Bulk 1)number of
cells/mouse

Bulk 2



color 2 [lg]
color 1 [lg]

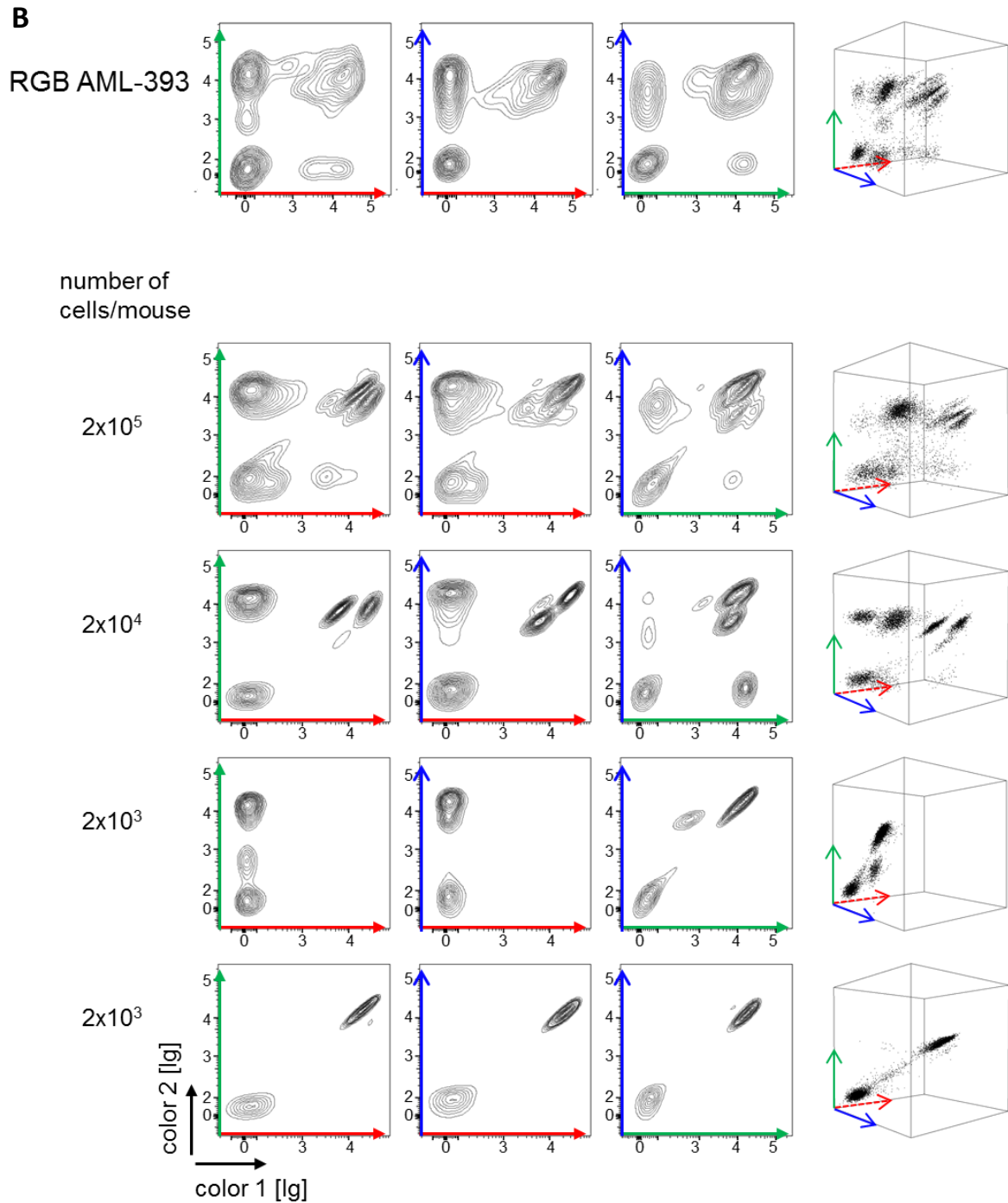


Figure 15: Transplantation of low cell numbers decreased the amount of differently colored populations. Cells of RGB ALL-265 (A) and RGB AML-393 (B) were transplanted at limiting dilution as described in Table 12 and Table 11. Expression of mCherry, Venus and mTagBFP was assessed by flow cytometry in spleen derived cells of all recipient mice. Color expression of one representative mouse for the indicated LDA group is shown in 2- and 3-dimensional plots. Depicted dot plots are pregated on living cells and on muCD45 negative cells as shown in Figure 4.

6.3.4. Generating single cell clones of ALL-265

We decided to restrict our further studies to sample PDX ALL-265. As described in 6.3.3, limiting dilution transplantation of RGB ALL-265 resulted in generation of numerous individually colored single cell clones. In those LDA samples of RGB ALL-265, in which either only one single cell had engrafted or engrafted single cell clones could clearly be separated from each other by flow cytometry, clones were purified for further studies using flow cytometry (5.5.8). This was the case in groups in which 33, 100 or 333 cells had been transplanted per mouse. To have enough cells for all functional analyses, sorted cells of each single cell clone were injected into two recipient mice for amplification in two biological replicates. Two samples without limiting dilution, but at different passages were used as control for further experiments and called “Bulk 1” and “Bulk 2”; Bulk 2 was obtained by amplification of 1×10^5 cells of Bulk 1. The experimental procedure for generation of single cell clones is summarized in Figure 16.

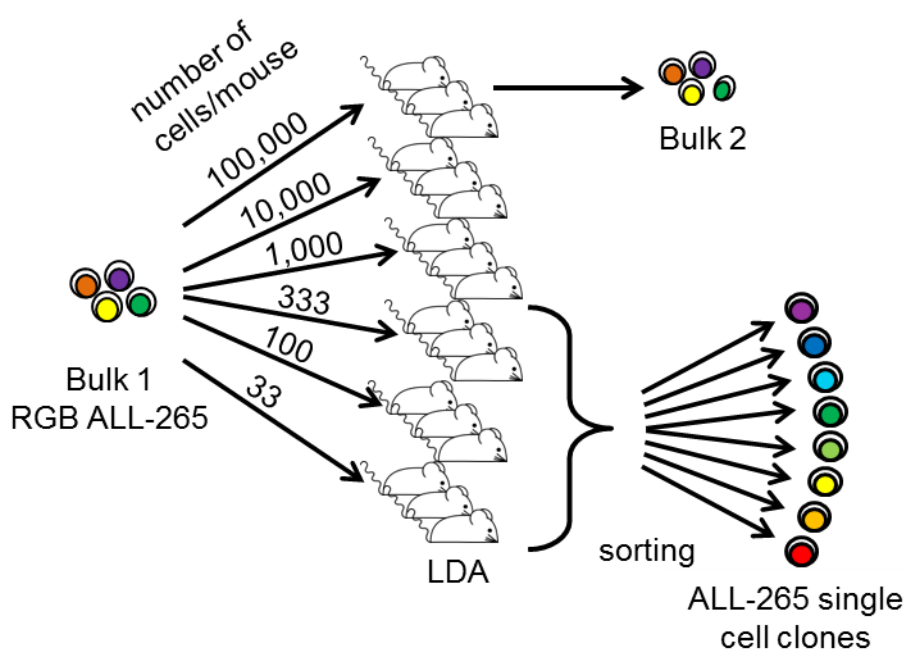


Figure 16: Procedure for generation of single cell clones expressing unique colors.

RGB ALL-265 Bulk 1 cells were transplanted at limiting dilution (Table 12, Figure 15A). Individually colored single cell clones could be distinguished upon injection of low cell numbers (333, 1×10^2 or 33 cells/mouse) and purified using flow cytometry. Bulk 2 was generated by transplantation of 1×10^5 cells of Bulk 1.

Thus, I generated eight single cell clones by limiting dilution transplantation of a RGB marked PDX ALL-265 sample. Since all clones originated from clonal expansion of single individually

colored LSCs, they were defined by unique colors and could be distinguished from each other using flow cytometry. Specific color expression was determined for each clone and could be illustrated in 2- or 3-dimensional plots as shown in Figure 17. As major advantage, single cell clones revealed highly distinct colors so that they could be distinguished from each other in mixtures using flow cytometry – an important characteristic for the later functional competitive analyses in mice.

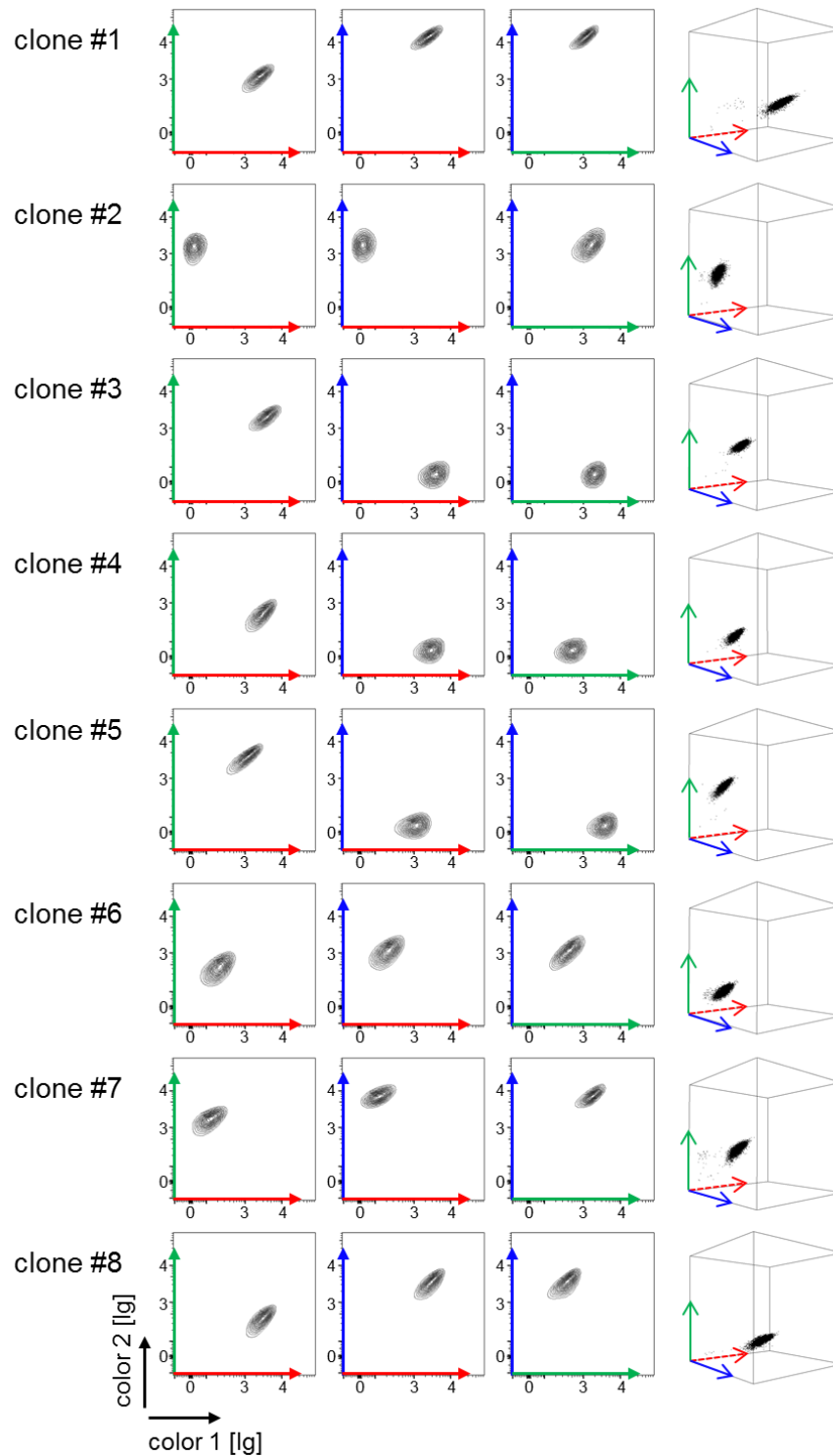


Figure 17: Generated ALL-265 single cell clones.

8 clones were sorted using flow cytometry and re-passaged for amplification (1×10^5 cells/mouse; 2 biological replicates/clone). Human cells were purified out of mouse spleens and measured by flow cytometry. Depicted are 2- and 3-dimensional plots to illustrate color expression of each cell clone. Cells are gated on living cells and muCD45 negative cells according to Figure 4; shown is color distribution of 1 biological replicate per clone.

Although RGB marking indicates with a high likelihood that single cell clones resulted from a true single cell, two different cells might by chance receive and express the identical color combination. To verify that each clone was truly derived from a single cell at the beginning, our collaboration partner Kerstin Cornils (Forschungsabteilung Zell- und Gentherapie, UK Hamburg-Eppendorf, Hamburg, Germany) performed LM-PCR to identify viral integration sites in all clones. In contrast to flow cytometry which could distinguish single cell clones by expression of different colors, LM-PCR allowed discrimination of single cell clones on the molecular level based on individual viral integration sites. LM-PCR detected at least two individual integration sites per clone which served as an exclusive marker for that clone strengthening the hypothesis that all clones originated from clonal expansion of single cells.

In summary, combining the individualized xenograft mouse model with genetic engineering allowed multicolor staining of PDX cells. Limiting dilution transplantation enabled generating viable single cell clones from one patient's ALL expressing an individual color and Gaussia luciferase enabling bioluminescence in vivo imaging. Finally, we had extensive amounts of viable cells of each cell clone at hand which we subjected to functional characterization in vitro and in vivo regarding growth behavior and chemosensitivity.

6.4. Single cell clones differed in growth behavior in vivo

The subclonal architecture in ALL is complex including different subpopulations. Moreover, subclonal composition in ALL patients is dynamic and changes during disease progression (Anderson et al., 2011; Ma et al., 2015; Mullighan et al., 2008; van Delft et al., 2011). Accordingly, leukemic clones that were dominant at diagnosis may be small clones at relapse or may even have disappeared entirely. In contrast, minor clones at diagnosis may become dominant at relapse indicating either favorable growth behavior or impaired sensitivity to chemotherapy. Hence, subclones with a particular survival benefit may outcompete less fit clones over time.

Having now eight differently colored ALL-265 single cell clones at hand, we performed functional in vivo studies comparing the clones between each other using two bulk samples as controls.

We first asked, whether certain clones might exhibit adverse growth properties and especially show slow growth patterns which is associated with stemness and drug resistance. Slow growth might be considered as adverse clonal characteristic as it might be related to drug resistance. To

answer this question, we subjected single cell clones to competitive xenotransplantation experiments.

6.4.1. Competitive transplantation of five single cell clones uncovered divergent growth properties among clones

To investigate whether the single cell clones differed in growth behavior, differently RGB marked clones were transplanted into the same recipient mice in a competitive setting. Since I could distinguish up to five single cell clones via flow cytometry based on their individual colors, I mixed five clones in equal parts and injected them into immunocompromised mice. Finally, I assessed how clonal composition had changed during one mouse passage by comparing clonal composition before and after mouse passage (Figure 18).

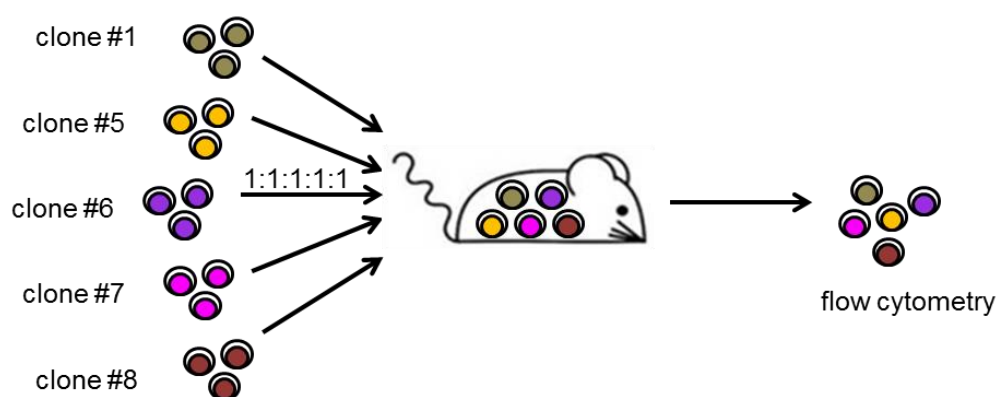


Figure 18: Experimental procedure for competitive transplantation of five clones.

Five differently colored clones were mixed in equal parts and injected into the same recipient mice (2.5×10^4 cells / mouse; $n = 4$). After mouse passage, leukemic cells were isolated out of mouse spleens and percentage of each clone was assessed by flow cytometry.

Due to individual color expression, the clones could clearly be separated from each other by flow cytometry (Figure 19). All five clones were mixed so that each clone accounted for 20% of total cells. When mice showed advanced disease, leukemic cells were analyzed for the presence of all five clones. Flow cytometry analysis of leukemic cells after mouse passage revealed marked changes in constitution of leukemic cells: two clones had overgrown the remaining three clones. In detail, we found clone #7 and clone #5 to be considerably enriched whereas clone #1, clone #8 and clone #6 had markedly decreased (Figure 19).

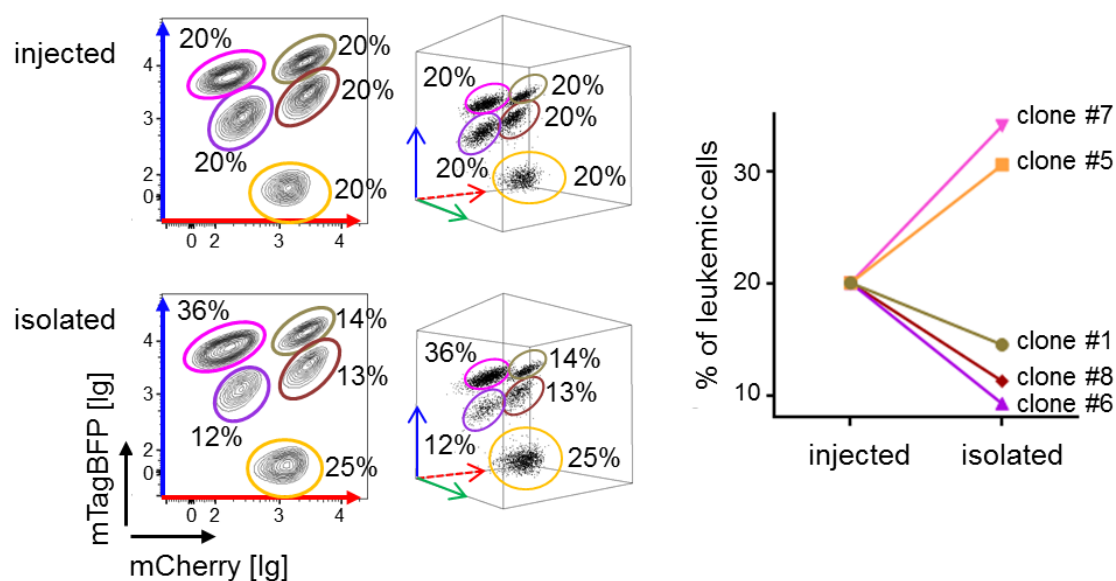


Figure 19: Competitive transplantation of five clones uncovered divergent growth behavior.

Equal numbers of clones #1, #5, #6, #7 and #8 were mixed (left side, upper panel) and transplanted (2.5×10^5 cells / mouse; $n = 4$). Percentage of each clone in spleen derived cells was assessed by flow cytometry after transplantation (left side, lower panel). Depicted are dot plots illustrating expression of mCherry and mTagBFP for all clones and cubes to illustrate color expression in 3D. Shown is one representative mouse out of four. Cells are pre-gated on living cells in FSC/SSC and muCD45 negative cells (Figure 4). The graph (right side) illustrates the percentage of each clone before and after transplantation (depicted are mean values for each clone, $n = 4$; SDs: clone #1 1.4%, #5 5.0%, #6 2.5%, #7 3.9%, #8 1.5%; results of single mice are illustrated in Figure 23C).

Our data indicate that single PDX ALL cell clones reveal a marked heterogeneity regarding in vivo growth behavior and that certain clones show an especially slow growth pattern.

6.4.2. Competitive transplantation of two single cell clones confirmed differences in growth behavior

Competitive engraftment experiments with five clones clearly demonstrated the selective growth advantage of clone #7 and clone #5 compared to clone #1, clone #8 and clone #6. To further validate these findings, I reduced the complexity and repeated the experiment as depicted in Figure 20 with combinations of only two clones to test if clone #5 maintained its growth advantage when transplanted together with only one additional clone in a competitive

setting. This second, complementary experimental approach allows understanding, whether growth advantage is clone-inherent or a condition relying on the entire complex tumor.

Accordingly, clone #5 was either combined with clone #6 or with clone #8 or in another experiment, I tested the combination of clone #6 and clone #8.

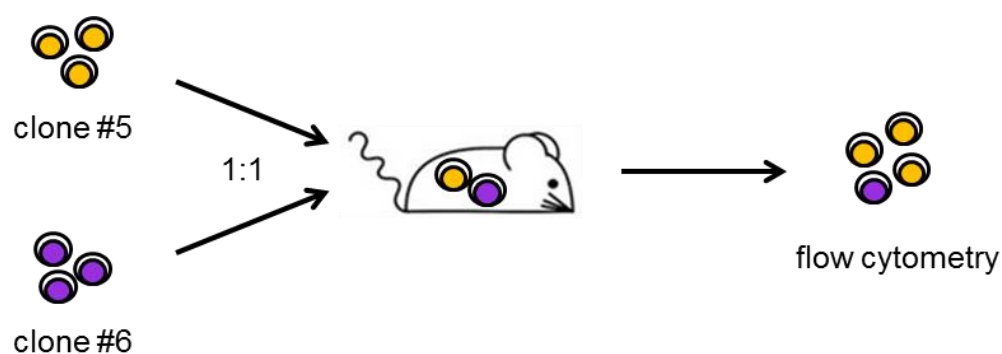


Figure 20: Procedure for competitive transplantation of two clones.

Two differently marked clones were mixed in equal parts and transplanted into mice (1×10^5 cells / mouse; $n = 5$). After mouse passage, leukemic cells were isolated out of mouse spleens and the percentage of each clone was assessed by flow cytometry.

Competitive transplantation of clone #5 and clone #6 revealed that clone #5 had significantly overgrown clone #6 so that in average 93% of total leukemic cells belonged to clone #5 and only 7% to clone #6 (Figure 23A). The result taken from one representative mouse of this combination is depicted in Figure 21A.

The same experiment was performed with mixtures of clone #5 and clone #8 and of clone #6 and clone #8. The results of one representative mouse for each combination are depicted in Figure 21B and Figure 21C. Here, we could also detect differences in clonal composition before and after xenotransplantation. However, the effects were less prominent. In the combination of clone #5 and clone #8 we observed only a minor change in favor of clone #5 so that in average 62% belonged to clone #5 and 38% to clone #8. Combination of clone #6 and clone #8 resulted in a slight outgrowth of clone #8 to 75% in average combined with a decrease of clone #6 to 25% in average (Figure 23A).

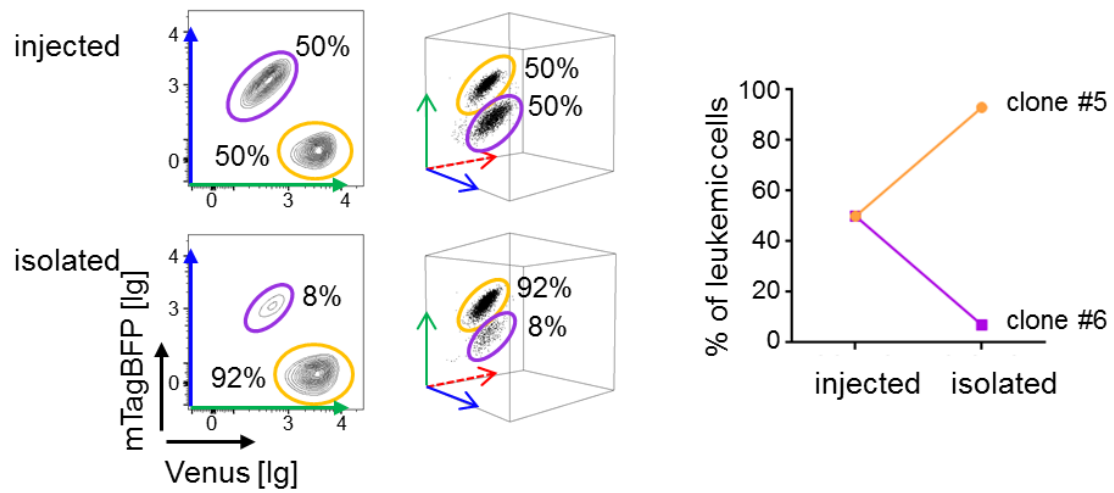
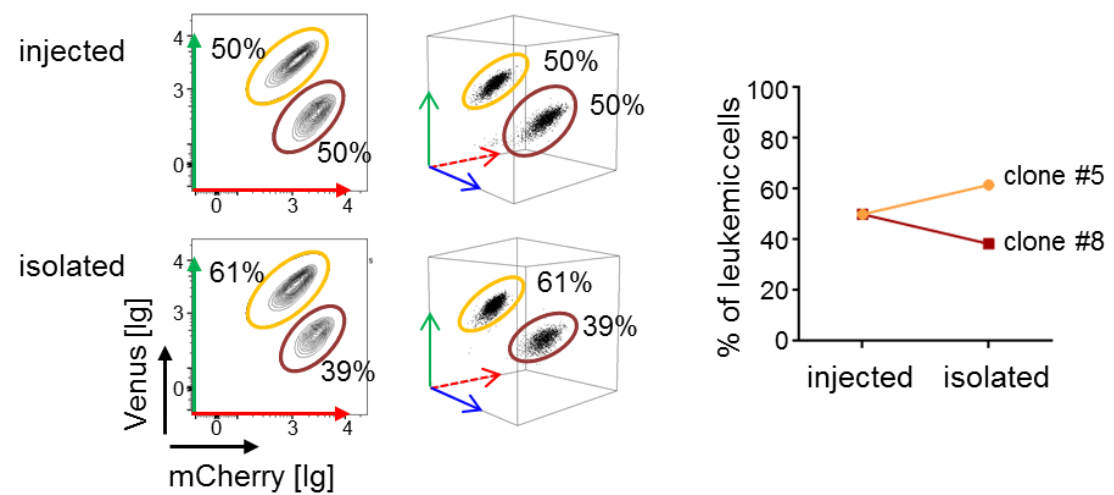
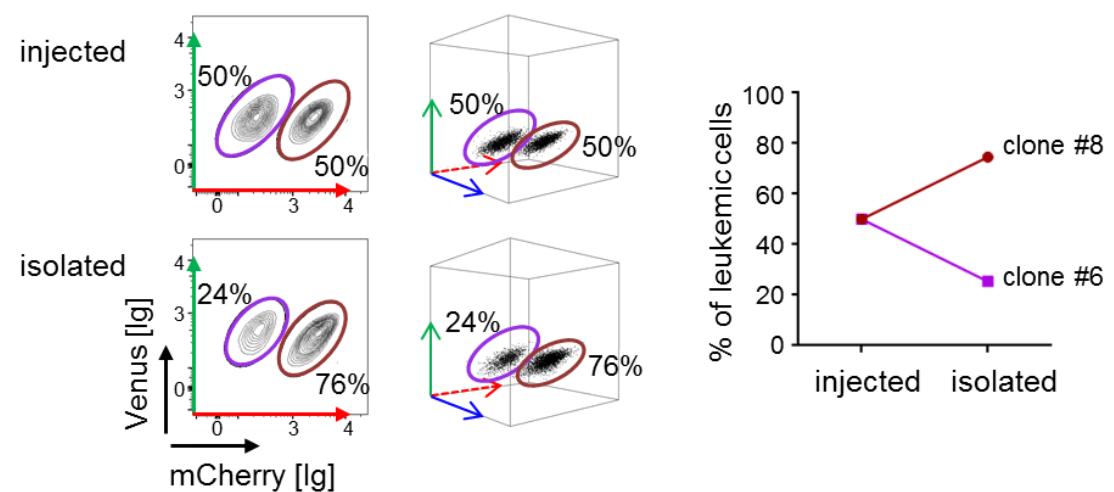
A clone #5 + clone #6**B clone #5 + clone #8****C clone #6 + clone #8**

Figure 21: Competitive transplantation of two clones confirmed different growth properties in vivo.

Cells of two differently marked clones were mixed in equal parts (upper panels) and transplanted (1×10^5 cells/mouse; $n = 5$). Shown is one representative mouse for each of the three different combinations. (A-C) Results for competitive transplantation of indicated clone pairs. Percentage of each clone in spleen derived cells was determined by flow cytometry (lower panels). Depicted dot plots are gated on living cells in FSC/SSC and muCD45 negative cells (Figure 4). Graphs show ratios of both clones before and after mouse passage ($n = 5$, mean values; A: SD 1.2%; B: SD 3.2%; C: SD 5.0%; results of single mice are illustrated in Figure 23A).

These results were consistent with our previous observations, obtained in the experiment in which we transplanted five clones described in 6.4.1, and confirmed that clone #5 kept its growth advantage in vivo irrespectively whether it was transplanted with one or four clones into the same mouse. Furthermore, clone #8 and, particularly, clone #6 exhibited impaired growth behavior when transplanted together with clone #5. In summary, these data indicate that the three clones tested showed divergent growth properties in vivo when mixed and transplanted in a competitive setting in pairs of two clones. Especially, the prominent increase of clone #5 when combined with clone #6 was remarkable and independent from the presence of other clones from the tumor.

To investigate whether the growth advantage of clone #5 would persist over prolonged periods of time, we tested whether clone #5 would continue to overgrow clone #6 and clone #8 upon serial re-transplantation. Cells of two representative samples of the first competition cycle of the combination of clone #5 and clone #6 depicted in Figure 21A and of the combination of clone #5 and clone #8 depicted in Figure 21B were chosen and each injected into secondary recipient mice. As shown in Figure 22, clonal outgrowth of clone #5 proceeded also upon secondary transplantation for both combinations underlining favorable growth properties of clone #5 compared to clone #6 and clone #8.

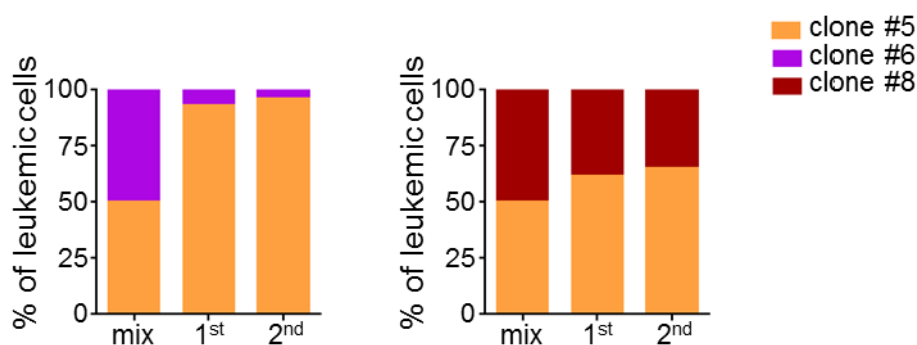


Figure 22: Growth advantage of clone #5 continued upon re-transplantation.

2 representative samples of clone #5 plus clone #6 (Figure 21A) and clone #5 plus clone #8 (Figure 21B) were injected into secondary recipient mice ($n = 3$ for each combination; 1×10^4 cells/mouse); percentages for both clones were determined by flow cytometry, respectively. Graphs show mean values ($n = 6$: 2 biological and 3 technical replicates) of the percentages of each clone as injected (mix) and after first and second transplantation (for results of single mice and statistical data see Figure 23A and Figure 23B).

Remarkably, for all competitive engraftment experiments the results were highly comparable between all mice with astonishingly low inter-mouse variances. Upon transplantation of two single cell clones in a competitive setting, we detected only minor standard deviations between 1.2% and 5.0% (Figure 23A). This was also true for the re-transplantation experiments of samples consisting of two clones in which two representative samples were transplanted into secondary recipient mice. Here, we discovered standard deviations of only 1.6% and 7.8%, although two different biological replicates were used for secondary transplantation (Figure 23B). Ultimately, the percentages for each clone were also highly reproducible among all biological replicates with very low standard deviations between 1.4% and 5% when five clones were injected into the same mouse.

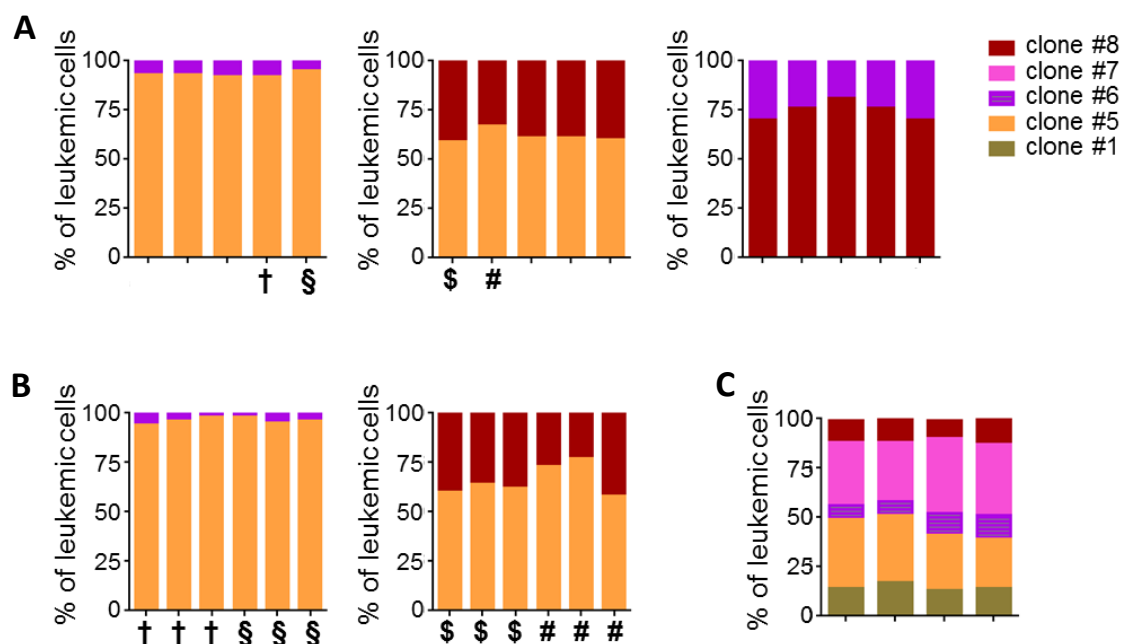


Figure 23: Outcompete experiments yielded reproducible results in all mice.

Flow cytometry analysis of leukemic cells re-isolated after primary (A) or secondary (B) transplantation of mixtures of the indicated single cell clones. (A) Competitive transplantation of different pairs of clones as depicted in Figure 21. Clone #5 + clone #6: mean #5 93%, #6 7%, SD 1.2%; clone #5 + clone #8: mean #5 62%, #8 38%, SD 3.2%; clone #6 + clone #8: mean #6 25% #8 75%, SD 5.0%. †, \$, § and # indicate samples that were injected into secondary recipients (B) Secondary transplantation as shown in Figure 22. Clone #5 + clone #6: mean #5 96%, #6 4%, SD 1.6, clone #5 + clone #8: mean #5 66%, #8 34%, SD 7.8. (C) Competitive transplantation of five clones as illustrated in Figure 19. Mean values: clone #1 15%, #5 31%, #6 9%, #7 34%, #8 12%, SDs: #1 1.4%, #5 5.0%, #6 2.5%, #7 3.9%, #8 1.5%. Each bar illustrates analysis of cells re-isolated out of one single mouse.

In summary, we could show that five single cell clones derived from PDX ALL-265 exhibited divergent growth behavior when transplanted into the same recipient mice. Using transplantation experiments with different combinations of two clones, we could confirm the tendencies observed in the competitive transplantation experiment with five clones: clone #6 and clone #8 showed the putatively adverse characteristic of slow growth in all competitive in vivo proliferation assays.

6.5. Single cell clones differed in chemosensitivity in vitro and in vivo

A highly important functional characteristic of tumor cells determining the prognosis of patients is their response to treatment and potential drug resistance described in 3.2.2. Minimal residual disease cells described in 3.1.2 may survive therapy, regrow and induce relapse. Since leukemias

are life-threatening diseases, patients receive treatment immediately after diagnosis. Consequently, the impact that chemotherapy has on clonal evolution has to be taken into account. Selective pressure of treatment may promote outgrowth of resistant subclones and, in addition, chemotherapy might even induce new mutations that may confer resistance to treatment.

In a next step, I investigated, whether the generated ALL clones were heterogeneous in terms of chemosensitivity, in order to identify drug resistant subclones.

6.5.1. Single cell clones differed in drug sensitivity in vitro

To check if the clones exhibited differences regarding chemosensitivity in vitro, I systematically analyzed sensitivity of all clones towards specific drugs in vitro. Since PDX ALL cells do not grow in vitro and show markedly reduced viability after freezing and thawing, PDX ALL-265 cells freshly isolated from mice were subjected to short term culture with or without cytotoxic drugs (5.3.7, Table 7). In these cultures, PDX ALL cells show rapid spontaneous death so that experiments of a maximum of 72 hours can be performed. After 72 hours, the amount of apoptotic cells was quantified by flow cytometry using forward-side scatter analysis and specific apoptosis rates were calculated based on spontaneous apoptosis rates of untreated cells.

At first, in order to validate the gating strategy for assessing the amount of apoptotic cells, non-transgenic PDX ALL-265 cells were treated with four different concentrations of cytarabine (AraC) for 72 hours. Specific apoptosis was measured by flow cytometry by gating on living cells in FSC/SSC as well as by double staining with DAPI and with anti Annexin V-APC antibody (5.3.6). The amount of apoptotic cells assessed by these two different strategies correlated very well as shown in Figure 24. As a consequence, we assessed the number of apoptotic cells after in vitro drug treatment of single cell clones by gating on living cells in FSC/SSC.

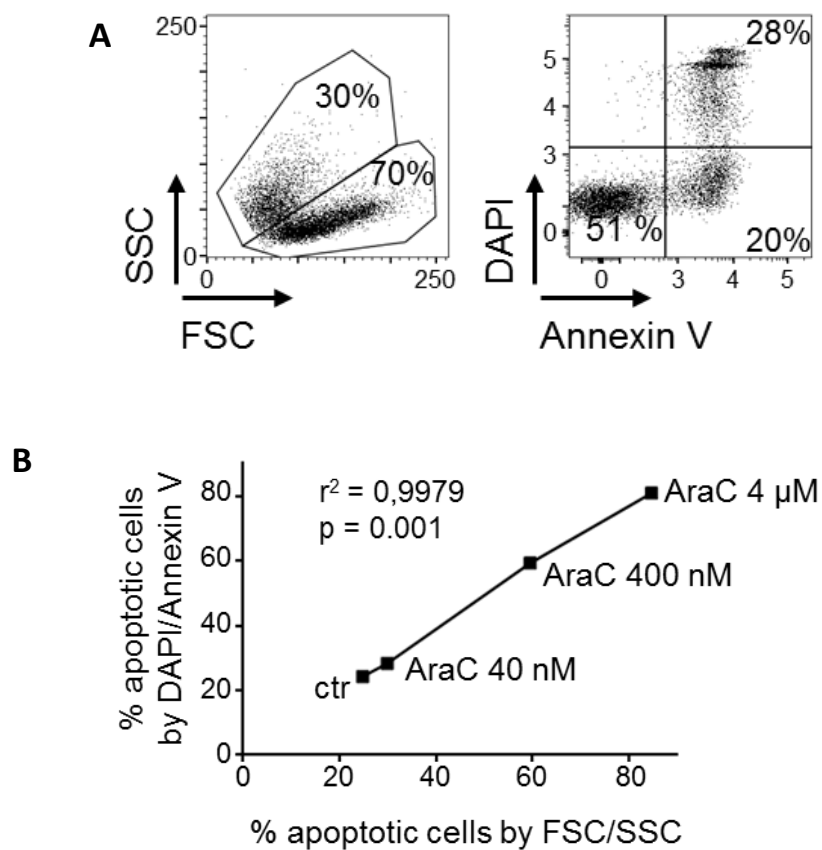


Figure 24: Percentage of specific apoptosis is independent from gating strategy

PDX ALL-265 cells were treated with different concentrations of cytarabine (AraC) for 72 hours. (A) Cells were stained with DAPI and with anti Annexin V-APC. Flow cytometry analysis was performed and the amount of apoptotic cells was assessed by two different strategies: gating on living cells in FSC/SSC and on cells double positive for DAPI and Annexin V. Debris was excluded in a first gating step. (B) Both strategies yielded similar results.

We first asked, whether the spontaneous apoptosis rate would differ between the clones, but did not detect major differences regarding spontaneous apoptosis rates among all single cell clones and bulk cells (Figure 25).

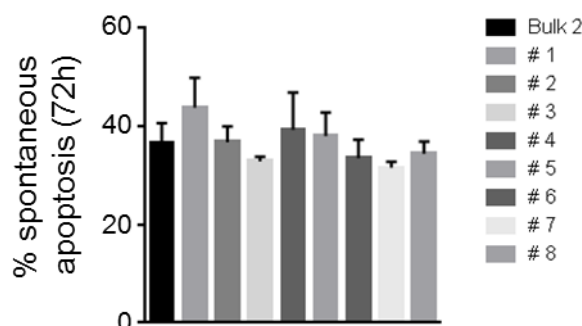


Figure 25: Single cell clones exhibited similar spontaneous apoptosis rates in vitro.

Fresh cells of each clone were cultured without treatment (1×10^5 cells / well; 2 biological replicates and 2 technical replicates / clone; $n = 4$). Spontaneous apoptosis rates after 72 hours were determined by flow cytometry by gating on living cells in FSC/SSC as described.

Upon drug treatment, remarkably, the measured specific apoptosis rates were highly reproducible with very low standard deviations between duplicate wells and even between biological replicates (Figure 26 and Figure 27).

In general, I discovered profound diversity in drug response among all eight clones tested; specific apoptosis rates after stimulation with different drugs were diverse among all clones. Response to some drugs was rather homogeneous while sensitivity towards other drugs was different among clones. For instance, I detected only minor variances upon stimulation with the three anthracyclines daunorubicine, doxorubicine and epirubicine (Figure 26A). But still, I found these differences to be significant in some cases. For example sensitivity of clone #6 which was the least affected and clone #8 which was the most sensitive towards stimulation with all three anthracyclines differed significantly. Strikingly, even if I observed only small differences in sensitivity against all three anthracyclines among all clones, the trends were similar so that, for instance, clone #6 was least susceptible against all three compounds while bulk cells, clones #1, #2, #7 and #8 were always highly sensitive.

Upon treatment with cytarabine and L-asparaginase, the results were more heterogeneous (Figure 26B). Here, measured drug response between several clones and bulk cells varied profoundly. For example, bulk cells, clone #7 and clone #8 were highly sensitive to cytarabine while clone #5 and clone #6 were less susceptible. Upon stimulation with L-asparaginase, I observed major differences, too: bulk cells, clone #1, clone #7 and clone #8 were more sensitive

compared to the other clones. Remarkably, clone #3 which was sensitive towards all anthracyclines and towards cytarabine, was less affected by L-asparaginase treatment.

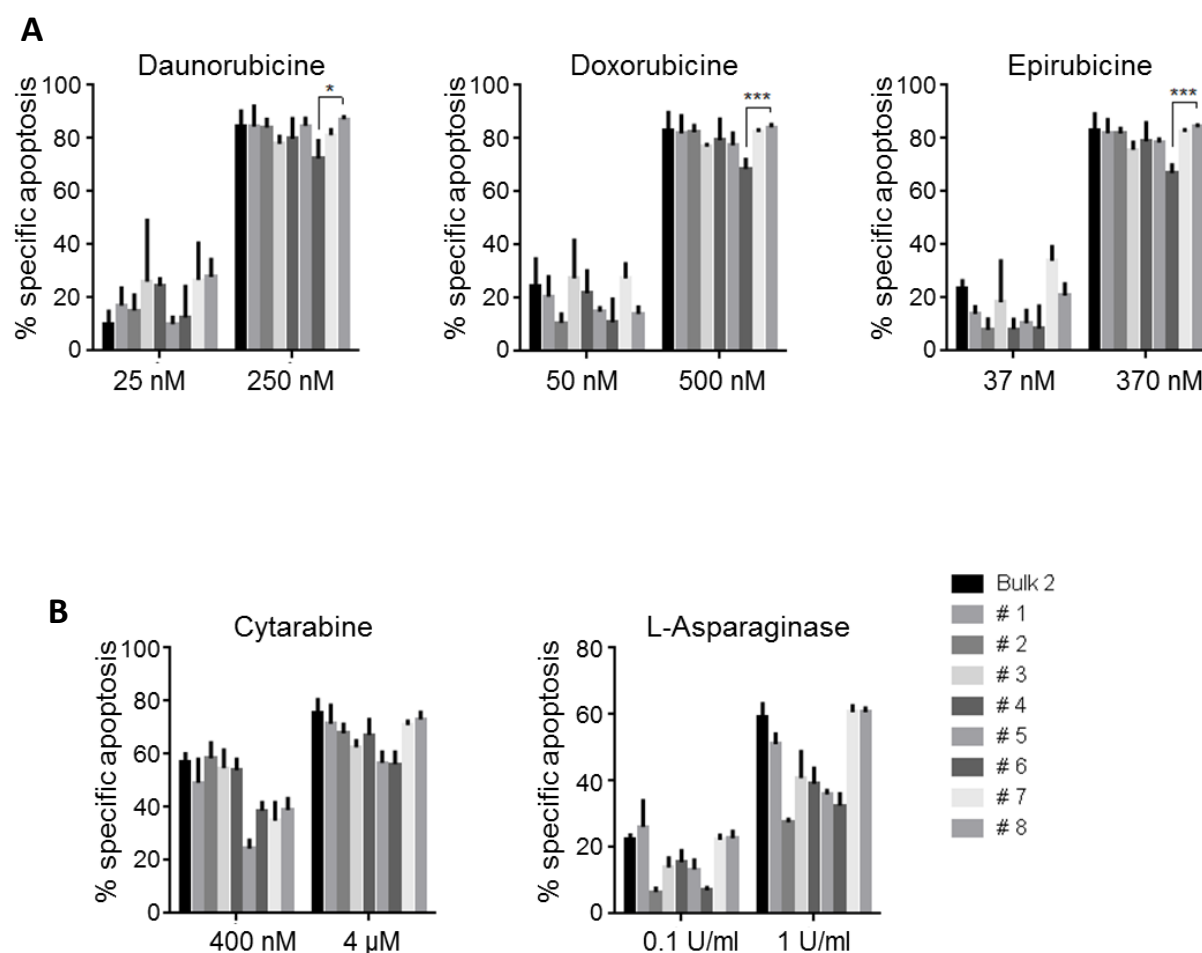


Figure 26: Drug sensitivities were diverse among all clones.

Freshly isolated cells of each single cell clone and cells of Bulk 2 were stimulated with different drugs at indicated concentrations in vitro (1×10^5 cells/well, 2 biological replicates/clone, 2 technical replicates/concentration; $n = 4$). The amount of apoptotic cells was determined by flow cytometry after 72 hours and specific apoptosis rates were calculated compared to untreated control as described in 5.3.7. (A) Stimulation with different concentrations of daunorubicine, doxorubicine and epirubicine. Sensitivity of clone #6 and clone #8 differed significantly in the indicated concentrations. Depicted are mean values with SD. * $p < 0.05$, *** $p < 0.001$ by two-tailed unpaired t-test (doxorubicine) and two-tailed unpaired t-test with Welch's correction (daunorubicine, epirubicine) (B) Stimulation with different concentrations of cytarabine and L-asparaginase.

Upon stimulation with the glucocorticoids (GCs) dexamethasone (Dexa) and prednisolone (Pred), we detected the most striking differences between the clones (Figure 27). This finding was particularly interesting because GCs are important drugs in clinical treatment of ALL patients (Inaba et al., 2013; Pui et al., 2012). Furthermore, GC resistance is a common reason for treatment failure in ALL (Bhadri et al., 2012; Inaba & Pui, 2010).

As shown in Figure 27, clone #6 was markedly less affected by stimulation with both GCs. In contrast, clone #5 was highly sensitive to Dexa and Pred treatment in vitro in all concentrations tested. Sensitivity of all clones against Dexa and Pred was comparable: clones were either sensitive or resistant to both drugs.

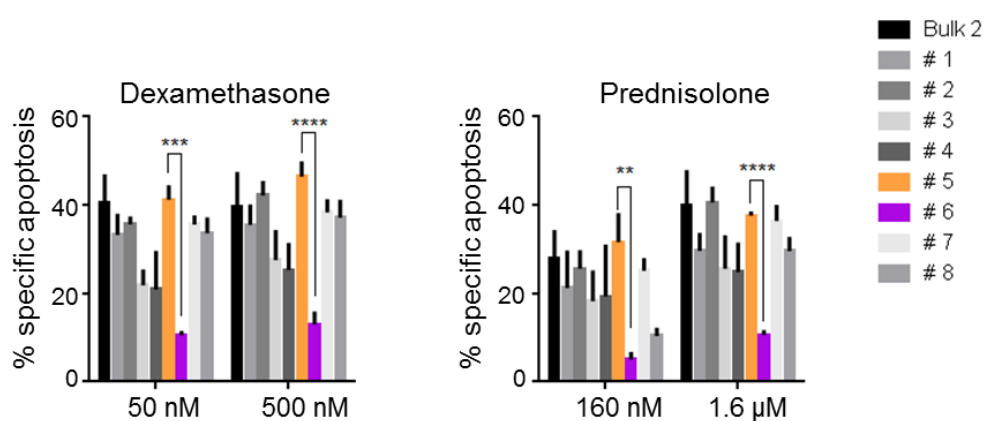


Figure 27: Clones exhibited major differences regarding glucocorticoid sensitivity.

Fresh cells of each single cell clone and of Bulk 2 were treated with dexamethasone or prednisolone at indicated concentrations in vitro (1×10^5 cells/well, 2 biological replicates/clone, 2 technical replicates/concentration; $n = 4$). The amount of apoptotic cells was assessed after 72 hours and specific apoptosis rates were calculated, respectively. Specific apoptosis rates of clone #5 and clone #6 differed significantly in all 4 concentrations tested. Depicted are mean values with SD. ** $p < 0.01$, *** $p < 0.001$, **** $p < 0.0001$ by two-tailed unpaired t-test (Dexa 500 nM, Pred 1.6 μ M) and two-tailed unpaired t-test with Welch's correction (Dexa 50 nM, Pred 160 nM).

In summary, I discovered a prominent heterogeneity in sensitivity against different drugs in vitro among all clones and bulk cells. Sensitivities against some drugs were similar while response towards others was diverse, including resistant clones. In general, clone #6 seemed to be less sensitive towards most drugs. In contrast, bulk cells, clone #7 and clone #8 were generally more affected. Clone #3 was sensitive towards all drugs except L-asparaginase. Importantly,

stimulation with GCs revealed prominent differences in sensitivities among all clones, with clone #5 being highly sensitive and clone #6 being rather resistant against GCs in vitro.

6.5.2. Single cell clones differed in drug sensitivity in vivo

Our previous investigations revealed that the generated single cell clones were heterogeneous in terms of growth properties in vivo (6.4) and in terms of drug sensitivity in vitro (6.5.1).

Ultimately, we aimed at studying drug sensitivity of single cell clones in vivo in order to investigate whether the in vitro data would be transferable to in vivo conditions.

Since we observed profound differences regarding GC sensitivity in vitro and since GC resistance is a prominent challenge for ALL therapy, we chose Dexa for in vivo treatment. Based on the observed in vitro sensitivity against Dexa depicted in Figure 27, we chose clone #5 (highly sensitive in vitro; rapid in vivo growth) and clone #6 (less susceptible in vitro; slow in vivo growth) for the in vivo study. Both clones were mixed in equal parts and the mixture was transplanted into groups of mice. The mice were either treated with different concentrations of Dexa or with PBS for five days per week and five consecutive weeks as shown in Figure 28. Subsequently, percentages of clone #5 and clone #6 in bone marrows of treated and untreated mice were quantified.

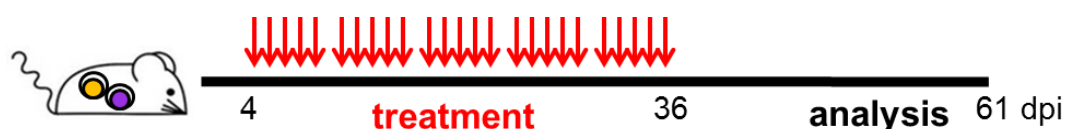


Figure 28: Experimental procedure for in vivo therapy with dexamethasone.

Clone #5 and clone #6 were mixed in equal parts and injected into mice (1×10^5 cells / mouse; $n = 5$). After 4 days, mice were treated with Dexa (2 or 8 mg/kg BW ip) or with PBS from Monday to Friday for 5 consecutive weeks. Bone marrow cells of treated and untreated mice were analyzed for the presence of clone #5 and clone #6 by flow cytometry (untreated: days 54 – 57; treated: days 62 - 64). dpi = days post injection.

Weekly bioluminescence in vivo imaging based on transgenic expression of luciferase enabled visualization of disease progression in treated and untreated animals (5.2.4). In vivo imaging

revealed that treatment with dexamethasone markedly delayed disease progression in mice as illustrated in Figure 29.

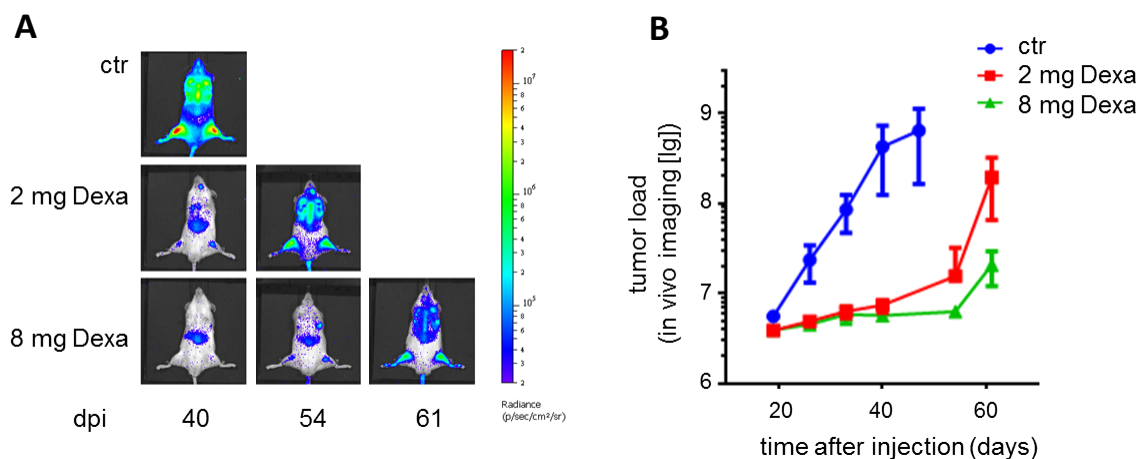


Figure 29: Disease progression was delayed in treated animals.

Expression of *Gaussia luciferase* in single cell clones enabled bioluminescence in vivo imaging of mice engrafted with clone #5 and clone #6. Pictures were taken once a week to follow disease progression over time. (A) Shown are pictures of one mouse per group taken at day 40, 54 and 61 after transplantation (units in rainbow color scales are photons per second per cm² per steradian (photons s⁻¹ cm²⁻¹ sr⁻¹)). (B) Quantification of imaging signals as shown in (A).

In good reliability to the proliferation experiments described in 6.4, flow cytometric analyses of bone marrow cells of untreated mice revealed that clone #5 overgrew clone #6 so that in average 88% of cells were derived from clone #5 and only 12% from clone #6 at the end of the experiment. Importantly, clone #6 was markedly less affected by Dexa treatment compared to clone #5 so that bone marrows of mice treated with Dexa contained considerably more clone #6 cells, in average 44% in mice treated with 2 mg Dexa and even 54% in mice treated with 8 mg Dexa (see Figure 32). Accordingly, in mice treated with 8 mg Dexa, clone #6 had overgrown clone #5 suggesting that Dexa affected primarily clone #5 but less clone #6. The results for one mouse of each group are depicted in Figure 30.

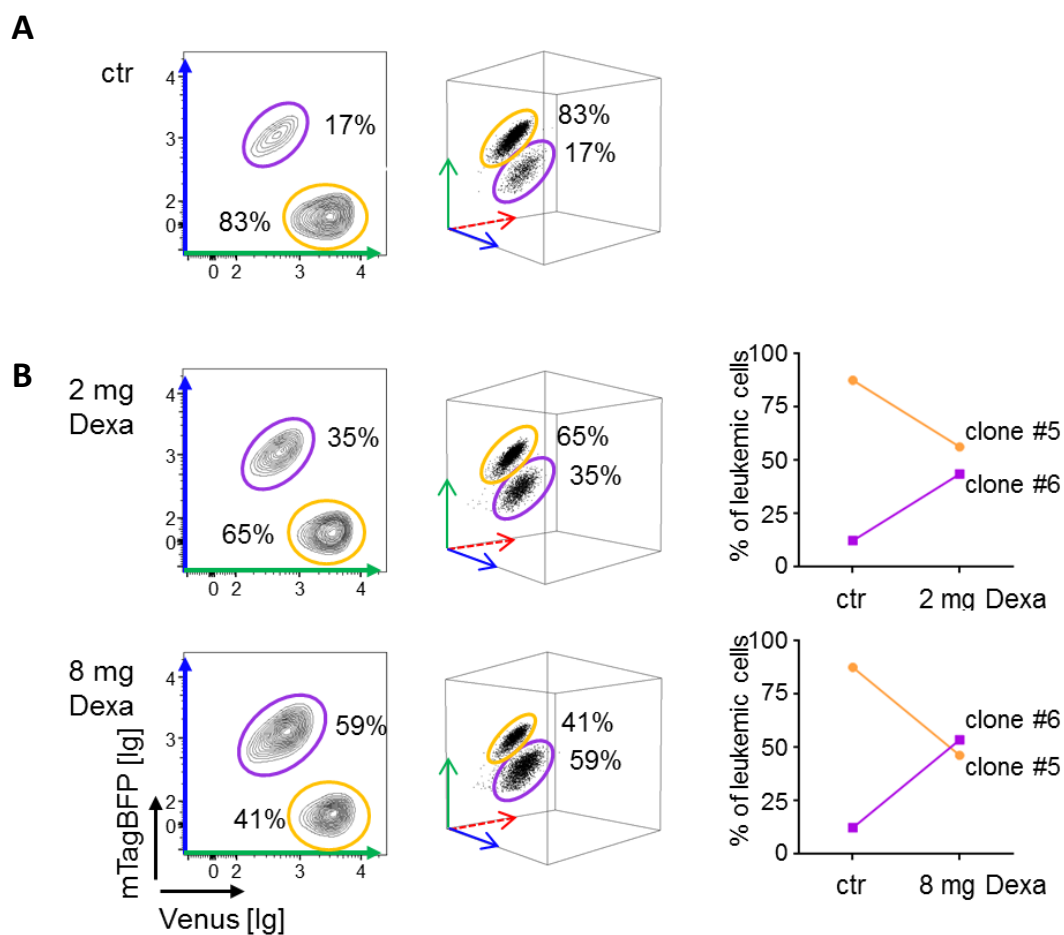


Figure 30: Dexamethasone treatment of mice engrafted with clone #5 and clone #6 particularly decreased clone #5.

Flow cytometry analysis of bone marrows of (A) untreated (ctr) and (B) mice treated with 2 mg or 8 mg Dexa. Shown are one dot plot illustrating expression of Venus and mTagBFP and one cube of a control mouse and a mouse treated with 2 mg or 8 mg Dexa (one mouse close to the mean for each group) to illustrate color expression in 2D and 3D. Depicted dot plots are gated on living cells in FSC/SSC and μ CD45 negative cells as shown in Figure 4. Graphs show mean values of percentages of clone #5 and clone #6 for treated and untreated animals ($n = 5$; control: SD 2.7%; 2 mg Dexa: SD 28.6%; 8 mg Dexa: SD 25.6%; results of single mice are illustrated in Figure 32).

In summary, the results obtained in the in vivo treatment experiment were fully consistent with the in vitro data. Clone #5 was considerably reduced upon Dexa treatment in vivo, whereas clone #6 was less susceptible to Dexa. Moreover, we observed that eradication of clone #5 was dose dependent as, in average, treatment with 8 mg Dexa was more effective compared to treatment with 2 mg Dexa (Figure 31).

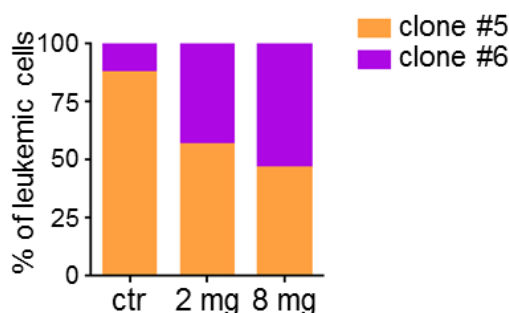


Figure 31: Eradication of clone #5 was dose dependent.

Mice engrafted with clone #5 and clone #6 were either treated with Dexa (2 or 8 mg/kg BW ip) or with buffer for 5 weeks. Depicted are percentages of each clone (mean values) in untreated (ctr) and Dexa treated (2 mg, 8 mg) mice (for results of single mice and statistical data see Figure 32).

Unfortunately and in contrast to the reliable results observed in competitive transplant experiments without additional treatment depicted in Figure 23, eradication of clone #6 was less constant between different mice (Figure 32). Variations were much higher among treated mice than among control mice, suggesting that some mice responded better to treatment than others. Thus, either an unknown mouse recipient-dependent influence exists on Dexa sensitivity or clones might have derived new sub-clonal heterogeneities upon repetitive passaging.

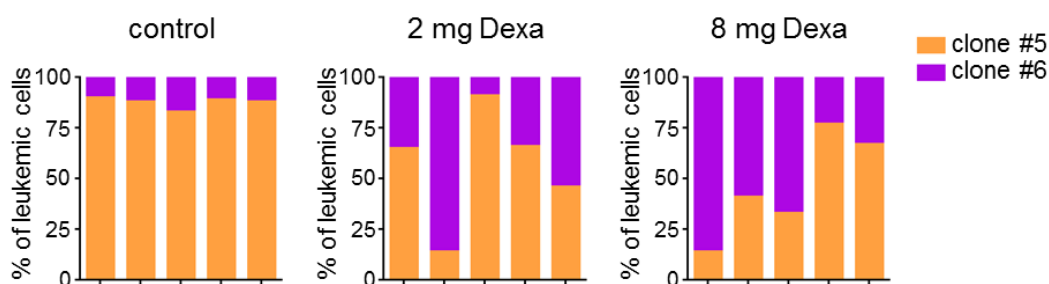


Figure 32: In vivo therapy yielded high variations in treated mice.

Percentages of clone #5 and clone #6 in bone marrows of untreated (control) and treated (2 mg, 8 mg Dexa) mice. Each bar represents one single mouse. Control: mean #5 88%, #6 12%, SD 2.7%; 2 mg Dexa: mean #5 56%, #6 44%, SD 28.6%; 8 mg Dexa: #5 46%, #6 54%, SD 25.6%.

Taken together, our previous experiments revealed prominent differences of ALL single cell clones regarding functional properties. We could demonstrate profound diversity in respect to growth behavior in vivo and to chemosensitivity in vitro and in vivo. Clone #6 was specifically interesting as it revealed a combination of two unfavorable characteristics: slow growth associated with or even causing increased resistance against Dexa treatment in vitro and in vivo.

7. Discussion

Subclonal heterogeneity represents a major challenge for acute leukemia patients as a single, rare, unfavorable subclone is sufficient to induce relapse with poor prognosis (Inaba et al., 2013; Kreso & Dick, 2014; Pui et al., 2012).

Still, the biology underlying more aggressive and therapy resistant subclones is not fully understood. Since the most aggressive subpopulation defines the patient's outcome, a better characterization of challenging subclones is urgently needed in order to develop novel therapies that eliminate them.

In this study, I characterized eight single cell clones from a child with ALL regarding their clonal growth behavior and drug sensitivity in a xenograft mouse model *in vivo*. I found that a slowly growing subclone showed resistance against dexamethasone treatment *in vivo*.

7.1. Molecular marking of PDX cells using RGB

To generate single cell clones from acute leukemia PDX samples, I used RGB marking, an innovative multicolor staining based on lentiviral transduction. Weber and colleagues established RGB marking in cell line cells (Weber et al., 2011). However, cell lines are no suitable model to study clonal subpopulations as they putatively are monoclonal. Besides, during the process of immortalization and extensive passaging *in vitro*, important functional characteristics may be altered. In contrast, PDX cells represent the complexity of the individual patient's leukemia and reproduce the heterogeneity of ALL and AML. Therefore, I adapted the RGB system to acute leukemia PDX cells that were amplified in mice. Towards this aim, I combined RGB marking with our established individualized xenograft mouse model of acute leukemia which enabled multicolor staining of PDX cells.

Weber and colleagues used fluorescence microscopy to analyze specifically colored cell clones. Since microscopy does not allow cell enrichment and sorting, I introduced flow cytometry analyses of RGB marked cells. In addition, I replaced the original blue fluorescent protein cerulean because, in contrast to cell line cells, it was not expressed brightly enough in PDX cells. Thus, we cloned mTagBFP as a blue component into our lentiviral vector which was expressed much brighter in PDX cells (Subach et al., 2008). Flow cytometry allowed evaluating more cells per sample compared to fluorescence microscopy and enabled analyzing several, differently marked clones within a cell mixture. Furthermore, RGB marking combined with flow cytometry

allowed enriching single cell clones to increase clonal purity which is impossible if other types of molecular marking are used such as genetic barcoding (Bystrykh, de Haan, & Verovskaya, 2014).

For genetic engineering of cell line cells and PDX cells, I used a third generation lentiviral vector system (Dull et al., 1998; Naldini et al., 1996; Zufferey et al., 1999). This system enabled transduction of non-dividing cells which is important as xenograft cells generally do not cycle in vitro (Terziyska et al., 2012). Lentiviral integration into the genome of xenograft cells could possibly alter their properties. However, until now, we could not detect any alterations in behavior of xenograft cells that could have been caused by lentiviral transduction (Terziyska et al., 2012; Vick et al., 2015).

For efficient RGB marking, high transduction efficiencies of around 50% for each vector were required to have a sufficient color overlap. Low efficiencies would only result in cells expressing either red, or green, or blue and no double and triple transgenic cells expressing two or three colors. But only when the majority of the cells expressed more than one color, single cells or clones could clearly be distinguished. In general, PDX cells cannot easily be transduced and it is challenging to obtain such high transduction efficiencies. Since I could only work with those PDX samples that could be most efficiently transduced I optimized virus production by concentrating the viral particles to a high extent to obtain very high virus titers. In addition, I cloned novel smaller lentiviral vectors encoding a red, a green and a blue fluorescent protein without Gaussia luciferase because, in general, smaller constructs allow generation of viruses with higher titers compared to larger constructs. Finally, I only used viruses with titers of 1×10^9 to 1×10^{11} TU / ml (assessed on NALM-6 cells) for successful RGB marking of PDX cells. Still, sufficient RGB marking could only be achieved in two AML PDX samples, AML-346 and AML-393, by simultaneous transduction with all three lentiviral vectors. Transductions with three lentiviral vectors at the same time yielded in general lower efficiencies for each single vector compared to consecutive transductions with only one vector. For this reason, I performed three consecutive lentiviral transductions with only one virus to generate efficiently RGB marked ALL-265 cells.

Basically, we chose RGB marking because it allowed separation and isolation of living cells according to their unique color. Using RGB marking enabled discrimination and isolation of different cell clones based on their individual color by flow cytometry. Hence, I had numerous living cells of the same cell clone at hand, which I extensively characterized regarding functional properties. Yet, RGB marking has some limitations which have to be taken into account.

First, one color can possibly contain different clones. Two cells can potentially be transduced with the same vector combination resulting in two clones, although genetically diverse,

expressing the same color. However, LM-PCR performed as a quality control detected different integration sites for all eight clones proving their clonal uniqueness.

Second, one single clone might also have different colors since cells that belong to the same cell clone could be stained differently. Nevertheless, I detected profound differences among all clones regarding functional features strengthening the hypothesis that I clonally amplified single cells belonging to at least partially diverse clones.

Third, RGB marking cannot visualize clonal evolution which took place after the clone was already RGB marked. To limit proliferation times and putative clonal evolution therein, each clone was amplified in two biological replicates and cells were viably frozen. All experiments were subsequently performed with these cells without additional amplification.

Despite these limitations, RGB marking offers the unique possibility to isolate viable cells of different single cell clones based on their specific color and to analyze these cells. Using RGB marking, we could trace single cell clones by flow cytometry in outcompete and treatment experiments. Thus, RGB marking represents an exclusive tool to generate viable single cell clones from a patient's sample for further functional and genetic analyses.

7.2. Limiting dilution transplantation allowed visualization of selective engraftment of leukemic stem cells

Comparing color expression of the same freshly RGB marked cells before and after xenotransplantation enabled visualization how the colors of an acute leukemia PDX sample changed during one mouse passage equaling approximately six weeks. Comparing expressed colors directly after transduction and after mouse passage revealed a loss of colors among the transplanted cells indicating that certain cells got lost upon transplantation. The two tested AML samples became patchy upon first transplantation and in one ALL sample we detected clonal outgrowth after serial-transplantation over three mouse passages. This experiment allowed an estimation how representatively PDX samples are propagated when many cells (1×10^6) are transplanted. Clonal outgrowth suggested that not all RGB marked cells engrafted in the mouse and that some clones were more dominant compared to others. Accordingly, upon each mouse passage, several cells got lost and clonal outgrowth aggravated over passaging.

Only LSCs can initiate leukemia in immunocompromised mice and maintain the disease upon serial transplantation. Thus, PDX samples are propagated by their containing LSCs while non-LSCs are not able to establish a full leukemia in immunocompromised mice (Clarke et al.,

2006; Kreso & Dick, 2014). We assume that by comparing the amount of colors before and after mouse passage, we have visualized engrafting LSCs. Since non-LSCs will not engraft, the amount of patchiness may be determined by the amount of homing LSCs. The fact that the two AML samples tested became patchy already after first transplantation while in one ALL sample clonal outgrowth became visible only after serial transplantation would argue for a reduced amount of LSCs in the AML samples. Consequently, 1×10^6 cells of AML-393 and of AML-346 would comprise less LSCs able to home in mice than 1×10^6 cells of ALL-265. Correspondingly, some publications could show that in B-ALL many cells exhibit leukemia propagating activity whereas in AML stem cell frequencies tend to be markedly lower (Kelly et al., 2007; Rehe et al., 2013; Sarry et al., 2011). In fact, for ALL-265, we determined a very high LSC frequency of 1 stem cell in 27 cells using limiting dilution transplantation assay. However, we did not clearly define the stem cell frequencies of AML-393 and AML-346. For AML-393, the amount of stem cells in the sample has to be at least 1 in 2,000 cells since all of the mice that had been transplanted with 2×10^3 cells developed leukemia, but it may be even higher. Consequently, more experiments would be needed to prove this hypothesis. Still, our findings may suggest that ALL and AML samples differ in the amount of LSCs but more experiments would be required to strengthen this idea. In summary, these findings indicate that RGB marking combined with xenotransplantation enabled visualization of engraftment of leukemia propagating cells in mice.

By transplanting limiting numbers of RGB ALL-265 and RGB AML-393 cells, we discovered that the amount of differently colored populations after the additional mouse passage was dependent on the amount of transplanted cells as expected. Transplantation of many cells caused only small changes in expressed colors whereas upon transplantation of few cells, we observed a prominent decrease of colors. Ultimately, transplantation of only some hundred cells resulted in engraftment of single cells and in generation of single cell clones.

Since ALL and AML PDX samples are defined by the amount of containing LSCs or their stem cell frequency (Clarke et al., 2006; Clevers, 2011; Kreso & Dick, 2014), the number of transplanted LSCs is dependent on the total amount of transplanted cells. The fewer cells are transplanted, the fewer LSCs are transplanted, respectively. Consequently, the number of LSCs among all transplanted cells would determine the amount of colors.

Upon transplantation of 2×10^3 cells of AML-393 we could clearly distinguish single cell clones. In contrast, single cell clones of ALL-265 could only be distinguished after transplantation of as few as 333 cells or less. These findings would, again, implicate that the same amount of cells of AML-393 comprised less LSCs compared to ALL-265. Besides, all single cell clones originated

from clonal expansion of single LSCs. Conversely, for RGB ALL-265 we determined a stem cell frequency of 1 in 27 cells. Nevertheless, upon transplantation of only 333 or 100 cells per mouse, we observed engraftment of only one or two cells in most cases, even if, according to the determined LSC frequency, there should have engrafted up to 12 cells according to theoretical calculations. In none of the mice injected with 333 cells we detected engraftment of 12 cells. This might be caused by experimental conditions like the hostile environment in the mouse, but might also challenge the suggested proportional correlation between numbers of PDX cells injected and numbers of PDX cells engrafted.

7.3. Competitive transplantation experiments revealed divergent growth behavior of clonal subpopulations

Unique color expression of RGB marked single cell clones allowed reliable separation of individually colored single cell clones by flow cytometry. However, due to overlap in colors and the surprisingly high diversity in color expression within each single cell clone resulting in a large 3-dimensional space obtained by each clone in flow cytometric analysis, we could only measure up to five differently marked clones in parallel.

To detect differences regarding growth behavior among single cell clones, I performed competitive engraftment experiments in which differently colored clones were injected into the same recipient mice. Competitive transplantation of five clones clearly demonstrated the growth advantage of clone #5 and clone #7. I could further strengthen these findings as I discovered the same tendencies when I transplanted different combinations of two clones. Still, the effects were more pronounced when only two clones grew in the same mouse indicating that expansion is hampered when more clones grow in the same mouse and that outcompete would take longer. Serial transplantation of these samples might result in more pronounced effects. However, trends were similar indicating that predominant clones kept their growth advantage irrespective of competing with one or four clones. Taken together, these findings suggest that subclones exhibited divergent growth properties most probably determined by clone-intrinsic features.

Using the individualized xenograft mouse model enabled investigating the growth behavior of subclones from one patient's leukemia without the impact of drugs. The xenograft mouse model of acute leukemia is the best model system available to simulate the complex biology of ALL that exists in the patient (Lee et al., 2007; Liem et al., 2004). In this respect, xenografts in

immunocompromised mice allow studies on clonal evolution that cannot be investigated in patients.

In line with published data, I could show that subclones of one patient's leukemia exhibited divergent growth behavior since I observed that some clones overgrew others when transplanted in a competitive setting (Jan & Majeti, 2013; Ma et al., 2015).

One explanation for the increase of clone #5 and clone #7 could be that these two clones have enhanced proliferation rates and grow quicker than the other clones. Consequently, clones that grow slower would be overgrown by clones that grow faster.

Additional gene expression analyses may give a hint if "slow" clones and "fast" clones differ in expression of particular genes that are implicated in proliferation. For instance, it would be interesting to check if proliferation pathways are altered in clone #5 and clone #7 compared to clone #1, clone #6 and clone #8. In this respect, differentially expressed genes might serve as candidate genes for knock-down experiments that could give evidence if particular functional features are caused by specific genotypes.

Another explanation for the impaired expansion of clone #6, clone #8 and clone #1 would be that these clones contained more resting stem cells than clone #5 and clone #7. The presence of many quiescent, non-cycling LSCs that do not contribute to sustained tumor growth would explain why clone #6, clone #8 and clone #1 were overgrown by clone #5 and clone #7. In addition, this may as well explain why the clones with inferior growth properties in outcompete experiments were still present in the bulk sample, considering the rounds of xenotransplantation of this PDX sample. Resting stem cells may persist without proliferating for a long time but may finally start to cycle again (Clevers, 2011; Dick, 2008; Greaves, 2013). Consequently, an increased number of LSCs might delay growth, but when the dormant cells restart to cycle, the clone would reappear.

In general, it would be highly interesting to know the LSC frequencies of all clones in order to understand if slowly growing clones contained less LSCs compared to clone #5 and clone #7.

Unfortunately, comparing LSC frequencies among the generated single cell clones is technically highly demanding. As few as 33 cells per mouse of ALL-265 engrafted and caused leukemia in all mice. Consequently, to detect an increased LSC frequency in single cell clones, transplantation of even less than 33 cells per mouse would be necessary. In addition, to minimize experimental variations (variability in cell counting and in injection into the tail vein, decreased viability due to experimental stress) and mouse specific variations (variability in engraftment) each dilution

requires a very high number of mice as slight differences in LSC frequencies may always be based on technical variations. Due to the technical challenges and a low likelihood to generate reliable data, we did not undertake these highly resource intensive experiments.

In summary, these findings provide that PDX samples are still comprised of divergent subclones even after passaging in immunocompromised mice. Additionally, these results demonstrate that even without the selective pressure and the mutagenic effect that chemotherapy may have on leukemic subclones, differences regarding growth behavior have an impact on clonal composition in leukemia. Fast growing clones may contribute to a quickly growing tumor load while slowly growing and eventually resistant clones could be the reason for recurrent leukemia after treatment.

7.4. Drug treatment of single cell clones revealed heterogeneity in drug response

Using competitive engraftment experiments, I identified divergent growth properties among five single cell clones. Next, I investigated whether the clones also differed in respect to drug sensitivity. To identify drug resistant clones, I performed a drug screening in which I tested several drugs in various concentrations in vitro. Remarkably, in the in vitro assays I obtained stable results with very low standard deviations between biological and technical replicates indicating the high quality of the experiment. Furthermore, I discovered highly comparable results for drugs belonging to the same groups (anthracyclines, glucocorticoids). In summary, I detected similar sensitivities towards some drugs while I discovered prominent differences in response to others among all clones and bulk cells. However, I identified profound diversity in specific apoptosis rates upon stimulation with cytarabine, L-asparaginase, dexamethasone and prednisolone. Bulk cells were usually sensitive towards treatment. Clone #6 was generally less susceptible to treatment while other clones were sensitive to some drugs and resistant to others.

Since glucocorticoids (GCs) play an essential role in treatment of ALL patients, the observed diversity in sensitivity against GCs in vitro was very interesting. The initial response to GCs represents an important prognostic factor and patients responding poorly to initial GC treatment typically have a worse outcome compared to GC good responders (Dordelmann et al., 1999; Inaba & Pui, 2010). Especially the great difference between clone #5 and clone #6 was surprising: clone #5 was highly sensitive whereas clone #6 was quite resistant. When we subjected mice that were engrafted with clone #5 and clone #6 to treatment with Dexa we observed that Dexa treatment particularly eliminated clone #5 while clone #6 was less impaired.

These findings were fully consistent with the *in vitro* drug response of these two clones. As expected and in accordance with the outcompete proliferation assay, in the untreated control group, clone #5 significantly overgrew clone #6 indicating that clone #5 had a growth advantage compared to clone #6. In summary, despite its inferior growth rate, clone #6 was increased in the treated mice implicating that Dexa treatment selected for the resistant clone #6.

Heterogeneity of tumor subpopulations regarding drug sensitivity is a central problem for therapy of leukemia (Hanahan & Weinberg, 2011; Marusyk et al., 2012). Patients can only be cured when all relevant leukemic subclones are eradicated by chemotherapy. Since survival of treatment-refractory cells may be the reason for MRD and disease relapse, a better understanding of the characteristics of resistant cell clones is of particular importance. In line with published data, I could show that treatment selected for outgrowth of the resistant clone supporting the hypothesis that selective pressure of therapy promotes expansion of resistant clones (Greaves & Maley, 2012; Landau et al., 2014). Consistent with Nowell's clonal evolution model, I observed that Dexa treatment contributed to the progression towards a more aggressive disease with an increased amount of the resistant cell clone after Dexa treatment (Nowell, 1976). Besides, these findings are consistent with numerous publications that have uncovered that even a minor clone at diagnosis may be dominant at relapse and thus ultimately lethal for the patient (Anderson et al., 2011; Ma et al., 2015; Mullighan et al., 2008; Shlush et al., 2012; van Delft et al., 2011).

Since clone #6 could potentially comprise more quiescent stem cells compared to clone #5, this would explain its slow growth. However, it does not explain the impaired sensitivity against Dexa because the mechanism of action of Dexa should be independent from cell cycle. Consequently, also non-cycling cells should be eradicated by Dexa (Bhadri et al., 2012; Inaba & Pui, 2010). Here, further analyses are required to investigate the mechanisms of GC resistance of clone #6 on the molecular level. Since the current knowledge about GC resistance is still fragmentary (Bhadri et al., 2012), genetic characterization of clone #6 might help to increase the knowledge about alterations that are associated with a decreased sensitivity towards GCs. Nevertheless, resting stem cells might reside in another niche of the bone marrow than cycling cells. Since LSCs might be protected by the micro-environmental conditions in their niche, they would be less affected by treatment which would explain the impaired sensitivity of a cell clone containing more stem cells (Ishikawa et al., 2007; Shlush et al., 2012).

Still, it would be interesting to perform the same experiment with drugs that specifically target cycling cells, for instance antimetabolites. Against cytarabine, clone #5 and clone #6 were

similarly sensitive in vitro (Figure 26). Since PDX cells hardly cycle in vitro, differences in sensitivity would mainly be observed under in vivo conditions with actively cycling cells. Therefore, cytarabine treatment of mice engrafted with these two clones may give another hint if the clones differ in the amount of containing LSCs. Accordingly, clone #6 would be less impaired by cytarabine in vivo compared to clone #5.

Furthermore, it would be interesting to check whether genes known to be implicated in apoptosis pathways are differentially regulated in sensitive and resistant cell clones.

Remarkably, I observed a high variability in response to treatment among all mice. In average, mice treated with a higher concentration of Dexamethasone contained less clone #5 but standard deviations for the percentages of both clones were quite high among all mice. Variations in drug applications and metabolic differences in individual mice could be the reason for these discrepancies. In contrast, in untreated mice, standard deviations were marginal.

Taken together, I could show that within the heterogeneous tumor bulk aggressive subclones exist showing slow tumor growth and drug resistance.

7.5. Conclusion and outlook

In summary, my studies represent the first experimental in vivo evidence that functionally heterogeneous subclones exist within a single ALL PDX sample. Functional characterization detected profound diversity in terms of growth behavior and drug sensitivity among the single cell clones.

As conclusion, we have established a technique which now allows targeting functionally adverse subclones specifically by combining the individualized mouse model of acute leukemia with genetic engineering, multicolor molecular staining, limiting dilution transplantation assays and competitive in vivo functional assays.

By combining in vivo functional assays with genetic characterization, the approach allows characterizing adverse single cell clones in order to establish novel treatment options against them. As outlook, our detected functional results require further studies in order to reveal any putative causative relationship between functional phenotype and genotype. My studies highlight that it is important to characterize adverse single cell clones and develop treatment options against the most resistant clone within a single tumor. It is important to address adverse

functional characteristics such as quiescence and drug resistance in order to completely eliminate an entire tumor and to improve prognosis and survival of cancer patients.

8. List of tables and list of figures

List of tables

| | |
|---|----|
| Table 1: Primers..... | 27 |
| Table 2: Enzymes..... | 28 |
| Table 3: Plasmids..... | 28 |
| Table 4: Cell lines..... | 29 |
| Table 5: Antibodies..... | 29 |
| Table 6: Commercial kits..... | 29 |
| Table 7: Drugs and dilutions for in vitro stimulation of single cell clones..... | 36 |
| Table 8: Filter settings of the BD LSRfortessa..... | 44 |
| Table 9: PDX samples..... | 47 |
| Table 10: Transduction efficiencies of lentivirally transduced RGB PDX samples..... | 56 |
| Table 11: Numbers of cells and mice used for LDA of RGB AML-393..... | 60 |
| Table 12: Numbers of cells and mice used for LDA of RGB ALL-265..... | 61 |

List of figures

| | |
|---|----|
| Figure 1: Functional heterogeneity of acute leukemia cells..... | 14 |
| Figure 2: Subclonal architecture in ALL is complex..... | 20 |
| Figure 3: Relationship of diagnosis and relapse samples in ALL..... | 21 |
| Figure 4: Gating strategy for analysis of PDX cells by flow cytometry..... | 45 |
| Figure 5: The principle of RGB marking..... | 49 |
| Figure 6: Transfer vectors for production of third generation lentiviruses..... | 50 |
| Figure 7: Color expression of RGB marked cell line cells assessed by fluorescence microscopy..... | 51 |
| Figure 8: Color expression of RGB marked cell line cells assessed by flow cytometry..... | 53 |
| Figure 9: Experimental procedure for generation of RGB ALL-265..... | 55 |
| Figure 10: Experimental procedure for generation of RGB AML-393 and RGB AML-346..... | 56 |
| Figure 11: Amplification, lentiviral transduction and in vitro co-culture of RGB PDX cells..... | 57 |
| Figure 12: RGB marking of AML PDX cells revealed clonal outgrowth upon in vivo transplantation..... | 58 |
| Figure 13: Clonal outgrowth aggravated upon passaging in ALL-265..... | 59 |

| | |
|--|----|
| Figure 14: Kaplan Meier survival curves for LDAs with cells of RGB ALL-265 and AML-393..... | 62 |
| Figure 15: Transplantation of low cell numbers decreased the amount of differently colored populations..... | 65 |
| Figure 16: Procedure for generation of single cell clones expressing unique colors. | 66 |
| Figure 17: Generated ALL-265 single cell clones. | 68 |
| Figure 18: Experimental procedure for competitive transplantation of five clones. | 70 |
| Figure 19: Competitive transplantation of five clones uncovered divergent growth behavior. ... | 71 |
| Figure 20: Procedure for competitive transplantation of two clones..... | 72 |
| Figure 21: Competitive transplantation of two clones confirmed different growth properties in vivo..... | 74 |
| Figure 22: Growth advantage of clone #5 continued upon re-transplantation. | 75 |
| Figure 23: Outcompete experiments yielded reproducible results in all mice. | 76 |
| Figure 24: Percentage of specific apoptosis is independent from gating strategy | 78 |
| Figure 25: Single cell clones exhibited similar spontaneous apoptosis rates in vitro. | 79 |
| Figure 26: Drug sensitivities were diverse among all clones..... | 80 |
| Figure 27: Clones exhibited major differences regarding glucocorticoid sensitivity..... | 81 |
| Figure 28: Experimental procedure for in vivo therapy with dexamethasone. | 82 |
| Figure 29: Disease progression was delayed in treated animals..... | 83 |
| Figure 30: Dexamethasone treatment of mice engrafted with clone #5 and clone #6 particularly decreased clone #5..... | 84 |
| Figure 31: Eradication of clone #5 was dose dependent..... | 85 |
| Figure 32: In vivo therapy yielded high variations in treated mice. | 85 |

9. List of abbreviations

| | |
|---------|-------------------------------------|
| A | Adenine |
| ALL | acute lymphoblastic leukemia |
| AML | acute myeloid leukemia |
| APC | allophycocyanin |
| B-ALL | B-cell acute lymphoblastic leukemia |
| bp | base pair |
| C | Cytosine |
| °C | degree Celsius |
| CI | confidence interval |
| CSC | cancer stem cell |
| d | day |
| DAPI | 4',6-diamidino-2-phenylindole |
| Dexa | dexamethasone |
| DMSO | dimethyl sulfoxide |
| DNA | deoxyribonucleic acid |
| dpi | days post injection |
| E. coli | Escherichia coli |
| EDTA | Ethylenediaminetetraacetic acid |
| FCS | fetal calf serum |
| FSC | forward scatter |
| GC | glucocorticoid |
| G | Guanine |
| g | gram |
| h | hour |
| k | kilo |
| l | liter |
| LB | lysogeny broth |

| | |
|-------------------|--|
| LDA | limiting dilution transplantation assay |
| LSC | leukemic stem cell |
| M | molar [1 M = 1 mol/l] |
| m | milli (10^{-3}) |
| μ | mikro (10^{-6}) |
| MCS | multiple cloning site |
| min | minute |
| mRNA | messenger ribonuclein acid |
| n | nano (10^{-9}) |
| NSG | non obese diabetic / severe combined immunodeficiency / gamma chain depleted (NOD.Cg-Prkdc ^{scid} Il2rg ^{tm1Wjl} /SzJ) |
| OD ₆₀₀ | optical density, absorbance at a wavelength of 600 nm |
| PBS | phosphate buffered saline |
| PCR | polymerase chain reaction |
| PDX | patient-derived xenograft |
| Pred | prednisolone |
| RGB | red-green-blue |
| RNA | ribonucleic acid |
| rt | room temperature |
| SD | standard deviation |
| sec | second |
| SSC | side scatter |
| sr | steradian |
| T | Thymine |
| Tm | melting temperature |
| UV | ultraviolet |
| V | volt |

10. References

- Almendro, V., Marusyk, A., & Polyak, K. (2013). Cellular heterogeneity and molecular evolution in cancer. *Annu Rev Pathol*, 8, 277-302. doi: 10.1146/annurev-pathol-020712-163923
- Anderson, K., Lutz, C., van Delft, F. W., Bateman, C. M., Guo, Y., Colman, S. M., . . . Greaves, M. (2011). Genetic variegation of clonal architecture and propagating cells in leukaemia. *Nature*, 469(7330), 356-361. doi: 10.1038/nature09650
- Aparicio, S., & Caldas, C. (2013). The implications of clonal genome evolution for cancer medicine. *N Engl J Med*, 368(9), 842-851. doi: 10.1056/NEJMra1204892
- Barber, L. J., Davies, M. N., & Gerlinger, M. (2014). Dissecting cancer evolution at the macro-heterogeneity and micro-heterogeneity scale. *Curr Opin Genet Dev*, 30C, 1-6. doi: 10.1016/j.gde.2014.12.001
- Barrett, D. M., Seif, A. E., Carpenito, C., Teachey, D. T., Fish, J. D., June, C. H., . . . Reid, G. S. (2011). Noninvasive bioluminescent imaging of primary patient acute lymphoblastic leukemia: a strategy for preclinical modeling. *Blood*, 118(15), e112-117. doi: 10.1182/blood-2011-04-346528
- Berdasco, M., & Esteller, M. (2010). Aberrant epigenetic landscape in cancer: how cellular identity goes awry. *Dev Cell*, 19(5), 698-711. doi: 10.1016/j.devcel.2010.10.005
- Bhadri, V. A., Trahair, T. N., & Lock, R. B. (2012). Glucocorticoid resistance in paediatric acute lymphoblastic leukaemia. *J Paediatr Child Health*, 48(8), 634-640. doi: 10.1111/j.1440-1754.2011.02212.x
- Bhatla, T., Jones, C. L., Meyer, J. A., Vitanza, N. A., Raetz, E. A., & Carroll, W. L. (2014). The biology of relapsed acute lymphoblastic leukemia: opportunities for therapeutic interventions. *J Pediatr Hematol Oncol*, 36(6), 413-418. doi: 10.1097/MPH.0000000000000179
- Bomken, S., Buechler, L., Rehe, K., Ponthan, F., Elder, A., Blair, H., . . . Heidenreich, O. (2013). Lentiviral marking of patient-derived acute lymphoblastic leukaemic cells allows in vivo tracking of disease progression. *Leukemia*, 27(3), 718-721. doi: 10.1038/leu.2012.206
- Bonnet, D., & Dick, J. E. (1997). Human acute myeloid leukemia is organized as a hierarchy that originates from a primitive hematopoietic cell. *Nat Med*, 3(7), 730-737.
- Bruggemann, M., Raff, T., & Kneba, M. (2012). Has MRD monitoring superseded other prognostic factors in adult ALL? *Blood*, 120(23), 4470-4481. doi: 10.1182/blood-2012-06-379040

- Bullinger, L., & Armstrong, S. A. (2010). HELP for AML: methylation profiling opens new avenues. *Cancer Cell*, 17(1), 1-3. doi: 10.1016/j.ccr.2009.12.033
- Burrell, R. A., McGranahan, N., Bartek, J., & Swanton, C. (2013). The causes and consequences of genetic heterogeneity in cancer evolution. *Nature*, 501(7467), 338-345. doi: 10.1038/nature12625
- Burrell, R. A., & Swanton, C. (2014). Tumour heterogeneity and the evolution of polyclonal drug resistance. *Mol Oncol*, 8(6), 1095-1111. doi: 10.1016/j.molonc.2014.06.005
- Bystrykh, L. V., de Haan, G., & Verovskaya, E. (2014). Barcoded vector libraries and retroviral or lentiviral barcoding of hematopoietic stem cells. *Methods Mol Biol*, 1185, 345-360. doi: 10.1007/978-1-4939-1133-2_23
- Chiu, P. P., Jiang, H., & Dick, J. E. (2010). Leukemia-initiating cells in human T-lymphoblastic leukemia exhibit glucocorticoid resistance. *Blood*, 116(24), 5268-5279. doi: 10.1182/blood-2010-06-292300
- Choi, S., Henderson, M. J., Kwan, E., Beesley, A. H., Sutton, R., Bahar, A. Y., . . . Norris, M. D. (2007). Relapse in children with acute lymphoblastic leukemia involving selection of a preexisting drug-resistant subclone. *Blood*, 110(2), 632-639. doi: 10.1182/blood-2007-01-067785
- Clarke, M. F., Dick, J. E., Dirks, P. B., Eaves, C. J., Jamieson, C. H., Jones, D. L., . . . Wahl, G. M. (2006). Cancer stem cells--perspectives on current status and future directions: AACR Workshop on cancer stem cells. *Cancer Res*, 66(19), 9339-9344. doi: 10.1158/0008-5472.CAN-06-3126
- Clevers, H. (2011). The cancer stem cell: premises, promises and challenges. *Nat Med*, 17(3), 313-319. doi: 10.1038/nm.2304
- Davis, H. E., Rosinski, M., Morgan, J. R., & Yarmush, M. L. (2004). Charged polymers modulate retrovirus transduction via membrane charge neutralization and virus aggregation. *Biophys J*, 86(2), 1234-1242. doi: 10.1016/S0006-3495(04)74197-1
- Dawson, M. A., & Kouzarides, T. (2012). Cancer epigenetics: from mechanism to therapy. *Cell*, 150(1), 12-27. doi: 10.1016/j.cell.2012.06.013
- Dick, J. E. (2008). Stem cell concepts renew cancer research. *Blood*, 112(13), 4793-4807. doi: 10.1182/blood-2008-08-077941
- Ding, L., Ley, T. J., Larson, D. E., Miller, C. A., Koboldt, D. C., Welch, J. S., . . . DiPersio, J. F. (2012). Clonal evolution in relapsed acute myeloid leukaemia revealed by whole-genome sequencing. *Nature*, 481(7382), 506-510. doi: 10.1038/nature10738
- Dohner, K., Paschka, P., & Dohner, H. (2015). [Acute myeloid leukemia]. *Internist (Berl)*. doi: 10.1007/s00108-014-3596-5

- Dordelmann, M., Reiter, A., Borkhardt, A., Ludwig, W. D., Gotz, N., Viehmann, S., . . . Schrappe, M. (1999). Prednisone response is the strongest predictor of treatment outcome in infant acute lymphoblastic leukemia. *Blood*, *94*(4), 1209-1217.
- Downing, J. R., Wilson, R. K., Zhang, J., Mardis, E. R., Pui, C. H., Ding, L., . . . Evans, W. E. (2012). The Pediatric Cancer Genome Project. *Nat Genet*, *44*(6), 619-622. doi: 10.1038/ng.2287
- Dull, T., Zufferey, R., Kelly, M., Mandel, R. J., Nguyen, M., Trono, D., & Naldini, L. (1998). A third-generation lentivirus vector with a conditional packaging system. *J Virol*, *72*(11), 8463-8471.
- Eppert, K., Takenaka, K., Lechman, E. R., Waldron, L., Nilsson, B., van Galen, P., . . . Dick, J. E. (2011). Stem cell gene expression programs influence clinical outcome in human leukemia. *Nat Med*, *17*(9), 1086-1093. doi: 10.1038/nm.2415
- Esparza, S. D., & Sakamoto, K. M. (2005). Topics in pediatric leukemia--acute lymphoblastic leukemia. *MedGenMed*, *7*(1), 23.
- Estey, E., & Dohner, H. (2006). Acute myeloid leukaemia. *Lancet*, *368*(9550), 1894-1907. doi: 10.1016/S0140-6736(06)69780-8
- Estey, E. H. (2014). Acute myeloid leukemia: 2014 update on risk-stratification and management. *Am J Hematol*, *89*(11), 1063-1081. doi: 10.1002/ajh.23834
- Evans, W. E., Crews, K. R., & Pui, C. H. (2013). A health-care system perspective on implementing genomic medicine: pediatric acute lymphoblastic leukemia as a paradigm. *Clin Pharmacol Ther*, *94*(2), 224-229. doi: 10.1038/clpt.2013.9
- Figuroa, M. E., Chen, S. C., Andersson, A. K., Phillips, L. A., Li, Y., Sotzen, J., . . . Mullighan, C. G. (2013). Integrated genetic and epigenetic analysis of childhood acute lymphoblastic leukemia. *J Clin Invest*, *123*(7), 3099-3111. doi: 10.1172/JCI66203
- Figuroa, M. E., Lugthart, S., Li, Y., Erpelinck-Verschueren, C., Deng, X., Christos, P. J., . . . Melnick, A. (2010). DNA methylation signatures identify biologically distinct subtypes in acute myeloid leukemia. *Cancer Cell*, *17*(1), 13-27. doi: 10.1016/j.ccr.2009.11.020
- Galmarini, C. M., Mackey, J. R., & Dumontet, C. (2001). Nucleoside analogues: mechanisms of drug resistance and reversal strategies. *Leukemia*, *15*(6), 875-890.
- Garraway, L. A., & Janne, P. A. (2012). Circumventing cancer drug resistance in the era of personalized medicine. *Cancer Discov*, *2*(3), 214-226. doi: 10.1158/2159-8290.CD-12-0012

- Gawad, C., Koh, W., & Quake, S. R. (2014). Dissecting the clonal origins of childhood acute lymphoblastic leukemia by single-cell genomics. *Proc Natl Acad Sci U S A*, *111*(50), 17947-17952. doi: 10.1073/pnas.1420822111
- Geng, H., Brennan, S., Milne, T. A., Chen, W. Y., Li, Y., Hurtz, C., . . . Melnick, A. M. (2012). Integrative epigenomic analysis identifies biomarkers and therapeutic targets in adult B-acute lymphoblastic leukemia. *Cancer Discov*, *2*(11), 1004-1023. doi: 10.1158/2159-8290.CD-12-0208
- Gerlinger, M., McGranahan, N., Dewhurst, S. M., Burrell, R. A., Tomlinson, I., & Swanton, C. (2014). Cancer: evolution within a lifetime. *Annu Rev Genet*, *48*, 215-236. doi: 10.1146/annurev-genet-120213-092314
- Greaves, M. (2010). Cancer stem cells: back to Darwin? *Semin Cancer Biol*, *20*(2), 65-70. doi: 10.1016/j.semcancer.2010.03.002
- Greaves, M. (2013). Cancer stem cells as 'units of selection'. *Evol Appl*, *6*(1), 102-108. doi: 10.1111/eva.12017
- Greaves, M., & Maley, C. C. (2012). Clonal evolution in cancer. *Nature*, *481*(7381), 306-313. doi: 10.1038/nature10762
- Guzman, M. L., & Allan, J. N. (2014). Concise review: Leukemia stem cells in personalized medicine. *Stem Cells*, *32*(4), 844-851. doi: 10.1002/stem.1597
- Hanahan, D., & Weinberg, R. A. (2011). Hallmarks of cancer: the next generation. *Cell*, *144*(5), 646-674. doi: 10.1016/j.cell.2011.02.013
- Harrison, C. J. (2009). Cytogenetics of paediatric and adolescent acute lymphoblastic leukaemia. *Br J Haematol*, *144*(2), 147-156. doi: 10.1111/j.1365-2141.2008.07417.x
- Hogan, L. E., Meyer, J. A., Yang, J., Wang, J., Wong, N., Yang, W., . . . Carroll, W. L. (2011). Integrated genomic analysis of relapsed childhood acute lymphoblastic leukemia reveals therapeutic strategies. *Blood*, *118*(19), 5218-5226. doi: 10.1182/blood-2011-04-345595
- Hope, K. J., Jin, L., & Dick, J. E. (2004). Acute myeloid leukemia originates from a hierarchy of leukemic stem cell classes that differ in self-renewal capacity. *Nat Immunol*, *5*(7), 738-743. doi: 10.1038/ni1080
- Hu, Y., & Smyth, G. K. (2009). ELDA: extreme limiting dilution analysis for comparing depleted and enriched populations in stem cell and other assays. *J Immunol Methods*, *347*(1-2), 70-78. doi: 10.1016/j.jim.2009.06.008
- Hutter, G., Nickenig, C., Garritsen, H., Hellenkamp, F., Hoerning, A., Hiddemann, W., & Dreyling, M. (2004). Use of polymorphisms in the noncoding region of the human mitochondrial genome to identify potential contamination of human leukemia-lymphoma cell lines. *Hematol J*, *5*(1), 61-68. doi: 10.1038/sj.thj.6200317

- Inaba, H., Greaves, M., & Mullighan, C. G. (2013). Acute lymphoblastic leukaemia. *Lancet*, 381(9881), 1943-1955. doi: 10.1016/S0140-6736(12)62187-4
- Inaba, H., & Pui, C. H. (2010). Glucocorticoid use in acute lymphoblastic leukaemia. *Lancet Oncol*, 11(11), 1096-1106. doi: 10.1016/S1470-2045(10)70114-5
- Ishikawa, F., Yoshida, S., Saito, Y., Hijikata, A., Kitamura, H., Tanaka, S., . . . Shultz, L. D. (2007). Chemotherapy-resistant human AML stem cells home to and engraft within the bone-marrow endosteal region. *Nat Biotechnol*, 25(11), 1315-1321. doi: 10.1038/nbt1350
- Jacoby, E., Chien, C. D., & Fry, T. J. (2014). Murine models of acute leukemia: important tools in current pediatric leukemia research. *Front Oncol*, 4, 95. doi: 10.3389/fonc.2014.00095
- Jan, M., & Majeti, R. (2013). Clonal evolution of acute leukemia genomes. *Oncogene*, 32(2), 135-140. doi: 10.1038/onc.2012.48
- Kamel-Reid, S., Letarte, M., Sirard, C., Doedens, M., Grunberger, T., Fulop, G., . . . Dick, J. E. (1989). A model of human acute lymphoblastic leukemia in immune-deficient SCID mice. *Science*, 246(4937), 1597-1600.
- Kelly, P. N., Dakic, A., Adams, J. M., Nutt, S. L., & Strasser, A. (2007). Tumor growth need not be driven by rare cancer stem cells. *Science*, 317(5836), 337. doi: 10.1126/science.1142596
- Klco, J. M., Spencer, D. H., Miller, C. A., Griffith, M., Lamprecht, T. L., O'Laughlin, M., . . . Ley, T. J. (2014). Functional heterogeneity of genetically defined subclones in acute myeloid leukemia. *Cancer Cell*, 25(3), 379-392. doi: 10.1016/j.ccr.2014.01.031
- Kreso, A., & Dick, J. E. (2014). Evolution of the cancer stem cell model. *Cell Stem Cell*, 14(3), 275-291. doi: 10.1016/j.stem.2014.02.006
- Kronke, J., Bullinger, L., Teleanu, V., Tschurtz, F., Gaidzik, V. I., Kuhn, M. W., . . . Dohner, K. (2013). Clonal evolution in relapsed NPM1-mutated acute myeloid leukemia. *Blood*, 122(1), 100-108. doi: 10.1182/blood-2013-01-479188
- Kuiper, R. P., Schoenmakers, E. F., van Reijmersdal, S. V., Hehir-Kwa, J. Y., van Kessel, A. G., van Leeuwen, F. N., & Hoogerbrugge, P. M. (2007). High-resolution genomic profiling of childhood ALL reveals novel recurrent genetic lesions affecting pathways involved in lymphocyte differentiation and cell cycle progression. *Leukemia*, 21(6), 1258-1266. doi: 10.1038/sj.leu.2404691
- Landau, D. A., Carter, S. L., Getz, G., & Wu, C. J. (2014). Clonal evolution in hematological malignancies and therapeutic implications. *Leukemia*, 28(1), 34-43. doi: 10.1038/leu.2013.248

- Lapidot, T., Sirard, C., Vormoor, J., Murdoch, B., Hoang, T., Caceres-Cortes, J., . . . Dick, J. E. (1994). A cell initiating human acute myeloid leukaemia after transplantation into SCID mice. *Nature*, *367*(6464), 645-648. doi: 10.1038/367645a0
- le Viseur, C., Hotfilder, M., Bomken, S., Wilson, K., Rottgers, S., Schrauder, A., . . . Vormoor, J. (2008). In childhood acute lymphoblastic leukemia, blasts at different stages of immunophenotypic maturation have stem cell properties. *Cancer Cell*, *14*(1), 47-58. doi: 10.1016/j.ccr.2008.05.015
- Lee, E. M., Bachmann, P. S., & Lock, R. B. (2007). Xenograft models for the preclinical evaluation of new therapies in acute leukemia. *Leuk Lymphoma*, *48*(4), 659-668. doi: 10.1080/10428190601113584
- Liem, N. L., Papa, R. A., Milross, C. G., Schmid, M. A., Tajbakhsh, M., Choi, S., . . . Lock, R. B. (2004). Characterization of childhood acute lymphoblastic leukemia xenograft models for the preclinical evaluation of new therapies. *Blood*, *103*(10), 3905-3914. doi: 10.1182/blood-2003-08-2911
- Ma, X., Edmonson, M., Yergeau, D., Muzny, D. M., Hampton, O. A., Rusch, M., . . . Zhang, J. (2015). Rise and fall of subclones from diagnosis to relapse in pediatric B-acute lymphoblastic leukaemia. *Nat Commun*, *6*, 6604. doi: 10.1038/ncomms7604
- Magee, J. A., Piskounova, E., & Morrison, S. J. (2012). Cancer stem cells: impact, heterogeneity, and uncertainty. *Cancer Cell*, *21*(3), 283-296. doi: 10.1016/j.ccr.2012.03.003
- Marusyk, A., Almendro, V., & Polyak, K. (2012). Intra-tumour heterogeneity: a looking glass for cancer? *Nat Rev Cancer*, *12*(5), 323-334. doi: 10.1038/nrc3261
- Meacham, C. E., & Morrison, S. J. (2013). Tumour heterogeneity and cancer cell plasticity. *Nature*, *501*(7467), 328-337. doi: 10.1038/nature12624
- Mehdipour, P., Santoro, F., & Minucci, S. (2014). Epigenetic alterations in acute myeloid leukemias. *FEBS J*. doi: 10.1111/febs.13142
- Mullighan, C. G. (2012). The molecular genetic makeup of acute lymphoblastic leukemia. *Hematology Am Soc Hematol Educ Program*, *2012*, 389-396. doi: 10.1182/asheducation-2012.1.389
- Mullighan, C. G., Phillips, L. A., Su, X., Ma, J., Miller, C. B., Shurtleff, S. A., & Downing, J. R. (2008). Genomic analysis of the clonal origins of relapsed acute lymphoblastic leukemia. *Science*, *322*(5906), 1377-1380. doi: 10.1126/science.1164266
- Mullighan, C. G., Zhang, J., Kasper, L. H., Lerach, S., Payne-Turner, D., Phillips, L. A., . . . Downing, J. R. (2011). CREBBP mutations in relapsed acute lymphoblastic leukaemia. *Nature*, *471*(7337), 235-239. doi: 10.1038/nature09727

- Naldini, L., Blomer, U., Gallay, P., Ory, D., Mulligan, R., Gage, F. H., . . . Trono, D. (1996). In vivo gene delivery and stable transduction of nondividing cells by a lentiviral vector. *Science*, *272*(5259), 263-267.
- Notta, F., Mullighan, C. G., Wang, J. C., Poepl, A., Doulatov, S., Phillips, L. A., . . . Dick, J. E. (2011). Evolution of human BCR-ABL1 lymphoblastic leukaemia-initiating cells. *Nature*, *469*(7330), 362-367. doi: 10.1038/nature09733
- Nowell, P. C. (1976). The clonal evolution of tumor cell populations. *Science*, *194*(4260), 23-28.
- Parkin, B., Ouilllette, P., Li, Y., Keller, J., Lam, C., Roulston, D., . . . Malek, S. N. (2013). Clonal evolution and devolution after chemotherapy in adult acute myelogenous leukemia. *Blood*, *121*(2), 369-377. doi: 10.1182/blood-2012-04-427039
- Patel, J. P., Gonen, M., Figueroa, M. E., Fernandez, H., Sun, Z., Racevskis, J., . . . Levine, R. L. (2012). Prognostic relevance of integrated genetic profiling in acute myeloid leukemia. *N Engl J Med*, *366*(12), 1079-1089. doi: 10.1056/NEJMoa1112304
- Pui, C. H., Carroll, W. L., Meshinchi, S., & Arceci, R. J. (2011). Biology, risk stratification, and therapy of pediatric acute leukemias: an update. *J Clin Oncol*, *29*(5), 551-565. doi: 10.1200/JCO.2010.30.7405
- Pui, C. H., & Evans, W. E. (2013). A 50-year journey to cure childhood acute lymphoblastic leukemia. *Semin Hematol*, *50*(3), 185-196. doi: 10.1053/j.seminhematol.2013.06.007
- Pui, C. H., Mullighan, C. G., Evans, W. E., & Relling, M. V. (2012). Pediatric acute lymphoblastic leukemia: where are we going and how do we get there? *Blood*, *120*(6), 1165-1174. doi: 10.1182/blood-2012-05-378943
- Rehe, K., Wilson, K., Bomken, S., Williamson, D., Irving, J., den Boer, M. L., . . . Vormoor, J. (2013). Acute B lymphoblastic leukaemia-propagating cells are present at high frequency in diverse lymphoblast populations. *EMBO Mol Med*, *5*(1), 38-51. doi: 10.1002/emmm.201201703
- Roberts, K. G., & Mullighan, C. G. (2015). Genomics in acute lymphoblastic leukaemia: insights and treatment implications. *Nat Rev Clin Oncol*. doi: 10.1038/nrclinonc.2015.38
- Saadatpour, A., Guo, G., Orkin, S. H., & Yuan, G. C. (2014). Characterizing heterogeneity in leukemic cells using single-cell gene expression analysis. *Genome Biol*, *15*(12), 525. doi: 10.1186/s13059-014-0525-9
- Saito, Y., Uchida, N., Tanaka, S., Suzuki, N., Tomizawa-Murasawa, M., Sone, A., . . . Ishikawa, F. (2010). Induction of cell cycle entry eliminates human leukemia stem cells in a mouse model of AML. *Nat Biotechnol*, *28*(3), 275-280. doi: 10.1038/nbt.1607

- Santos, E. B., Yeh, R., Lee, J., Nikhamin, Y., Punzalan, B., Punzalan, B., . . . Brentjens, R. J. (2009). Sensitive in vivo imaging of T cells using a membrane-bound *Gaussia princeps* luciferase. *Nat Med*, *15*(3), 338-344. doi: 10.1038/nm.1930
- Sarry, J. E., Murphy, K., Perry, R., Sanchez, P. V., Secreto, A., Keefer, C., . . . Carroll, M. (2011). Human acute myelogenous leukemia stem cells are rare and heterogeneous when assayed in NOD/SCID/IL2Rgammac-deficient mice. *J Clin Invest*, *121*(1), 384-395. doi: 10.1172/JCI41495
- Schafer, E., Irizarry, R., Negi, S., McIntyre, E., Small, D., Figueroa, M. E., . . . Brown, P. (2010). Promoter hypermethylation in MLL-r infant acute lymphoblastic leukemia: biology and therapeutic targeting. *Blood*, *115*(23), 4798-4809. doi: 10.1182/blood-2009-09-243634
- Schlenk, R. F., & Dohner, H. (2013). Genomic applications in the clinic: use in treatment paradigm of acute myeloid leukemia. *Hematology Am Soc Hematol Educ Program*, *2013*, 324-330. doi: 10.1182/asheducation-2013.1.324
- Schmitz, M., Breithaupt, P., Scheidegger, N., Cario, G., Bonapace, L., Meissner, B., . . . Bourquin, J. P. (2011). Xenografts of highly resistant leukemia recapitulate the clonal composition of the leukemogenic compartment. *Blood*, *118*(7), 1854-1864. doi: 10.1182/blood-2010-11-320309
- Secker-Walker, L. M., Lawler, S. D., & Hardisty, R. M. (1978). Prognostic implications of chromosomal findings in acute lymphoblastic leukaemia at diagnosis. *Br Med J*, *2*(6151), 1529-1530.
- Shackleton, M., Quintana, E., Fearon, E. R., & Morrison, S. J. (2009). Heterogeneity in cancer: cancer stem cells versus clonal evolution. *Cell*, *138*(5), 822-829. doi: 10.1016/j.cell.2009.08.017
- Shlush, L. I., Chapal-Ilani, N., Adar, R., Pery, N., Maruvka, Y., Spiro, A., . . . Shapiro, E. (2012). Cell lineage analysis of acute leukemia relapse uncovers the role of replication-rate heterogeneity and microsatellite instability. *Blood*, *120*(3), 603-612. doi: 10.1182/blood-2011-10-388629
- Shultz, L. D., Ishikawa, F., & Greiner, D. L. (2007). Humanized mice in translational biomedical research. *Nat Rev Immunol*, *7*(2), 118-130. doi: 10.1038/nri2017
- Shultz, L. D., Pearson, T., King, M., Giassi, L., Carney, L., Gott, B., . . . Greiner, D. L. (2007). Humanized NOD/LtSz-scid IL2 receptor common gamma chain knockout mice in diabetes research. *Ann N Y Acad Sci*, *1103*, 77-89. doi: 10.1196/annals.1394.002
- Stow, P., Key, L., Chen, X., Pan, Q., Neale, G. A., Coustan-Smith, E., . . . Campana, D. (2010). Clinical significance of low levels of minimal residual disease at the end of remission induction therapy in childhood acute lymphoblastic leukemia. *Blood*, *115*(23), 4657-4663. doi: 10.1182/blood-2009-11-253435

- Subach, O. M., Gundorov, I. S., Yoshimura, M., Subach, F. V., Zhang, J., Gruenwald, D., . . . Verkhusha, V. V. (2008). Conversion of red fluorescent protein into a bright blue probe. *Chem Biol*, *15*(10), 1116-1124. doi: 10.1016/j.chembiol.2008.08.006
- Swanton, C. (2012). Intratumor heterogeneity: evolution through space and time. *Cancer Res*, *72*(19), 4875-4882. doi: 10.1158/0008-5472.CAN-12-2217
- Swanton, C., & Beck, S. (2014). Epigenetic noise fuels cancer evolution. *Cancer Cell*, *26*(6), 775-776. doi: 10.1016/j.ccell.2014.11.003
- Taussig, D. C., Miraki-Moud, F., Anjos-Afonso, F., Pearce, D. J., Allen, K., Ridler, C., . . . Bonnet, D. (2008). Anti-CD38 antibody-mediated clearance of human repopulating cells masks the heterogeneity of leukemia-initiating cells. *Blood*, *112*(3), 568-575. doi: 10.1182/blood-2007-10-118331
- Taussig, D. C., Vargaftig, J., Miraki-Moud, F., Griessinger, E., Sharrock, K., Luke, T., . . . Bonnet, D. (2010). Leukemia-initiating cells from some acute myeloid leukemia patients with mutated nucleophosmin reside in the CD34(-) fraction. *Blood*, *115*(10), 1976-1984. doi: 10.1182/blood-2009-02-206565
- Terziyska, N., Castro Alves, C., Groiss, V., Schneider, K., Farkasova, K., Ogris, M., . . . Jeremias, I. (2012). In vivo imaging enables high resolution preclinical trials on patients' leukemia cells growing in mice. *PLoS One*, *7*(12), e52798. doi: 10.1371/journal.pone.0052798
- van Delft, F. W., Horsley, S., Colman, S., Anderson, K., Bateman, C., Kempinski, H., . . . Greaves, M. (2011). Clonal origins of relapse in ETV6-RUNX1 acute lymphoblastic leukemia. *Blood*, *117*(23), 6247-6254. doi: 10.1182/blood-2010-10-314674
- Vick, B., Rothenberg, M., Sandhofer, N., Carlet, M., Finkenzeller, C., Krupka, C., . . . Jeremias, I. (2015). An advanced preclinical mouse model for acute myeloid leukemia using patients' cells of various genetic subgroups and in vivo bioluminescence imaging. *PLoS One*, *10*(3), e0120925. doi: 10.1371/journal.pone.0120925
- Wang, J. C. (2007). Evaluating therapeutic efficacy against cancer stem cells: new challenges posed by a new paradigm. *Cell Stem Cell*, *1*(5), 497-501.
- Weber, K., Thomaschewski, M., Warlich, M., Volz, T., Cornils, K., Niebuhr, B., . . . Fehse, B. (2011). RGB marking facilitates multicolor clonal cell tracking. *Nat Med*, *17*(4), 504-509. doi: 10.1038/nm.2338
- Williams, D. L., Look, A. T., Melvin, S. L., Roberson, P. K., Dahl, G., Flake, T., & Stass, S. (1984). New chromosomal translocations correlate with specific immunophenotypes of childhood acute lymphoblastic leukemia. *Cell*, *36*(1), 101-109.

-
- Yang, X., Lay, F., Han, H., & Jones, P. A. (2010). Targeting DNA methylation for epigenetic therapy. *Trends Pharmacol Sci*, 31(11), 536-546. doi: 10.1016/j.tips.2010.08.001
- Yates, L. R., & Campbell, P. J. (2012). Evolution of the cancer genome. *Nat Rev Genet*, 13(11), 795-806. doi: 10.1038/nrg3317
- Zhang, J., Mullighan, C. G., Harvey, R. C., Wu, G., Chen, X., Edmonson, M., . . . Hunger, S. P. (2011). Key pathways are frequently mutated in high-risk childhood acute lymphoblastic leukemia: a report from the Children's Oncology Group. *Blood*, 118(11), 3080-3087. doi: 10.1182/blood-2011-03-341412
- Zufferey, R., Donello, J. E., Trono, D., & Hope, T. J. (1999). Woodchuck hepatitis virus posttranscriptional regulatory element enhances expression of transgenes delivered by retroviral vectors. *J Virol*, 73(4), 2886-2892.

11. Acknowledgment

Ein großes Dankeschön an....

meine Betreuerinnen Prof. Dr. Irmela Jeremias und PD Dr. Ursula Zimmer-Strobl, die es mir ermöglicht haben, meine Doktorarbeit in ihrer Arbeitsgruppe durchzuführen. Vielen Dank für die gute Betreuung!

Dr. Philipp Greif für die Planung der genetischen Analyse der Klone und für die konstruktiven Ideen im Rahmen des Thesis Committees.

Sebastian Vosberg für die Hilfe bei der Auswertung der genetischen Daten.

Dr. Kerstin Cornils für die zuverlässige Kooperation bei der Durchführung der LM-PCR.

alle Gruppenmitglieder der Arbeitsgruppe für die angenehme Arbeitsatmosphäre, die vielen Kuchenorgien, die tollen Laborausflüge, movie nights, grillen, Eis essen uvm...!!!

alle TAs der Gruppe für die immense Hilfe bei der Aufarbeitung der Mäuse, vor allem an Fabian für die Übernahme des Sortens der Klone und fürs Managen der genetischen Analysen in Heidelberg.

alle Mitarbeiter der Tierhaltung, vor allem Franziska Liebel für die Wochenendbereitschaft und fürs Anrufen bei Notfällen.

Michela für ein immer offenes Ohr und die Hilfe in allen Bereichen während der letzten drei Jahre.

Jenny, Erbey und Sarah - my best office mates.

Nina, Sybille und Steffi für die Aktivitäten fernab des Labors.

Thomas und Jan und vor allem meinen Eltern für die immerwährende Unterstützung und Hilfe.